

# Simulation of networks of spiking neurons: A review of tools and strategies

Romain Brette<sup>1</sup>, Michelle Rudolph<sup>2</sup>, Ted Carnevale<sup>3</sup>, Michael Hines<sup>3</sup>, David Beeman<sup>4</sup>,  
James M. Bower<sup>5</sup>, Markus Diesmann<sup>6,7</sup>, Abigail Morrison<sup>7</sup>, Philip H. Goodman<sup>8</sup>,  
Frederick C. Harris, Jr.<sup>8</sup>, Milind Zirpe<sup>8</sup>, Thomas Natschläger<sup>9</sup>, Dejan Pecevski<sup>10</sup>, Bard Ermentrout<sup>11</sup>,  
Mikael Djurfeldt<sup>12</sup>, Anders Lansner<sup>12</sup>, Olivier Rochel<sup>13</sup>, Thierry Vieville<sup>14</sup>, Eilif Muller<sup>15</sup>,  
Andrew P. Davison<sup>2</sup>, Sami El Boustani<sup>2</sup> and Alain Destexhe<sup>2\*</sup>

1: Ecole Normale Supérieure, Paris, France

2: CNRS, Gif-sur-Yvette, France

3: Yale University, New Haven, CT, USA

4: University of Colorado, Boulder, CO, USA

5: University of Texas, San Antonio, TX, USA

6: University of Freiburg, Germany

7: RIKEN Brain Science Institute, Wako City, Japan

8: University of Nevada, Reno NV, USA

9: Software Competence Center Hagenberg, Hagenberg, Austria

10: Technical University of Graz, Austria

11: University of Pittsburgh, Pittsburgh, PA, USA

12: KTH, Sweden

13: University of Leeds, UK

14: INRIA, Nice, France

15: University of Heidelberg, Germany

November 29, 2006

## Abstract

We review different aspects of the simulation of spiking neural networks. We start by reviewing the different types of simulation strategies and algorithms that are currently implemented. We next review the precision of those simulation strategies, in particular in cases where plasticity depends on the exact timing of the spikes. We overview different simulators and simulation environments presently available (restricted to those freely available, open source and documented). For each simulation tool, its advantages and pitfalls are reviewed, with an aim to allow the reader to identify which simulator is appropriate for a given task. Finally, we provide a series of benchmark simulations of different types of networks of spiking neurons, including Hodgkin-Huxley type, integrate-and-fire models, interacting with current-based or conductance-based synapses, using clock-driven or event-driven integration strategies. The same set of models are implemented on the different simulators, and the codes are made available. The ultimate goal of this review is to provide a resource to facilitate identifying the appropriate integration strategy and simulation tool to use for a given modeling problem related to spiking neural networks.

---

\*Address for correspondence: Alain Destexhe, Unité de Neurosciences Intégratives et Computationnelles (UNIC), CNRS (Bat 33),  
1 Avenue de la Terrasse, 91190 Gif-sur-Yvette, France (destexhe@iaf.cnrs-gif.fr)

1  
2  
3  
4  
5  
6  
7  
8  
9  
10  
11  
12  
13  
14  
15  
16  
17  
18  
19  
20  
21  
22  
23  
24  
25  
26  
27  
28  
29  
30  
31  
32  
33  
34  
35  
36  
37  
38  
39  
40  
41  
42  
43  
44  
45  
46  
47  
48  
49  
50  
51  
52  
53  
54  
55  
56  
57  
58  
59  
60  
61  
62  
63  
64  
65

# Introduction

The growing experimental evidence that spike timing may be important to explain neural computations has motivated the use of spiking neuron models, rather than the traditional rate-based models. At the same time, a growing number of tools have appeared, allowing the simulation of spiking neural networks. Such tools offer the user to obtain precise simulations of a given computational paradigm, as well as publishable figures in a relatively short amount of time. However, the range of computational problems related to spiking neurons is very large. It requires in some cases to use detailed biophysical representations of the neurons, for example when intracellular electrophysiological measurements are to be reproduced (e.g., see Destexhe and Sejnowski, 2001). In this case, one uses conductance-based models, such as the Hodgkin and Huxley (1952) type of models. In other cases, one does not need to realistically capture the spike generating mechanisms, and simpler models, such as the integrate-and-fire (IF) model are sufficient. IF type models are also very fast to simulate, and are particularly attractive for large-scale network simulations.

There are two families of algorithms for the simulation of neural networks: synchronous or “clock-driven” algorithms, in which all neurons are updated simultaneously at every tick of a clock, and asynchronous or “event-driven” algorithms, in which neurons are updated only when they receive or emit a spike (hybrid strategies also exist). Synchronous algorithms can be easily coded and apply to any model. Because spike times are typically bound to a discrete time grid, the precision of the simulation can be an issue. Asynchronous algorithms have been developed mostly for exact simulation, which is possible for simple models. For very large networks, the simulation time for both methods scale as the total number of spike transmissions, but each strategy has its own assets and disadvantages.

In this paper, we start by providing an overview of different simulation strategies, and outline to which extent the temporal precision of spiking events impacts on neuronal dynamics of single as well as small networks of IF neurons with plastic synapses. Next, we review the currently available simulators or simulation environments, with an aim to focus only on publically-available and non-commercial tools to simulate networks of spiking neurons. For each type of simulator, we describe the simulation strategy used, outline the type of models which are most optimal, as well as provide concrete examples. The ultimate goal of this paper is to provide a resource to enable the researcher to identify which strategy or simulator to use for a given modeling problem related to spiking neural networks.

## 1 Simulation strategies

This discussion is restricted to serial algorithms for brevity. The specific sections of NEST and SPLIT contain additional information on concepts for parallel computing.

There are two families of algorithms for the simulation of neural networks: synchronous or “clock-driven” algorithms, in which all neurons are updated simultaneously at every tick of a clock, and asynchronous or “event-driven” algorithms, in which neurons are updated only when they receive or emit a spike. These two approaches have some common features that we will first describe by expressing the problem of simulating neural networks in the formalism of hybrid systems, i.e., differential equations with discrete events (spikes). In this framework some common strategies for efficient representation and simulation appear.

Since we are going to compare algorithms in terms of computational efficiency, let us first ask ourselves the following question: how much time can it possibly take for a good algorithm to simulate a large network? Suppose there are  $N$  neurons whose average firing rate is  $F$  and average number of synapses is  $p$ . If all spike transmissions are taken into account, then a simulation lasting 1s (biological time) must process  $N \times p \times F$  spike transmissions. The goal of efficient algorithm design is to reach this minimal number of operations (of course, up to a constant multiplicative factor). If the simulation is not restricted to spike-mediated interactions, e.g. if the model includes gap junctions or dendro-dendritic interactions, then the optimal number of operations can be much larger, but in this review we chose not to address the problem of graded interactions.

1  
2  
3  
4  
5  
6  
7  
8  
9  
10  
11  
12  
13  
14  
15  
16  
17  
18  
19  
20  
21  
22  
23  
24  
25  
26  
27  
28  
29  
30  
31  
32  
33  
34  
35  
36  
37  
38  
39  
40  
41  
42  
43  
44  
45  
46  
47  
48  
49  
50  
51  
52  
53  
54  
55  
56  
57  
58  
59  
60  
61  
62  
63  
64  
65

## 1.1 A hybrid system formalism

Mathematically, neurons can be described as *hybrid systems*: the state of a neuron evolves continuously according to some biophysical equations, which are typically differential equations (deterministic or stochastic, ordinary or partial differential equations), and spikes received through the synapses trigger changes in some of the variables. Thus the dynamics of a neuron can be described as follows:

$$\begin{aligned} \frac{d\mathbf{X}}{dt} &= f(\mathbf{X}) \\ \mathbf{X} &\leftarrow g_i(\mathbf{X}) \quad \text{upon spike from synapse } i \end{aligned}$$

where  $\mathbf{X}$  is a vector describing the state of the neuron. In theory, taking into account the morphology of the neuron would lead to partial differential equations; however, in practice, one usually approximates the dendritic tree by coupled isopotential compartments, which also leads to a differential system with discrete events. Spikes are emitted when some threshold condition is satisfied, for instance  $V_m \geq \theta$  for integrate-and-fire models (where  $V_m$  is the membrane potential and would be the first component of vector  $\mathbf{X}$ ), and/or  $dV_m/dt \geq \theta$  for Hodgkin-Huxley type models. This can be summarized by saying that a spike is emitted whenever some condition  $\mathbf{X} \in \mathbf{A}$  is satisfied. For integrate-and-fire models, the membrane potential, which would be the first component of  $\mathbf{X}$ , is reset when a spike is produced. The reset can be integrated into the hybrid system formalism by considering for example that outgoing spikes act on  $\mathbf{X}$  through an additional (virtual) synapse:  $\mathbf{X} \leftarrow g_0(\mathbf{X})$ .

With this formalism, it appears clearly that *spike times need not be stored* (except of course if transmission delays are included), even though it would seem so from more phenomenological formulations. For example, consider the following integrate-and-fire model (described for example in Gütig and Sompolinsky (2006)):

$$V(t) = \sum_i \omega_i \sum_{t_i} K(t - t_i) + V_{\text{rest}}$$

where  $V(t)$  is the membrane potential,  $V_{\text{rest}}$  is the rest potential,  $\omega_i$  is the synaptic weight of synapse  $i$ ,  $t_i$  are the timings of the spikes coming from synapse  $i$ , and  $K(t - t_i) = \exp(-(t - t_i)/\tau) - \exp(-(t - t_i)/\tau_s)$  is the post-synaptic potential (PSP) contributed by each incoming spike. The model can be restated as a two-variables differential system with discrete events as follows:

$$\begin{aligned} \tau \frac{dV}{dt} &= V_{\text{rest}} - V + J \\ \tau_s \frac{dJ}{dt} &= -J \\ J &\leftarrow J + \frac{\tau - \tau_s}{\tau} w_i \quad \text{upon spike from synapse } i \end{aligned}$$

Virtually all post-synaptic potentials or currents described in the literature (e.g.  $\alpha$ -functions, bi-exponential functions) can be expressed this way. Several authors have described the transformation from phenomenological expressions to the hybrid system formalism for synaptic conductances and currents (Destexhe et al, 1994a, 1994b, Rotter and Diesmann, 1999, Giugliano, 2000), short-term synaptic depression (Giugliano et al, 1999), and spike-timing-dependent plasticity (Song et al, 2000). In many cases, the Spike Response Model (Gerstner and Kistler, 2002) is also the integral expression of a hybrid system. To derive the differential formulation of a given post-synaptic current or conductance (PSC), one way is to see the latter as the impulse response of a linear time-invariant system (which can be seen as a filter (Janke et al, 1998)) and use transformation tools from signal processing theory such as the Z-transform (Kohn and Wörgötter, 1998; see also Sanchez, 2001) or the Laplace transform (the Z-transform is the equivalent of the Laplace transform in the digital time domain, i.e., for synchronous algorithms).

## 1.2 Using linearities for fast synaptic simulation

In general, the number of state variables of a neuron (length of vector  $\mathbf{X}$ ) scales with the number of synapses, since each synapse has its own dynamics. This fact constitutes a major problem for efficient simulation of

neural networks, both in terms of memory consumption and computation time. However, several authors have observed that all synaptic variables sharing the same linear dynamics can be reduced to a single one (Wilson and Bower, 1989, Bernard et al, 1994, Lytton, 1996 and Song et al, 2000). For example, the following set of differential equations, describing an integrate-and-fire model with  $n$  synapses with exponential conductances:

$$\begin{aligned}
C \frac{dV}{dt} &= V_0 - V + \sum_i g_i(t)(V - E_s) \\
\tau_s \frac{dg_1}{dt} &= -g_1 \\
&\dots \\
\tau_s \frac{dg_n}{dt} &= -g_n \\
g_i &\leftarrow g_i + w_i \quad \text{upon spike arriving at synapse } i
\end{aligned}$$

is mathematically equivalent to the following set of two differential equations:

$$\begin{aligned}
C \frac{dV}{dt} &= V_0 - V + g(t)(V - E_s) \\
\tau_s \frac{dg}{dt} &= -g \\
g &\leftarrow g + w_i \quad \text{upon spike arriving at synapse } i
\end{aligned}$$

where  $g$  is the total synaptic conductance. The same reduction applies to synapses with higher dimensional dynamics, as long as it is linear and the spike-triggered changes ( $g_i \leftarrow g_i + w_i$ ) are additive and do not depend on the state of the synapse (e.g. the rule  $g_i \leftarrow g_i + w_i * f(g_i)$  would cause a problem). Some models of spike-timing dependent plasticity (with linear interactions between pairs of spikes) can also be simulated in this way (see e.g. Abbott and Nelson (2000)). However, some important biophysical models are not linear and thus cannot benefit from this optimization, in particular NMDA-mediated interactions and saturating synapses.

### 1.3 Synchronous or “clock-driven” algorithms

In a synchronous or “clock-driven” algorithm (see pseudo-code in figure 1), the state variables of all neurons (and possibly synapses) are updated at every tick of a clock:  $\mathbf{X}(t) \rightarrow \mathbf{X}(t + dt)$ . With non-linear differential equations, one would use an integration method such as Euler or Runge-Kutta (Press et al, 1993) or, for Hodgkin-Huxley models, implicit methods (Hines, 1984). Neurons with complex morphologies are usually spatially discretized and modelled as interacting compartments: they are also described mathematically by coupled differential equations, for which dedicated integration methods have been developed (for details see e.g. the specific section of Neuron in this review). If the differential equations are linear, then the update operation  $\mathbf{X}(t) \rightarrow \mathbf{X}(t + dt)$  is also linear, which means updating the state variables amounts simply to multiplying  $\mathbf{X}$  by a matrix:  $\mathbf{X}(t + dt) = \mathbf{A}\mathbf{X}(t)$  (Hirsch and Smale, 1974; see also Rotter and Diesmann (1999) for an application to neural networks), which is very convenient in vector-based scientific softwares such as Matlab or Scilab. Then, after updating all variables, the threshold condition is checked for every neuron. Each neuron that satisfies this condition produces a spike which is transmitted to its target neurons, updating the corresponding variables ( $\mathbf{X} \leftarrow g_i(\mathbf{X})$ ). For integrate-and-fire models, the membrane potential of every spiking neuron is reset.

### Computational complexity

The simulation time of such an algorithm consists of two parts: 1) state updates and 2) propagation of spikes. Assuming the number of state variables for the whole network scales with the number of neurons  $N$  in the network (which is the case when the reduction described in section 1.2 applies), the cost of the update phase is of order  $N$  for each step, so it is  $O(N/dt)$  per second of biological time ( $dt$  is the duration of the time bin). This component grows with the complexity of the neuron models and the precision of the simulation. Every second

(biological time), an average of  $F \times N$  spikes are produced by the neurons ( $F$  is the average firing rate), and each of these needs to be propagated to  $p$  target neurons. Thus, the propagation phase consists in  $F \times N \times p$  spike propagations per second. These are essentially additions of weights  $w_i$  to state variables, and thus are simple operations whose cost does not grow with the complexity of the models. Summing up, the total computational cost per second of biological time is of order

$$\begin{aligned} & \text{Update} + \text{Propagation} \\ & c_U \times \frac{N}{dt} + c_P \times F \times N \times p \quad (*) \end{aligned}$$

where  $c_U$  is the cost of one update and  $c_P$  is the cost of one spike propagation; typically,  $c_U$  is much higher than  $c_P$  but this is implementation-dependent. Therefore, for very dense networks, the total is dominated by the propagation phase and is linear in the number of synapses, which is optimal. However, in practice the first phase is negligible only when the following condition is met:

$$\frac{c_P}{c_U} \times F \times p \times dt \gg 1$$

For example, the average firing rate in the cortex might be as low as  $F = 1$  Hz (Olshausen and Field, 2005), and assuming  $p = 10,000$  synapses per neuron and  $dt = 0.1$  ms, we get  $F \times p \times dt = 1$ . In this case, considering that each operation in the update phase is heavier than in the propagation phase (especially for complex models), i.e.,  $c_P < c_U$ , the former is likely to dominate the total computational cost. Thus, it appears that even in networks with realistic connectivity, increases in precision (smaller  $dt$ , see section 2) can be detrimental to the efficiency of the simulation.

## Delays

For the sake of simplicity, we ignored transmission delays in the description above. However it is not very complicated to include them in a synchronous clock-driven algorithm. The straightforward way is to store the future synaptic events in a circular array. Each element of the array corresponds to a time bin and contains a list of synaptic events that are scheduled for that time (see e.g. Morrison et al, 2005). For example, if neuron  $i$  sends a spike to neuron  $j$  with delay  $d$  (in units of the time bin  $dt$ ), then the synaptic event “ $i \rightarrow j$ ” is placed in the circular array at position  $p + d$ , where  $p$  is the present position. Circularity of the array means the addition  $p + d$  is modular ( $(p + d) \bmod n$ , where  $n$  is the size of the array — which corresponds to the largest delay in the system).

What is the additional computational cost of managing delays? In fact, it is not very high and does not depend on the duration of the time bin. Since every synaptic event ( $i \rightarrow j$ ) is stored and retrieved exactly once, the computational cost of managing delays for one second of biological time is

$$c_D \times F \times N \times p$$

where  $c_D$  is the cost of one store and one retrieve operation in the circular array (which is low). In other words, managing delays increases the cost of the propagation phase in equation (\*) by a small multiplicative factor.

## Exact clock-driven simulation

The obvious drawback of clock-driven algorithms as described above is that spike timings are aligned to a grid (ticks of the clock), thus the simulation is approximate even when the differential equations are computed exactly. Other specific errors come from the fact that threshold conditions are checked only at the ticks of the clock, implying that some spikes might be missed (see section 2). However, in principle, it is possible to simulate a network exactly in a clock-driven fashion when the minimum transmission delay is larger than the time step. It implies that the precise timing of synaptic events is stored in the circular array (as described in Morrison et al, 2006). Then within each time bin, synaptic events for each neuron are sorted and processed in

1  
2  
3  
4 the right order, and when the neuron spikes, the exact spike timing is calculated. Neurons can be processed  
5 independently in this way only because the time bin is smaller than the smallest transmission delay (neurons  
6 have no influence on each other within one time bin).

7 Some sort of clock signals can also be used in general event-driven algorithms without the assumption of a  
8 minimum positive delay. For example, one efficient data structure used in discrete event systems to store events  
9 is a priority queue known as “calendar queue” (Brown, 1988), which is a dynamic circular array of sorted lists.  
10 Each “day” corresponds to a time bin, as in a classical circular array, and each event is placed in the calendar at  
11 the corresponding day; all events on a given day are sorted according to their scheduling time. If the duration  
12 of the day is correctly set, then insertions and extractions of events take constant time on average. Note that, in  
13 contrast with standard clock-driven simulations, the state variables are not updated at ticks of the clock and the  
14 duration of the days depends neither on the precision of the simulation or on the transmission delays (it is rather  
15 linked to the rate of events) — in fact, the management of the priority queue is separated from the simulation  
16 itself.

17 Note however that in all these cases, state variables need to be updated at the time of every incoming spike  
18 rather than at every tick of the clock in order to simulate the network exactly (e.g. simple vector-based updates  
19  $\mathbf{X} \leftarrow \mathbf{A}\mathbf{X}$  are not possible), so that the term *event-driven* may be a better description of these algorithms (the  
20 precise terminology may vary between authors).

## 21 22 23 24 25 **Noise in synchronous algorithms**

26  
27 Noise can be introduced in synchronous simulations by essentially two means: 1) adding random external  
28 spikes; 2) simulating a stochastic process.

29 Suppose a given neuron receives  $F$  random spikes per second, according to a Poisson process. Then the  
30 number of spikes in one time bin follows a Poisson distribution with mean  $F \times dt$ . Thus one can simulate  
31 random external spike trains by letting each tick of the clock trigger a random number of synaptic updates. If  
32  $F \times dt$  is low, the Poisson distribution is almost a Bernoulli distribution (i.e., there is one spike with probability  
33  $F \times dt$ ). It is straightforward to extend the procedure to inhomogeneous Poisson processes by allowing  $F$  to  
34 vary in time. The additional computational cost is proportional to  $F_{\text{ext}} \times N$ , where  $F_{\text{ext}}$  is the average rate of  
35 external synaptic events for each neuron and  $N$  is the number of neurons. Note that  $F_{\text{ext}}$  can be quite large  
36 since it represents the sum of firing rates of all external neurons (for example it would be 10,000 Hz for 10,000  
37 external synapses per neuron with rate 1 Hz).

38 To simulate a large number of external random spikes, it can be advantageous to simulate directly the  
39 total external synaptic input as a stochastic process, e.g. white or colored noise (Ornstein-Uhlenbeck). Lin-  
40 ear stochastic differential equations are analytically solvable, therefore the update  $\mathbf{X}(t) \rightarrow \mathbf{X}(t + dt)$  can be  
41 calculated exactly with matrix computations (Arnold, 1974) ( $\mathbf{X}(t + dt)$  is, conditionally to  $\mathbf{X}(t)$ , a normally dis-  
42 tributed random variable whose mean and covariance matrix can be calculated as a function of  $\mathbf{X}(t)$ ). Nonlinear  
43 stochastic differential equations can be simulated using approximation schemes, e.g. stochastic Runge-Kutta  
44 (Honeycutt, 1992).

## 45 46 47 48 49 50 **1.4 Asynchronous or “event-driven” algorithms**

51 Asynchronous or “event-driven” algorithms are not as widely used as clock-driven ones because they are sig-  
52 nificantly more complex to implement (see pseudo-code in figure 3) and less universal. Their key advantages  
53 are a potential gain in speed due to not calculating many small update steps for a neuron in which no event  
54 arrives and that spike timings are computed exactly (but see below for approximate event-driven algorithms);  
55 in particular, spike timings are not aligned to a time grid anymore (which is a source of potential errors, see  
56 section 2).

57 The problem of simulating dynamical systems with discrete events is a well established research topic in  
58 computer science (Ferscha, 1996; Sloot et al, 1999; Fujimoto, 2000; Zeigler et al, 2000; see also Rochel and  
59 Martinez, 2003 and Mayrhofer et al, 2002), with appropriate data structures and algorithms already available to  
60 the computational neuroscience community. We start by describing the simple case when synaptic interactions  
61  
62  
63  
64  
65

1  
2  
3  
4 are instantaneous, i.e., when spikes can be produced only at times of incoming spikes (no latency); then we will  
5 turn to the most general case.  
6

### 7 **Instantaneous synaptic interactions**

8  
9 In an asynchronous or “event-driven” algorithm, the simulation advances from one event to the next event.  
10 Events can be spikes coming from neurons in the network or external spikes (typically random spikes described  
11 by a Poisson process). For models in which spikes can be produced by a neuron only at times of incoming  
12 spikes, event-driven simulation is relatively easy (see pseudo-code in figure 2). Timed events are stored in a  
13 queue (which is some sort of sorted list). One iteration consists in 1) extracting the next event; 2) updating the  
14 state of the corresponding neuron (i.e., calculating the state according to the differential equation and adding the  
15 synaptic weight) 3) checking if the neuron satisfies the threshold condition, in which case events are inserted in  
16 the queue for each downstream neuron.  
17

18  
19 In the simple case of identical transmission delays, the data structure for the queue can be just a FIFO queue  
20 (first in, first out), which has fast implementations (Cormen et al, 2001). When the delays take values in a small  
21 discrete set, the easiest way is to use one FIFO queue for each delay value, as described in Mattia and Del  
22 Giudice (2000). It is also more efficient to use a separate FIFO queue for handling random external events (see  
23 paragraph about noise below).  
24

25 In the case of arbitrary delays, one needs a more complex data structure. In computer science, efficient  
26 data structures to maintain an ordered list of time-stamped events are grouped under the name *priority queues*  
27 (Cormen et al, 2001). The topic of priority queues is dense and well documented; examples are binary heaps,  
28 Fibonacci heaps (Cormen et al, 2001), calendar queues (Brown, 1988, Claverol et al, 2002) or van Emde Boas  
29 trees (van Emde Boas et al, 1976; see also Connolly et al (2003) in which various priority queues are compared).  
30 Using an efficient priority queue is a crucial element of a good event-driven algorithm. It is even more crucial  
31 when synaptic interactions are not instantaneous.  
32  
33

### 34 **Non-instantaneous synaptic interactions**

35  
36 For models in which spike times do not necessarily occur at times of incoming spikes, event-driven simulation  
37 is more complex. We first describe the basic algorithm with no delays and no external events (see pseudo-code  
38 in figure 3). One iteration consists in 1) finding which neuron is the next one to spike; 2) updating this neuron;  
39 3) propagating the spike, i.e., updating its target neurons. The general way to do that is to maintain a sorted list  
40 of the future spike timings of all neurons. These spike timings are only provisory since any spike in the network  
41 can modify all future spike timings. However, the spike with lowest timing in the list is certified. Therefore,  
42 the following algorithm for one iteration guarantees the correctness of the simulation (see figure 3): 1) extract  
43 the spike with lowest timing in the list; 2) update the state of the corresponding neuron and recalculate its  
44 future spike timing; 3) update the state of its target neurons; 4) recalculate the future spike timings of the target  
45 neurons.  
46  
47

48 For the sake of simplicity, we ignored transmission delays in the description above. Including them in an  
49 event-driven algorithm is not as straightforward as in a clock-driven algorithm, but it is a minor complication.  
50 When a spike is produced by a neuron, the future synaptic events are stored in another priority queue in which  
51 the timings of events are non-modifiable. The first phase of the algorithm (extracting the spike with lowest  
52 timing) is replaced by extracting the next event, which can be either a synaptic event or a spike emission. One  
53 can use two separate queues or a single one. External events can be handled in the same way. Although delays  
54 introduce complications in coding event-driven algorithms, they can in fact simplify the management of the  
55 priority queue for outgoing spikes. Indeed, the main difficulty in simulating networks with non-instantaneous  
56 synaptic interactions is that scheduled outgoing spikes can be canceled, postponed or advanced by future incom-  
57 ing spikes. If transmission delays are greater than some positive value  $\tau_{\min}$ , then all outgoing spikes scheduled  
58 in  $[t, t + \tau_{\min}]$  ( $t$  being the present time) are certified. Thus, algorithms can exploit the structure of delays to  
59 speed up the simulation (Lee and Farhat, 2001).  
60  
61  
62  
63  
64  
65

1  
2  
3  
4  
5  
6  
7  
8  
9  
10  
11  
12  
13  
14  
15  
16  
17  
18  
19  
20  
21  
22  
23  
24  
25  
26  
27  
28  
29  
30  
31  
32  
33  
34  
35  
36  
37  
38  
39  
40  
41  
42  
43  
44  
45  
46  
47  
48  
49  
50  
51  
52  
53  
54  
55  
56  
57  
58  
59  
60  
61  
62  
63  
64  
65

## Computational complexity

Putting aside the cost of handling external events (which is minor), we can subdivide the computational cost of handling one outgoing spike as follows (assuming  $p$  is the average number of synapses per neuron):

- extracting the event (in case of non-instantaneous synaptic interactions)
- updating the neuron and its targets:  $p + 1$  updates;
- inserting  $p$  synaptic events in the queue (in case of delays);
- updating the spike times of  $p + 1$  neurons (in case of non-instantaneous synaptic interactions);
- inserting or rescheduling  $p + 1$  events in the queue (future spikes for non-instantaneous synaptic interactions).

Since there are  $F \times N$  spikes per second of biological time, the number of operations is approximately proportional to  $F \times N \times p$ . The total computational cost per second of biological time can be written concisely as follows:

$$\begin{matrix} \textit{Update} & + & \textit{Spike} & + & \textit{Queue} \\ (c_U & + & c_S & + & c_Q) & \times F \times N \times p \end{matrix}$$

where  $c_U$  is the cost of one update of the state variables,  $c_S$  is the cost of calculating the time of the next spike (non-instantaneous synaptic interactions) and  $c_Q$  is the average cost of insertions and extractions in the priority queue(s). Thus, the simulation time is linear in the number of synapses, which is optimal. Nevertheless, we note that the operations involved are heavier than in the propagation phase of clock-driven algorithms (see previous section), therefore the multiplicative factor is likely to be larger. We have also assumed that  $c_Q$  is  $O(1)$ , i.e., that the dequeue and enqueue operations can be done in constant average time with the data structure chosen for the priority queue. In the simple case of instantaneous synaptic interactions and homogeneous delays, one can use a simple FIFO queue (First In, First Out), in which insertions and extractions are very fast and take constant time. For the general case, data structures for which dequeue and enqueue operations take constant average time ( $O(1)$ ) exist, e.g. calendar queues (Brown, 1988, Claverol et al, 2002), however they are quite complex, i.e.,  $c_Q$  is a large constant. In simpler implementations of priority queues such as binary heaps, the dequeue and enqueue operations take  $O(\log m)$  operations, where  $m$  is the number of events in the queue. Overall, it appears that the crucial component in general event-driven algorithms is the queue management.

## What models can be simulated in an event-driven fashion?

Event-driven algorithms implicitly assume that we can calculate the state of a neuron at any given time, i.e., we have an explicit solution of the differential equations (but see below for approximate event-driven simulation). This would not be the case with e.g. Hodgkin-Huxley models. Besides, when synaptic interactions are not instantaneous, we also need a function that maps the current state of the neuron to the timing of the next spike (possibly  $+\infty$  if there is none).

So far, algorithms have been developed for simple pulse-coupled integrate-and-fire models (Watts, 1994, Claverol et al, 2002, Delorme and Thorpe, 2003) and more complex ones such as some instances of the Spike Response Model (Makino, 2003, Marian et al, 2002, Gerstner and Kistler, 2002) (note that the SRM model can usually be restated in the differential formalism of section 1.1). Recently, Rudolph and Destexhe (2006) introduced several integrate-and-fire models with synaptic conductances which are suitable for event-driven simulation. Algorithms were also recently developed by Brette to simulate exactly integrate-and-fire models with exponential synaptic currents (Brette, 2006a) and conductances (Brette, 2006b), and Tonnelier et al (2006, submitted) extended this work to the quadratic model (Ermentrout and Kopell, 1986). However, there are still efforts to be made to design suitable algorithms for more complex models (for example the two-variable integrate-and-fire models of Izhikevich (2003) and Brette and Gerstner (2005)), or to develop more realistic models that are suitable for event-driven simulation.



1  
2  
3  
4  
5  
6  
7  
8  
9  
10  
11  
12  
13  
14  
15  
16  
17  
18  
19  
20  
21  
22  
23  
24  
25  
26  
27  
28  
29  
30  
31  
32  
33  
34  
35  
36  
37  
38  
39  
40  
41  
42  
43  
44  
45  
46  
47  
48  
49  
50  
51  
52  
53  
54  
55  
56  
57  
58  
59  
60  
61  
62  
63  
64  
65

### Noise in event-driven algorithms

As for synchronous algorithms, there are two ways to introduce noise in a simulation: 1) adding random external spikes; 2) simulating a stochastic process.

The former case is by far easier in asynchronous algorithms. It simply amounts to adding a queue with external events, which is usually easy to implement. For example, if external spikes are generated according to a Poisson process with rate  $F$ , the timing of the next event is a random variable with exponential distribution with  $1/F$ . If  $n$  neurons receive external spike trains given by independent Poisson processes with rate  $F$ , then the time of the next event is exponentially distributed with mean  $1/(nF)$  and the label of the neuron receiving this event is picked at random in  $\{1, 2, \dots, n\}$ . Inhomogeneous Poisson processes can be simulated exactly in a similar way (Daley and Vere-Jones, 1988). If  $r(t)$  is the instantaneous rate of the Poisson process and is bounded by  $M$  ( $r(t) \leq M$ ), then one way to generate a spike train according to this Poisson process in the interval  $[0, T]$  is as follows: generate a spike train in  $[0, T]$  according to a homogeneous Poisson process with rate  $T * M$ ; for each spike at time  $t_i$ , draw a random number  $x_i$  from a uniform distribution in  $[0, M]$ ; select all spikes such that  $x_i \leq r(t_i)$ .

Simulating directly a stochastic process in asynchronous algorithms is much harder because even for the simplest stochastic neuron models, there is no closed analytical formula for the distribution of the time to the next spike (see e.g. Tuckwell (1988)). It is however possible to use precalculated tables when the dynamical systems are low dimensional (Reutimann et al, 2003) (i.e., not more than 2 dimensions). Note that simulating noise in this way introduces provisory events in the same way as for non-instantaneous synaptic interactions.

### Approximate event-driven algorithms

We have described asynchronous algorithms for simulating neural networks exactly. For complex neuron models of the Hodgkin-Huxley type, Lytton and Hines (2005) have developed an asynchronous simulation algorithm which consists in using for each neuron an independent time step whose width is reduced when the membrane potential approaches the action potential threshold.

## 2 Precision of different simulation strategies

As shown in this paper, a steadily growing number of neural simulation environments does endow computational neuroscience with tools which, together with the steady improvement of computational hardware, allow to simulate neural systems with increasing complexity, ranging from detailed biophysical models of single cells up to large-scale neural networks. Each of these simulation tools pursues the quest for a compromise between efficiency in speed and memory consumption, flexibility in the type of questions addressable, and precision or exactness in the numerical treatment of the latter. In all cases, this quest leads to the implementation of a specific strategy for numerical simulations which is found to be optimal given the set of constraints set by the particular simulation tool. However, as shown recently (Hansel et al., 1998; Lee and Farhat, 2001; Morrison et al, 2006), quantitative results and their qualitative interpretation strongly depend on the simulation strategy utilized, and may vary across available simulation tools or for different settings within the same simulator. The specificity of neuronal simulations is that spikes induce either a discontinuity in the dynamics (integrate-and-fire models) or have very fast dynamics (Hodgkin-Huxley type models). When using approximation methods, this problem can be tackled by spike timing interpolation in the former case (Hansel et al., 1998; Shelley and Tao, 2001) or integration with adaptive time step in the latter case (Lytton and Hines, 2005). Specifically in networks of integrate-and-fire neurons, which to date remain almost exclusively the basis for accessing dynamics of large-scale neural populations (but see Section 3.7), crucial differences in the appearance of synchronous activity patterns were observed, depending on the temporal resolution of the neural simulator or the integration method used.

In this section we address this question using one of the most simple analytically solvable LIF neuron

model, namely the classic leaky integrate-and-fire neuron, described by the state equation

$$\tau_m \frac{dm(t)}{dt} + m(t) = 0, \quad (1)$$

where  $\tau_m = 20$  ms denotes the membrane time constant and  $0 \leq m(t) \leq 1$ . Upon arrival of a synaptic event at time  $t_0$ ,  $m(t)$  is updated by a constant  $\Delta m = 0.1$  ( $\Delta m = 0.0085$  in network simulations) after which it decays according to

$$m(t) = m(t_0) \exp\left[-\frac{t-t_0}{\tau_m}\right]. \quad (2)$$

If  $m$  exceeds a threshold  $m_{thres} = 1$ , the neuron fires and is afterwards reset to a resting state  $m_{rest} = 0$  in which it stays for an absolute refractory period  $t_{ref} = 1$  ms. The neurons were subject to non-plastic or plastic synaptic interactions. In the latter case, spike timing dependent synaptic plasticity was used according to a model by Song and Abbott (2001). In this case, upon arrival of a synaptic input at time  $t_{pre}$ , synaptic weights are changed according to

$$g \leftarrow g + F(\Delta t) g_{max}, \quad (3)$$

where

$$F(\Delta t) = \pm A_{\pm} \exp\{\pm \Delta t / \tau_{\pm}\} \quad (4)$$

for  $\Delta t = t_{pre} - t_{post} < 0$  and  $\Delta t \geq 0$ , respectively. Here,  $t_{post}$  denotes the time of the nearest postsynaptic spike,  $A_{\pm}$  quantify the maximal change of synaptic efficacy, and  $\tau_{\pm}$  determine the range of pre- to postsynaptic spike intervals in which synaptic weight changes occur. Comparing simulation strategies at the both ends of a wide spectrum, namely a clock-driven algorithm (see Section 1.3) and event-driven algorithm (see Section 1.4), we evaluate to which extent the temporal precision of spiking events impacts on neuronal dynamics of single as well as small networks. These results support the argument that the speed of neuronal simulations should not be the sole criteria for evaluation of simulation tools, but must complement an evaluation of their exactness.

## 2.1 Neuronal systems without STDP

In the case of a single LIF neuron with non-plastic synapses subject to a frozen synaptic input pattern drawn from a Poisson distribution with rate  $\nu_{inp} = 250$  Hz, differences in the discharge behavior seen in clock-driven simulations at different resolutions (0.1 ms, 0.01 ms, 0.001 ms) and event-driven simulations occurred already after short periods of simulated neural activity (Fig. 4A). These deviations were caused by subtle differences in the subthreshold integration of synaptic input events due to temporal binning, and “decayed” with a constant which depended on the membrane time constant. However, for a strong synaptic drive, subthreshold deviations could accumulate and lead to marked delays in spike times, cancellation of spikes or occurrence of additional spikes.

Although differences at the single cell level remained widely constrained and did not lead to changes in the statistical characterization of the discharge activity when long periods of neural activity were considered, already small differences in spike times of individual neurons can lead to crucial differences in the population activity, such as synchronization (see Hansel et al., 1998; Lee and Farhat, 2001), if neural networks are concerned. We investigated this possibility using a small network of  $15 \times 15$  LIF neurons with all-to-all excitatory connectivity with fixed weights and not distance-dependent synaptic transmission delay (0.2 ms), driven by a fixed pattern of superthreshold random synaptic inputs to each neuron (average rate 250 Hz; weight  $\Delta m = 0.1$ ). In such a small network, the activity remained primarily driven by the external inputs, i.e. the influence of intrinsic connectivity is small. However, due to small differences in spike times due to temporal binning could had severe effects on the occurrence of synchronous network events where all (or most) cells discharge at the same time. Such events could be delayed, canceled or generated depending on the simulation strategy or temporal resolution utilized (Fig. 4B).

## 2.2 Neuronal systems with STDP

The above described differences in the behavior of neural systems simulated by using different simulation strategies remain constrained to the observed neuronal dynamics and are minor if some statistical measures, such as average firing rates, are considered. More severe effects can be expected if biophysical mechanisms which depend on the exact times of spikes are incorporated into the neural model. One of these mechanisms is short-term synaptic plasticity, in particular spike-timing dependent synaptic plasticity (STDP). In this case, the self-organizing capability of the neural system considered will yield different paths along which the systems will develop, and, thus, possibly lead to a neural behavior which not only quantitatively but also qualitatively may differ across various tools utilized for the numerical simulation.

To explain why such small differences in the exact timing of events are crucial if models with STDP are considered, consider a situation in which multiple synaptic input events arrive in between two state updates at  $t$  and  $t + dt$  in a clock-driven simulation. In the latter case, the times of these events are assigned to the end of the interval (Fig. 5A). In the case these inputs drive the cell over firing threshold, the synaptic weights of all three synaptic input channels will be facilitated by the same amount according to the used STDP model. In contrast, if exact times are considered, the same input pattern could cause a discharge already after only two synaptic inputs. In this case the synaptic weights linked to these inputs will be facilitated, whereas the weight of the input arriving after the discharge will be depressed.

Although the chance for the occurrence of situations such as those described above may appear small, already one instance will push the considered neural system onto a different path in its self-organization. The latter may lead to systems whose qualitative behavior may, after some time, markedly vary from a system with the same initial state but simulated by another, temporally more or less precise simulation strategy. Such a scenario was investigated by using a single LIF neuron ( $\tau_m = 4.424$  ms) with 1,000 plastic synapses ( $A_+ = 0.005$ ,  $A_-/A_+ = 1.05$ ,  $\tau_+ = 20$  ms,  $\tau_- = 20$  ms,  $g_{max} = 0.4$ ) driven by the same pattern of Poisson-distributed random inputs (average rate 5 Hz,  $\Delta m = 0.1$ ). Simulating only 1,000 s neural activity led to marked differences in the temporal development of the average rate between clock-driven simulations with a temporal resolution of 0.1 ms and event-driven simulations (Fig. 5B). Considering the average firing rate over the whole simulated window, clock-driven simulations led to an about 10 % higher value compared to the event-driven approach, and approached the value observed in event-driven simulations only when the temporal resolution was increased by two orders of magnitude. Moreover, different simulation strategies and temporal resolutions led also to a significant difference in the synaptic weight distribution at different times (Fig. 5C).

Both findings show that the small differences in the precision of synaptic events can have a severe impact even on statistically very robust measures, such as average rate or weight distribution. Considering the temporal development of individual synaptic weights, both depression and facilitation were observed depending on the temporal precision of the numerical simulation. Indeed, the latter could have severe impact on the qualitative interpretation of the temporal dynamics of structured networks, as this result suggests that synaptic connections in otherwise identical models can be strengthened or weakened due to the influence of the utilized simulation strategy or simulation parameters.

In conclusion, the results presented in this section suggest that the strategy and temporal precision used for neural simulations can severely alter simulated neural dynamics. Although dependent on the neural system modeled, observed differences may turn out to be crucial for the qualitative interpretation of the result of numerical simulations, in particular in simulations involving biophysical processes depending on the exact order or time of spike events (e.g. as in STDP). Thus, the search for an optimal neural simulation tool or strategy for the numerical solution of a given problem should be guided not only by its absolute speed and memory consumption, but also its numerical exactness.

### 3 Overview of simulation environments

#### 3.1 NEURON

##### 3.1.1 NEURON's domain of utility

NEURON is a simulation environment for creating and using empirically-based models of biological neurons and neural circuits. Initially it earned a reputation for being well-suited for conductance-based models of cells with complex branched anatomy, including extracellular potential near the membrane, and biophysical properties such as multiple channel types, inhomogeneous channel distribution, ionic accumulation and diffusion, and second messengers. In the early 1990s, NEURON was already being used in some laboratories for network models with many of thousands of cells, and over the past decade it has undergone many enhancements that make the construction and simulation of large-scale network models easier and more efficient.

To date, more than 600 papers and books have described NEURON models that range from a membrane patch to large scale networks with tens of thousands of conductance-based or artificial spiking cells<sup>1</sup>. In 2005, over 50 papers were published on topics such as mechanisms underlying synaptic transmission and plasticity (Banitt et al. 2005), modulation of synaptic integration by subthreshold active currents (Prescott and De Koninck 2005), dendritic excitability (Day et al. 2005), the role of gap junctions in networks (Migliore et al. 2005), effects of synaptic plasticity on the development and operation of biological networks (Saghatelian et al. 2005), neuronal gain (Azouz 2005), the consequences of synaptic and channel noise for information processing in neurons and networks (Badoual et al. 2005), cellular and network mechanisms of temporal coding and recognition (Kanold and Manis 2005), network states and oscillations (Wolf et al. 2005), effects of aging on neuronal function (Markaki et al. 2005), cortical recording (Moffitt and McIntyre 2005), deep brain stimulation (Grill et al. 2005), and epilepsy resulting from channel mutations (Vitko et al. 2005) and brain trauma (Houweling et al. 2005).

##### 3.1.2 How NEURON differs from other neurosimulators

The chief rationale for domain-specific simulators over general purpose tools lies in the promise of improved conceptual control, and the possibility of exploiting the structure of model equations for the sake of computational robustness, accuracy, and efficiency. Some of the key differences between NEURON and other neurosimulators are embodied in the way that they approach these goals.

###### *Conceptual control*

The cycle of hypothesis formulation, testing, and revision, which lies at the core of all scientific research, presupposes that one can infer the consequences of a hypothesis. The principal motivation for computational modeling is its utility for dealing with hypotheses whose consequences cannot be determined by unaided intuition or analytical approaches. The value of any model as a means for evaluating a particular hypothesis depends critically on the existence of a close match between model and hypothesis. Without such a match, simulation results cannot be a fair test of the hypothesis. From the user's viewpoint, the first barrier to computational modeling is the difficulty of achieving conceptual control, i.e. making sure that a computational model faithfully reflects one's hypothesis.

NEURON has several features that facilitate conceptual control, and it is acquiring more of them as it evolves to meet the changing needs of computational neuroscientists. Many of these features fall into the general category of "native syntax" specification of model properties: that is, key attributes of biological neurons and networks have direct counterparts in NEURON. For instance, NEURON users specify the gating properties of voltage- and ligand-gated ion channels with kinetic schemes or families of Hodgkin-Huxley style differential equations. Another example is that models may include electronic circuits constructed with the LinearCircuitBuilder, a GUI tool whose palette includes resistors, capacitors, voltage and current sources, and operational amplifiers. NEURON's most striking application of native syntax may lie in how it handles the cable properties of neurons, which is very different from any other neurosimulator. NEURON users never have to deal

---

<sup>1</sup><http://www.neuron.yale.edu/neuron/bib/usednrm.html>

1  
2  
3  
4 directly with compartments. Instead, cells are represented by unbranched neurites, called sections, which can  
5 be assembled into branched architectures (the topology of a model cell). Each section has its own anatomical  
6 and biophysical properties, plus a discretization parameter that specifies the local resolution of the spatial  
7 grid. The properties of a section can vary continuously along its length, and spatially inhomogeneous variables  
8 are accessed in terms of normalized distance along each section ((Hines and Carnevale 2001), chapter 5 in  
9 (Carnevale and Hines 2006)). Once the user has specified cell topology, and the geometry, biophysical properties,  
10 and discretization parameter for each section, NEURON automatically sets up the internal data structures  
11 that correspond to a family of ODEs for the model's discretized cable equation.  
12

### 13 *Computational robustness, accuracy, and efficiency*

14 NEURON's spatial discretization of conductance-based model neurons uses a central difference approximation  
15 that is second order correct in space. The discretization parameter for each section can be specified by  
16 the user, or assigned automatically according to the `d_lambda` rule (see (Hines and Carnevale 2001), chapters 4  
17 and 5 in (Carnevale and Hines 2006)).  
18

19 For efficiency, NEURON's computational engine uses algorithms that are tailored to the model system  
20 equations (Hines 1984, 1989; Hines and Carnevale 2004). To advance simulations in time, users have a choice  
21 of built-in clock driven (fixed step backward Euler and Crank-Nicholson) and event driven methods (global  
22 variable step and local variable step with second order threshold detection); the latter are based on CVODES  
23 and IDA from SUNDIALS (Hindmarsh et al. 2005). Networks of artificial spiking cells are solved analytically  
24 by a discrete event method that is several orders of magnitude faster than continuous system simulation (Hines  
25 and Carnevale 2004). NEURON fully supports hybrid simulations, and models can contain any combination of  
26 conductance-based neurons and analytically computable artificial spiking cells. Simulations of networks that  
27 contain conductance-based neurons are second order correct if adaptive integration is used (Lytton and Hines  
28 2005).  
29

30  
31 Synapse and artificial cell models accept discrete events with input stream specific state information. It is  
32 often extremely useful for artificial cell models to send events to themselves in order to implement refractory  
33 periods and intrinsic firing properties; the delivery time of these "self events" can also be adjusted in response  
34 to intervening events. Thus instantaneous and non-instantaneous interactions of section 1.4 are supported.  
35

36 Built-in synapses exploit the methods described in section 1.2. Arbitrary delay between generation of an  
37 event at its source, and delivery to the target (including 0 delay events), is supported by a splay-tree queue  
38 (Sleator and Tarjan 1983) which can be replaced at configuration time by a calendar queue. If the minimum  
39 delay between cells is greater than 0, self events do not use the queue and parallel network simulations are  
40 supported. For the fixed step method, when queue handling is the rate limiting step, a bin queue can be selected.  
41 For the fixed step method with parallel simulations, when spike exchange is the rate limiting step, six-fold spike  
42 compression can be selected.  
43  
44

### 45 **3.1.3 Creating and using models with NEURON**

46  
47 Models can be created by writing programs in an interpreted language based on hoc (Kernighan and Pike  
48 1984), which has been enhanced to simplify the task of representing the properties of biological neurons and  
49 networks. Users can extend NEURON by writing new function and biophysical mechanism specifications in  
50 the NMODL language, which is then compiled and dynamically linked ((Hines and Carnevale 2000), chapter 9  
51 in (Carnevale and Hines 2006)). There is also a powerful GUI for conveniently building and using models; this  
52 can be combined with hoc programming to exploit the strengths of both (Fig. 6).  
53

54  
55 The past decade has seen many enhancements to NEURON's capabilities for network modeling. First  
56 and most important was the addition of an event delivery system that substantially reduces the computational  
57 burden of simulating spike-triggered synaptic transmission, and enabled the creation of analytic integrate-and-  
58 fire cell models which can be used in any combination with conductance-based cells. Just in the past year the  
59 event delivery system was extended so that NEURON can now simulate models of networks and cells that are  
60 distributed over parallel hardware (see NEURON in a parallel environment below).  
61

### 62 *The GUI*

1  
2  
3  
4 The GUI contains a large number of tools that can be used to construct models, exercise simulations, and  
5 analyze results, so that no knowledge of programming is necessary for the productive use of NEURON. In ad-  
6 dition, many GUI tools provide functionality that would be quite difficult for users to replicate by writing their  
7 own code. Some examples are:  
8

9  
10 *Model specification tools*

- 11 • Channel Builder—specifies voltage- and ligand-gated ion channels in terms of ODEs (HH-style, including  
12 Borg-Graham formulation) and/or kinetic schemes. Channel states and total conductance can be sim-  
13 ulated as deterministic (continuous in time), or stochastic (countably many channels with independent  
14 state transitions, producing abrupt conductance changes).  
15
- 16 • Cell Builder—manages anatomical and biophysical properties of model cells.  
17
- 18 • Network Builder—prototypes small networks that can be mined for reusable code to develop large-scale  
19 networks (chapter 11 in (Carnevale and Hines 2006)).  
20
- 21 • Linear Circuit Builder—specifies models involving gap junctions, ephaptic interactions, dual-electrode  
22 voltage clamps, dynamic clamps, and other combinations of neurons and electrical circuit elements.  
23  
24

25  
26 *Model analysis tools*

- 27 • Import3D—converts detailed morphometric data (Eutectic, NeuroLucida, and SWC formats) into model  
28 cells. It automatically fixes many common errors, and helps users identify complex problems that require  
29 judgment.  
30
- 31 • Model View—automatically discovers and presents a summary of model properties in a browsable textual  
32 and graphical form. This aids code development and maintenance, and is increasingly important as code  
33 sharing grows.  
34
- 35 • Impedance—compute and display voltage transfer ratios, input and transfer impedance, and the electro-  
36 tonic transformation.  
37  
38

39  
40 *Simulation control tools*

- 41 • Variable Step Control—automatically adjusts the state variable error tolerances that regulate adaptive in-  
42 tegration.  
43
- 44 • Multiple Run Fitter—optimizes function and model parameters.  
45  
46

47  
48 **3.1.4 NEURON in a parallel environment**

49  
50 NEURON supports three kinds of parallel processing.

51 1. Multiple simulations distributed over multiple processors, each processor executing its own simulation.  
52 Communication between master processor and workers uses a bulletin-board method similar to Linda (Carriero  
53 and Gelernter 1989).  
54

55 2. Distributed network models with gap junctions.

56 3. Distributed models of individual cells (each processor handles part of the cell). At present, setting up  
57 distributed models of individual cells requires considerable effort; in the future it will be made much more  
58 convenient.  
59

60 The four benchmark simulations of spiking neural networks (see Appendix 2) were implemented under  
61 NEURON. Figure 7A demonstrates the speedup that NEURON can achieve with distributed network models  
62 of the four types (conductance-based, current-based, Hodgkin-Huxley, event-based – see Appendix 2) on a  
63  
64  
65

1  
2  
3  
4 Beowulf cluster (dashed lines are "ideal"—run time inversely proportional to number of CPUs—and solid symbols  
5 are actual run times). Figure 7B shows that performance improvement scales with the number of processors and  
6 the size and complexity of the network; for this figure we ran a series of tests using a NEURON implementation  
7 of the single column thalamocortical network model described by Traub et al. (2005) on the Cray XT3 at the  
8 Pittsburgh Supercomputer Center. Similar performance gain has been documented in extensive tests on parallel  
9 hardware with dozens to thousands of CPUs, using published models of networks of conductance based neurons  
10 (Migliore et al., 2006). Speedup is linear with the number of CPUs, or even superlinear (due to larger effective  
11 high speed memory cache), until there are so many CPUs that each one is solving fewer than 100 equations.  
12  
13

### 14 15 **3.1.5 Future plans**

16  
17 NEURON undergoes a continuous cycle of improvement and revision, much of which is devoted to aspects of  
18 the program that are not immediately obvious to the user, e.g. improvement of computational efficiency. More  
19 noticeable are new GUI tools, such as the recently added Channel Builder. Many of these tools exemplify a  
20 trend toward "form-based" model specification, which is expected to continue. The use of form-based GUI tools  
21 increases the ability to exchange model specifications with other simulators through the medium of XML. With  
22 regard to network modeling, the emphasis will shift away from developing simulation infrastructure, which is  
23 reasonably complete, to the creation of new tools for network design and analysis.  
24  
25

### 26 27 **3.1.6 Software development, support, and documentation**

28  
29 Michael Hines directs the NEURON project, and is responsible for almost all code development. The other  
30 members of the development team have varying degrees of responsibility for activities such as documentation,  
31 courses, and user support. NEURON has benefited from significant contributions of time and effort by members  
32 of the community of NEURON users who have worked on specific algorithms, written or tested new code, etc..  
33 Since 2003, user contributions have been facilitated by adoption of an "open source development model" so  
34 that source code, including the latest research threads, can be accessed from an on-line repository<sup>2</sup>.

35  
36 Support is available by email, telephone, and consultation. Users can also post questions and share informa-  
37 tion with other members of the NEURON community via a mailing list and The NEURON Forum<sup>3</sup>. Currently  
38 the mailing list has more than 700 subscribers with "live" email addresses; the Forum, which was launched in  
39 May, 2005, has already grown to 300 registered users and 1700 posted messages.

40  
41 Tutorials and reference material are available<sup>4</sup>. The NEURON Book (Carnevale and Hines 2006) is the  
42 authoritative book on NEURON. Four books by other authors have made extensive use of NEURON (Destexhe  
43 and Sejnowski 2001; Johnston and Wu 1995; Lytton 2002; Moore and Stuart 2000), and several of them have  
44 posted their code online or provide it on CD with the book.

45  
46 Source code for published NEURON models is available at many WWW sites. The largest code archive is  
47 ModelDB<sup>5</sup>, which currently contains 238 models, 152 of which were implemented with NEURON.  
48

### 49 50 **3.1.7 Software availability**

51  
52 NEURON runs under UNIX/Linux/OS X, MSWin 98 or later, and on parallel hardware including Beowulf  
53 clusters, the IBM Blue Gene and Cray XT3. NEURON source code and installers are provided free of charge<sup>6</sup>,  
54 and the installers do not require "third party" software. The current standard distribution is version 5.9.39. The  
55 alpha version can be used as a simulator/controller in dynamic clamp experiments under real-time Linux<sup>7</sup> with  
56 a National Instruments M series DAQ card.  
57

---

58 <sup>2</sup><http://www.neuron.yale.edu/neuron/install.html>

59 <sup>3</sup><https://www.neuron.yale.edu/phpBB2/index.php>

60 <sup>4</sup><http://www.neuron.yale.edu/neuron/docs/docs.html>

61 <sup>5</sup><http://senselab.med.yale.edu/senselab/ModelDB>

62 <sup>6</sup><http://www.neuron.yale.edu>

63 <sup>7</sup><http://rtai.org>

## 3.2 GENESIS

### 3.2.1 GENESIS Capabilities and Design Philosophy

GENESIS (the GEneral NEural SIMulation System) was given its name because it was designed, at the outset, be an extensible general simulation system for the realistic modeling of neural and biological systems (Bower and Beeman, 1998). Typical simulations that have been performed with GENESIS range from subcellular components and biochemical reactions (Bhalla, 2004) to complex models of single neurons (De Schutter and Bower, 1994), simulations of large networks (Nenadic et al., 2003), and systems-level models (Stricanne and Bower, 1998). Here, "realistic models" are defined as those models that are based on the known anatomical and physiological organization of neurons, circuits and networks (Bower, 1995). For example, realistic cell models typically include dendritic morphology and a large variety of ionic conductances, whereas realistic network models attempt to duplicate known axonal projection patterns.

Parallel GENESIS (PGENESIS) is an extension to GENESIS that runs on almost any parallel cluster, SMP, supercomputer, or network of workstations where MPI and/or PVM is supported, and on which serial GENESIS itself is runnable. It is customarily used for large network simulations involving tens of thousands of realistic cell models (for example, see Hereld et al., 2005).

GENESIS has a well-documented process for users themselves to extend its capabilities by adding new user-defined GENESIS object types (classes), or script language commands without the need to understand or modify the GENESIS simulator code. GENESIS comes already equipped with mechanisms to easily create large scale network models made from single neuron models that have been implemented with GENESIS.

While users have added, for example, the Izhikevich (2003) simplified spiking neuron model (now built in to GENESIS), and they could also add IF or other forms of abstract neuron models, these forms of neurons are not realistic enough for the interests of most GENESIS modelers. For this reason, GENESIS is not normally provided with IF model neurons, and no GENESIS implementations have been provided for the IF model benchmarks (see Appendix 2). Typical GENESIS neurons are multicompartmental models with a variety of Hodgkin-Huxley type voltage- and/or calcium-dependent conductances.

### 3.2.2 Modeling with GENESIS

GENESIS is an object-oriented simulation system, in which a simulation is constructed of basic building blocks (GENESIS elements). These elements communicate by passing messages to each other, and each contains the knowledge of its own variables (fields) and the methods (actions) used to perform its calculations or other duties during a simulation. GENESIS elements are created as instantiations of a particular precompiled object type that acts as a template. Model neurons are constructed from these basic components, such as neural compartments and variable conductance ion channels, linked with messages. Neurons may be linked together with synaptic connections to form neural circuits and networks. This object-oriented approach is central to the generality and flexibility of the system, as it allows modelers to easily exchange and reuse models or model components. Many GENESIS users base their simulation scripts on the examples that are provided with GENESIS or in the GENESIS Neural Modeling Tutorials package (Beeman, 2005).

GENESIS uses an interpreter and a high-level simulation language to construct neurons and their networks. This use of an interpreter with pre-compiled object types, rather than a separate step to compile scripts into binary machine code, gives the advantage of allowing the user to interact with and modify a simulation while it is running, with no sacrifice in simulation speed. Commands may be issued either interactively to a command prompt, by use of simulation scripts, or through the graphical interface. The 268 scripting language commands and the 125 object types provided with GENESIS are powerful enough that only a few lines of script are needed to specify a sophisticated simulation. For example, the GENESIS "cell reader" allows one to build complex model neurons by reading their specifications from a data file.

GENESIS provides a variety of mechanisms to model calcium diffusion and calcium-dependent conductances, as well as synaptic plasticity. There are also a number of "device objects" that may be interfaced to a simulation to provide various types of input to the simulation (pulse and spike generators, voltage clamp cir-



1  
2  
3  
4 cuitry, etc.) or measurements (peristimulus and interspike interval histograms, spike frequency measurements,  
5 auto- and cross-correlation histograms, etc.). Object types are also provided for the modeling of biochemical  
6 pathways (Bhalla and Iyengar, 1999). A list and description of the GENESIS object types, with links to full doc-  
7 umentation, may be found in the *Objects* section of the hypertext GENESIS Reference Manual, downloadable  
8 or viewable from the GENESIS web site.  
9

### 10 11 **3.2.3 GENESIS Graphical User Interfaces** 12

13 Very large scale simulations are often run with no GUI, with the simulation output to either text or binary format  
14 files for later analysis. However, GENESIS is usually compiled to include its graphical interface XODUS,  
15 which provides object types and script-level commands for building elaborate graphical interfaces, such as the  
16 one shown in Fig. 8 for the dual exponential variation of the HH benchmark simulation (Benchmark 3 in  
17 Appendix 2). GENESIS also contains graphical environments for building and running simulations with no  
18 scripting, such as Neurokit (for single cells) and Kinetikit (for modeling biochemical reactions). These are  
19 themselves created as GENESIS scripts, and can be extended or modified. This allows for the creation of the  
20 many educational tutorials that are included with the GENESIS distribution (Bower and Beeman, 1998).  
21  
22

### 23 24 **3.2.4 Obtaining GENESIS and User Support** 25

26 GENESIS and its graphical front-end XODUS are written in C and are known to run under most Linux or  
27 UNIX-based systems with the X Window System, as well as Mac OS/X and MS Windows with the Cygwin  
28 environment. The current release of GENESIS and PGENESIS (ver. 2.3, March 17, 2006) is available from the  
29 GENESIS web site<sup>8</sup> under the GNU General Public License. The GENESIS source distribution contains full  
30 source code and documentation, as well as a large number of tutorial and example simulations. Documentation  
31 for these tutorials is included along with online GENESIS help files and the hypertext GENESIS Reference  
32 Manual. In addition to the source distribution, precompiled binary versions are available for Linux, Mac OS/X,  
33 and Windows with Cygwin. The GENESIS Neural Modeling Tutorials (Beeman, 2005) are a set of HTML  
34 tutorials intended to teach the process of constructing biologically realistic neural models with the GENESIS  
35 simulator, through the analysis and modification of provided example simulation scripts. The latest version of  
36 this package is offered as a separate download from the GENESIS web site.  
37  
38

39 Support for GENESIS is provided through email to [genesis@genesis-sim.org](mailto:genesis@genesis-sim.org), and through the GEN-  
40 ESIS Users Group, BABEL. Members of BABEL receive announcements and exchange information through  
41 a mailing list, and are entitled to access the BABEL web page. This serves as a repository for the latest con-  
42 tributions by GENESIS users and developers, and contains hypertext archives of postings from the mailing  
43 list.  
44

45 Rallpacks are a set of benchmarks for evaluating the speed and accuracy of neuronal simulators for the  
46 construction of single cell models (Bhalla, et al., 1992). However, it does not provide benchmarks for network  
47 models. The package contains scripts for both GENESIS and NEURON, as well as full specifications for  
48 implementation on other simulators. It is included within the GENESIS distribution, and is also available for  
49 download from the GENESIS web site.  
50  
51

### 52 53 **3.2.5 GENESIS Implementation of the HH Benchmark** 54

55 The HH benchmark network model (Benchmark 3 in Appendix 2) provides a good example of the type of model  
56 that should probably NOT be implemented with GENESIS. The Vogels and Abbott (2005) integrate-and-fire  
57 network on which it is based is an abstract model designed to study the propagation of signals under very  
58 simplified conditions. The identical excitatory and inhibitory neurons have no physical location in space, and  
59 no distance-dependent axonal propagation delays in the connections. The benchmark model simply replaces  
60 the IF neurons with single-compartment cells containing fast sodium and delayed rectifier potassium channels  
61

---

62 <sup>8</sup><http://www.genesis-sim.org/GENESIS>  
63  
64  
65

1  
2  
3  
4 that fire tonically and display no spike frequency adaptation. Such models offer no advantages over IF cells for  
5 the study of the situation explored by Vogels and Abbott.

6 Nevertheless, it is a simple matter to implement such a model in GENESIS, using a simplification of existing  
7 example scripts for large network models, and the performance penalty for “using a sledge hammer to crack a  
8 peanut” is not too large for a network of this size. The simulation script for this benchmark illustrates the power  
9 of the GENESIS scripting commands for creating networks. Three basic commands are used for filling a region  
10 with copies of prototype cells, making synaptic connections with a great deal of control over the connectivity,  
11 and setting propagation delays.  
12

13 The instantaneous rise in the synaptic conductances makes this a very efficient model to implement with  
14 a simulator specialized for IF networks, but such a non-biological conductance is not normally provided by  
15 GENESIS. Therefore, two implementations of the benchmark have been provided. The Dual Exponential VA  
16 HH Model script implements synaptic conductances with a dual exponential form having a 2 msec time-to-  
17 peak, and the specified exponential decay times of 5 msec for excitatory connections and 10 msec for inhibitory  
18 connections. The Instantaneous Conductance VA HH Model script uses a user-added *isynchan* object type that  
19 can be compiled and linked into GENESIS to provide the the specified conductances with an instantaneous rise  
20 time. There is little difference in the behavior of the two versions of the simulation, although the Instantaneous  
21 Conductance model executes somewhat faster.  
22

23  
24 Figure 8 shows the implementation of the Dual Exponential VA HH Model with a GUI that was created by  
25 making small changes to the example *RSnet.g*, *protodefs.g*, and *graphics.g* scripts, which are provided in the  
26 GENESIS Modeling Tutorial (Beeman, 2005) section *Creating Large Networks with GENESIS*.  
27

28 These scripts and the tutorial specify a rectangular grid of excitatory neurons. An exercise suggests adding  
29 an additional layer of inhibitory neurons. The GENESIS implementations of the HH benchmark use a layer  
30 of  $64 \times 50$  excitatory neurons and a layer of  $32 \times 25$  inhibitory neurons. A change of one line in the example  
31 *RSnet.g* script allows the change from the nearest-neighbor connectivity of the model to the required infinite-  
32 range connectivity with 2% probability.  
33

34 The identical excitatory and inhibitory neurons used in the network are implemented as specified in App. 2.  
35 For both versions of the model, Poisson-distributed random spike inputs with a mean frequency of 70 Hz were  
36 applied to the excitatory synapses of the all excitatory neurons. The the simulation was run for 0.05 sec, the  
37 random input was removed, and it was then run for an additional 4.95 sec.  
38

39 The Control Panel at the left is used to run the simulation and to set parameters such as maximal synaptic  
40 conductances, synaptic weight scaling, and propagation delays. There are options to provide current injection  
41 pulses, as well as random synaptic activation. The plots in the middle show the membrane potentials of three  
42 excitatory neurons (0, 1536, and 1567), and inhibitory neuron 0. The netview displays at the right show the  
43 membrane potentials of the excitatory neurons (top) and inhibitory neurons (bottom). With no propagation  
44 delays, the positions of the neurons on the grid are irrelevant. Nevertheless, this two-dimensional representation  
45 of the network layers makes it easy to visualize the number of cells firing at any time during the simulation.  
46

47 Figure 9 shows the plots for the membrane potential of the same neurons as those displayed in Fig. 8, but  
48 produced by the Instantaneous Conductance VA HH Model script. The plot at the right shows a zoom of the  
49 interval between 3.2 and 3.4 sec.  
50

51 In both figures, excitatory neuron 1536 has the lowest ratio of excitatory to inhibitory inputs of the four neu-  
52 rons plotted. It fires only rarely, whereas excitatory neuron 0, which has the highest ratio, fires most frequently.  
53

### 54 3.2.6 Future Plans for GENESIS

55  
56 The GENESIS simulator is now undergoing a major redevelopment effort, which will result in GENESIS 3. The  
57 core simulator functionality is being reimplemented in C++ using an improved scheme for messaging between  
58 GENESIS objects, and with a platform-independent and browser-friendly Java-based GUI. This will result in  
59 not only improved performance and portability to MS Windows and non-UNIX platforms, but will also allow  
60 the use of alternate script parsers and user interfaces, as well as the ability to communicate with other modeling  
61 programs and environments. The GENESIS development team is participating in the NeuroML (Goddard et  
62  
63  
64  
65

1  
2  
3  
4  
5  
6  
7  
8  
9  
10  
11  
12  
13  
14  
15  
16  
17  
18  
19  
20  
21  
22  
23  
24  
25  
26  
27  
28  
29  
30  
31  
32  
33  
34  
35  
36  
37  
38  
39  
40  
41  
42  
43  
44  
45  
46  
47  
48  
49  
50  
51  
52  
53  
54  
55  
56  
57  
58  
59  
60  
61  
62  
63  
64  
65

al., 2001; Crook et al., 2005) project<sup>9</sup>, along with the developers of NEURON. This will enable GENESIS 3 to export and import model descriptions in a common simulator-independent XML format. Development versions of GENESIS are available from the Sourceforge GENESIS development site<sup>10</sup>.

---

<sup>9</sup><http://www.neuroml.org>

<sup>10</sup><http://sourceforge.net/projects/genesis-sim>

### 3.3 NEST

#### 3.3.1 The NEST initiative

The problem of simulating neuronal networks of biologically realistic size and complexity has long been underestimated. This is reflected in the limited number of publications on suitable algorithms and data structures in high-level journals. The lack of awareness of researchers and funding agencies of the need for progress in simulation technology and sustainability of the investments may partially originate from the fact that a mathematically correct simulator for a particular neuronal network model can be implemented by an individual in a few days. However, this has routinely resulted in a cycle of unscalable and unmaintainable code being rewritten in unmaintainable fashion by novices, with little progress in the theoretical foundations.

Due to the increased availability of computational resources, simulation studies are becoming ever more ambitious and popular. Indeed, many neuroscientific questions are presently only accessible through simulation. An unfortunate consequence of this trend is that it is becoming ever harder to reproduce and verify the results of these studies. The ad hoc simulation tools of the past cannot provide us with the appropriate degree of comprehensibility. Instead we require carefully crafted, validated, documented and expressive neuronal network simulators with a wide user community. Moreover, the current progress towards more realistic models demands correspondingly more efficient simulations. This holds especially for the nascent field of studies on large-scale network models incorporating plasticity. This research is entirely infeasible without parallel simulators with excellent scaling properties, which is outside the scope of ad hoc solutions. Finally, to be useful to a wide scientific audience over a long time, simulators must be easy to maintain and to extend.

On the basis of these considerations, the NEST initiative was founded as a long term collaborative project to support the development of technology for neural systems simulations (Diesmann et al., 2002). The NEST simulation tool is the reference implementation of this initiative. The software is provided to the scientific community under an open source license through the NEST initiative's website<sup>11</sup>. The license requests researchers to give reference to the initiative in work derived from the original code and, more importantly, in scientific results obtained with the software. The website also provides references to material relevant to neuronal network simulations in general and is meant to become a scientific resource of network simulation information. Support is provided through the NEST website and a mailing list. At present NEST is used in teaching at international summer schools and in regular courses at the University of Freiburg.

#### 3.3.2 The NEST simulation tool

In the following we give a brief overview of the NEST simulation tool and its capabilities.

##### *Domain and design goals*

The domain of NEST is large neuronal networks with biologically realistic connectivity. The software easily copes with the threshold network size of  $10^5$  neurons (Morrison et al., 2005) at which each neuron can be supplied with the natural number of synapses and simultaneously a realistic sparse connectivity can be maintained. Typical neuron models in NEST have one or a small number of compartments. The simulator supports heterogeneity in neuron and synapse types. In networks of realistic connectivity the memory consumption and work load is dominated by the number of synapses. Therefore, much emphasis is placed on the efficient representation and update of synapses. In many applications network construction has the same computational costs as the integration of the dynamics. Consequently, NEST parallelizes both. NEST is designed to guarantee strict reproducibility: the same network is required to generate the same results independent of the number of machines participating in the simulation. It is considered an important principle of the project that the development work is carried out by neuroscientists operating on a joint code base. No developments are made without the code being directly tested in neuroscientific research projects. This implements an incremental and iterative development cycle. Extensibility and long-term maintainability are explicit design goals.

##### *Infrastructure*

---

<sup>11</sup><http://www.nest-initiative.org>

1  
2  
3  
4 The primary user interface is a simulation language interpreter which processes a rather high level expressive  
5 language with an extremely simple syntax which incorporates heterogeneous arrays, dictionaries, and pure (i.e.  
6 unnamed) functions and is thus suited for interactive work. There is no built-in graphical user interface as it  
7 would not be particularly helpful in NEST’s domain: network specification is procedural, and data analysis is  
8 generally performed off-line for reasons of convenience and efficiency. The simulation language is used for data  
9 pre- and post-processing, specification of parameters, and for the compact description of the network structure  
10 and the protocol of the virtual experiment. The neuron models and synapse types are not expressed in the  
11 simulation language as this would result in a slower performance. They are implemented as derived classes on  
12 the C++ level such that all models provide the same minimal functionality and are thus easily interchangeable  
13 on the simulation language level. A mechanism for error handling propagates errors messages through all levels  
14 of the software. Connections between nodes (i.e. neurons, generators and recording devices) are checked for  
15 consistency at the time of creation. User level documentation is provided in a browsable format (the “helpdesk”)  
16 and is generated directly from source code.

17  
18  
19 The code of NEST is modularized to facilitate the development of new neuron models that can be loaded at  
20 run time and to decouple the development of extensions from a specific NEST release. In the framework of the  
21 FACETS project a Python interface and a “facetsmodule” has been created. In addition to providing an interface  
22 between user-defined modules and the core code, NEST can interface with other software - for example, in order  
23 to provide a graphical user interface. The primary strategy used is interpreter-interpreter interaction, whereby  
24 each interpreter emits code that the other interpreter accepts as its native language. This approach minimizes  
25 the need to define protocols and the dependency of NEST on foreign libraries.

### 26 *Kernel*

27  
28  
29 There is a common perception that event-driven algorithms are exact and time-driven algorithms are approx-  
30 imate. We have recently shown that both parts of this perception are generally false; it depends on the dynamics  
31 of the neuron model whether an event-driven algorithm can find an exact solution, just as it does for time-driven  
32 algorithms (Morrison et al., 2006b). NEST is designed for large scale simulations where performance is a critical  
33 issue. We have therefore argued that when comparing different integration strategies, one should evaluate  
34 the efficiency, i.e. the simulation time required to achieve a given integration error, rather than the plain simu-  
35 lation time (Morrison et al., 2006b). This philosophy is reflected in the simulation kernel of NEST. Although it  
36 implements a globally time-driven algorithm with respect to the ordering of neuron updates and the delivery of  
37 events, spike times are not necessarily constrained to the discrete time grid. Neuron implementations treating  
38 incoming and outgoing spikes in continuous time are seamlessly integrated into the time-driven infrastructure  
39 with no need for a central event queue. This permits a great flexibility in the range of neuron models which  
40 can be represented, including exactly solvable continuous time neuron models, models requiring approximation  
41 techniques to locate threshold passing and models with grid-constrained dynamics and spike times.

42  
43  
44 The simulation kernel of NEST supports parallelization by multi-threading and message passing, which  
45 allows distribution of a simulation over multiple processors of an SMP machine or over multiple machines in a  
46 cluster. Communication overhead is minimized by only communicating in intervals of the minimum propaga-  
47 tion delay between neurons, and communication bulk is minimized by storing synapses on the machine where  
48 the post-synaptic neuron is located (Morrison et al., 2005). This results in supra-linear speed-up in distributed  
49 simulations; scaling in multi-threaded simulations is reasonable, but more research is required to understand and  
50 overcome present constraints. The user only needs to provide a serial script, as the distribution is performed  
51 automatically. Interactive usage of the simulator is presently only possible in purely multi-threaded operation.  
52 Reproducibility of results independent of the number of machines/processors is achieved by dividing a simula-  
53 tion task into a fixed number of abstract (virtual) processes which are distributed amongst the actual machines  
54 used (Morrison et al., 2005).

### 55 **3.3.3 Performance**

56  
57  
58  
59 The supplementary material contains simulation scripts for all of the benchmarks specified in Appendix 2.  
60 Considering the domain of NEST, the benchmarks can only demonstrate NEST’s capabilities in a limited way.  
61  
62  
63  
64  
65

1  
2  
3  
4 Therefore, a fifth benchmark is included which is not only significantly larger than the other benchmarks (three  
5 times as many neurons and forty times as many synapses), but also incorporates spike-timing dependent plas-  
6 ticity in its excitatory-excitatory synapses. The neuron model for this benchmark is the same as for benchmark  
7 2. All the benchmarks were simulated on a Sun Fire V40z equipped with four dual core AMD Opteron 875  
8 processors at 2.2 GHz and 32 Gbytes RAM running Ubuntu 6.06.1 LTS with kernel 2.6.15-26-amd64-server.  
9 Simulation jobs were bound to specific cores using the `taskset` command. The simulations were performed  
10 with a synaptic propagation delay of 0.1 ms and a computation time step of 0.1 ms unless otherwise stated.

11  
12 Fig. 10A shows the simulation time for one biological second of Benchmarks 1 – 3. To compare the bench-  
13 marks fairly despite their different firing rates, the spiking was suppressed in all three benchmarks by removing  
14 the initial stimulus, and in the case of Benchmark 2, the intrinsic firing was suppressed by setting the resting  
15 potential to be lower than the threshold. For networks of integrate-and-fire neurons of this size and activity, the  
16 delivery of spikes does not contribute significantly to the simulation times, which are dominated by the neu-  
17 ron updates. If the spiking is not suppressed, the simulation times for Benchmarks 1 and 2 are less than 10%  
18 longer. The simulation time for Benchmark 3 is about 15% longer because of the computational cost associated  
19 with the integration of the action potential. Benchmark 2 (current-based integrate-and-fire neuron model) is  
20 significantly faster than the other two as its linear subthreshold dynamics permits the use of exact integration  
21 techniques (see Rotter and Diesmann, 1999). The non-linear dynamics of the conductance based integrate-  
22 and-fire neuron model in Benchmark 1 and the Hodgkin-Huxley neuron in benchmark 3 are propagated by one  
23 global computation time step by one or more function calls to the standard adaptive time stepping method of  
24 the GNU Scientific Library (GSL; Galassi et al., 2001) with a required accuracy of  $1 \mu V$ . The ODE-solver  
25 used is the embedded Runge-Kutta-Fehlberg (4,5) provided by the GSL, but this is not a constraint of NEST  
26 - a neuron model may employ any method for propagating its dynamics. In a distributed simulation, processes  
27 must communicate in intervals of the minimum synaptic delay in order to preserve causality (Morrison et al.,  
28 2005). It is therefore more efficient to simulate with realistic synaptic delays than with unrealistically short  
29 delays, as can be seen in Fig. 10A. The simulation times for the benchmark networks incorporating a synaptic  
30 delay of 1.5 ms are in all cases significantly shorter than the simulation times for the networks if the synaptic  
31 delay is assumed to be 0.1 ms.

32  
33 Benchmark 4 (integrate-and-fire neuron model with voltage jump synapses) is ideal for an event-driven  
34 simulation, as all spike times can be calculated analytically - they occur either when an excitatory spike is  
35 received, or due to the relaxation of the membrane potential to the resting potential, which is above the threshold.  
36 Therefore the size of the time steps in which NEST updates the neuron dynamics plays no role in determining  
37 the accuracy of the simulation. The primary constraint on the step size is that it must be less than or equal to  
38 the minimum synaptic delay between the neurons in the network. Fig. 10B shows the simulation time for one  
39 biological second of Benchmark 4 on two processors as a function of the minimum synaptic delay. Clearly, the  
40 simulation time is strongly dependent on the minimum delay in this system. At a realistic value of 1 ms, the  
41 network simulation is approximately a factor of 1.3 slower than real time; at a delay of 0.125 ms the simulation  
42 is approximately 7.3 times slower than real time. In the case of neuron models where the synaptic time course is  
43 not invertible, the computational time step determines the accuracy of the calculation of the threshold crossing.  
44 For a discussion of this case and the relevant quantitative benchmarks, see Morrison et al. (2006b).

45  
46 Fig. 10C shows the scaling of an application which lies in the domain of neural systems for which NEST  
47 is primarily designed. The simulated network contains 11250 neurons, of which 9000 are excitatory and 2250  
48 inhibitory. Each neuron receives 900 inputs randomly chosen from the population of excitatory neurons and  
49 225 inputs randomly chosen from the inhibitory population. The scaling is shown for the case that all the  
50 synapses are static, and for the case that the excitatory-excitatory synapses implement multiplicative spike-  
51 timing dependent plasticity with an all-to-all spike pairing scheme (Rubin et al., 2001). For implementation  
52 details of the STDP, see Morrison et al. (2006a), for further network parameters, see the supplementary material.  
53 The network activity is in the asynchronous irregular regime at 10 Hz. Both applications scale supra-linearly  
54 due to the exploitation of fast cache memory. When using eight processors, the static network is a factor of 6.5  
55 slower than real time and the plastic network is a factor of 14 slower. Compared to Benchmark 2, the network  
56 contains 3 times as many neurons, 40 times as many synapses and the firing rate is increased by a factor of 2.  
57  
58  
59  
60  
61  
62  
63  
64  
65

1  
2  
3  
4  
5  
6  
7  
8  
9  
10  
11  
12  
13  
14  
15  
16  
17  
18  
19  
20  
21  
22  
23  
24  
25  
26  
27  
28  
29  
30  
31  
32  
33  
34  
35  
36  
37  
38  
39  
40  
41  
42  
43  
44  
45  
46  
47  
48  
49  
50  
51  
52  
53  
54  
55  
56  
57  
58  
59  
60  
61  
62  
63  
64  
65

However, using the same number of processors (2), the static network simulation is only a factor of 17 slower, and the plastic network simulation is only a factor of 32 slower. This demonstrates that NEST is capable of simulating large, high-connectivity networks with computationally expensive synaptic dynamics with a speed suitable for interactive work. Although for this network the presence of the STDP synapses increases the simulation time by a factor of two, this factor generally depends on the number of synapses and the activity.

### 3.3.4 Perspectives

Future work on NEST will focus on an interactive mode for distributed computing, an improvement of performance with respect to modern multi-core computer clusters, and a rigorous test and validation suite. Further information on NEST and the current release can be found at the NEST web site<sup>12</sup>.

---

<sup>12</sup><http://www.nest-initiative.org>

### 3.4 NCS

The NeoCortical Simulator (NCS), as its name suggests, is optimized to model the horizontally dispersed, vertically layered distribution of neurons characteristic of the mammalian neocortex. NCS development began in 1997, a time at which fascinating details of synaptic plasticity and connectivity were being discovered (Markram et al., 1997a, 1997b) yet available simulators such as GENESIS and NEURON did not offer parallel architectures nor the degree of neuronal compartmental simplification required for reasonable performance times. Also emerging at the time were inexpensive clusters-of-workstations, also known as Beowulf clusters, operating under the LINUX operating system. Following a 1997 neuroscience fellowship with Rodney Douglas and Kevan Martin at the Institute for Neuroinformatics in Zürich, Philip Goodman programmed the first NCS using Matlab in collaboration with Henry Markram (then at the Weizmann Institute, now at the Swiss EPFL) and Thomas McKenna, Neural Computation Program Officer at the U.S. Office of Naval Research. Preliminary results led to ONR funding (award N000140010420) in 1999, which facilitated the subsequent collaboration with UNR computer scientists Sushil Louis and Frederick Harris, Jr. This led to a C++ implementation of NCS using LINUX MPI on a Beowulf cluster. NCS was first made available to outside investigators beginning in 2000, with further development targeting the following specifications:

1. Compartments: sampling frequency and membrane compartmental realism sufficient to capture biological response properties, arbitrary voltage- and ion-sensitive channel behaviors, and multicompartmental models distributed in 3-D (dendritic, somatic, and axonal systems);
2. Synapses: short-term depression and facilitation (Markram et al., 1998a), augmentation (Wang et al., 2006) and Hebbian spike-timing dependent plasticity (Markram et al., 1997b);
3. 3-D Connectionism: a layout to easily allocate neurons into subnetwork groupings, layers, column, and sheets separated by real micron- or millimeter spacings, with realistic propagation distances and axonal conduction speeds;
4. Parallelism: an inherently parallel, efficient method of passing messages of synaptic events among neurons;
5. Reporting: an efficient way to collect, sample and analyze selected compartmental and neuronal behaviors;
6. Stimulation: ability to (a) specify fixed, standard neurophysiological stimulation protocols, (b) port signals from an external device, and (c) export neuronal responses and await subsequent replies from external systems (e.g., dynamic clamps, in vitro or in vivo preparations, robotic emulations);
7. Freeze/resume system state: the ability to stop a simulation and hibernate all hardware and software parameters into a binary blob, for unpacking and resuming in later experiments;
8. Command files: simplicity in generating and modifying scripts.

As of 2005, NCS developers achieved all the objectives above, using an ASCII file based command input file to define a hierarchy of reusable brain objects (Figure 11A). NCS uses a clock-based integrate and fire neurons whose compartments contain conductance-based synaptic dynamics and Hodgkin-Huxley formulations of ionic channel gating particles<sup>13</sup>. Although a user-specified active spike template is usually used for our large simulations, Hodgkin-Huxley channel equations can be specified for the rapid sodium and delayed rectifier spike behavior. No nonlinear simplifications, such as the Izhikevich formulation, are supported. Compartments are allocated in 3-D space, and are connected by forward and reverse conductances without detailed cable equations. Synapses are conductance-based, with phenomenological modeling of depression, facilitation, augmentation, and STDP.

---

<sup>13</sup><http://brain.unr.edu/publications/thesis.ecw01.pdf>



1  
2  
3  
4 NCS runs on any LINUX cluster. We run NCS on our 200-CPU hybrid of Pentium and AMD processors,  
5 and also on the 8,000-CPU Swiss EPFL IBM Blue Brain. NCS can run in single-PC mode under LINUX or  
6 LINUX emulation (e.g., Cygwin) and on the new Pentium-based Macintosh.

7  
8 Although NCS was motivated by the need to model the complexity of the neocortex and hippocampus,  
9 limbic and other structures can be modeled by variably collapsing layers and specifying the relevant 3-D layouts.  
10 Large-scale models often require repetitive patterns of interconnecting brain objects, which can be tedious using  
11 only the basic ASCII command file. We therefore developed a suite of efficient Python-based scripting tools  
12 called Brainlab (Drewes, 2005). An Internet-based library and control system was also developed (Waikul et  
13 al., 2002).

14  
15 NCS delivers reports on any fraction of neuronal cell groups, at any specified interval. Reports include  
16 membrane voltage (current clamp mode), current (voltage clamp), spike-event-only timings (event-triggered),  
17 calcium concentrations, synaptic dynamics parameter states, and any Hodgkin-Huxley channel parameter. Al-  
18 though NCS does not provide any direct visualization software, report files are straightforward to view in any  
19 graphics environment. Two such Matlab-based tools are available for download from the lab's web site<sup>14</sup>.

20  
21 Benchmark. We ran the Vogels and Abbot (2005) benchmark under the conditions specified for the conductance-  
22 based integrate and fire model (see Benchmark 1 in Appendix 2), and obtained the expected irregularly-bursting  
23 sustained pattern (first second shown in Figure 11B). At the default 10:1 ratio of inhibitory to excitatory synaptic  
24 conductances, the overall mean firing rate was 15.9 Hz.

25  
26 The largest simulations to-date have been on the order of a million single-compartment neurons using mem-  
27 brane AHP, M, A-type channels. Neurons were connected by 1 trillion synapses using short-term and STDP  
28 dynamics; this required about 30 minutes on 120 CPUs to simulate one biological second (Ripplinger et al.,  
29 2004). Intermediate-complexity simulations have examined multimodal sensory integration and information  
30 transfer<sup>15</sup>, and genetic algorithm search for parameter sets which support learning of visual patterns (Drewes  
31 et al., 2004). Detailed work included evaluation of interneuronal membrane channels (Maciokas et al., 2005)  
32 underlying the spectrum of observed firing behaviors (Gupta et al., 2000), and potential roles in speech recog-  
33 nition (Blake and Goodman, 2002) and neuropathology (Kellogg et al., 1999; Wills et al., 1999; Wiebers et al.,  
34 2003; Opitz and Goodman, 2005). Recent developments focus on IP port-based real time input-output of the  
35 "brain" to remotely behaving and learning robots<sup>16</sup>.

36  
37 The UNR Brain Computation Laboratory is presenting collaborating with the Brain Mind Institute of the  
38 Swiss EPFL. Their 8,000-CPU Blue Brain cluster<sup>17</sup> currently runs NCS alone or as in a hybrid configuration as  
39 an efficient synaptic messaging system with CPU-resident instances of NEURON. The Reno and Swiss teams  
40 are exploring ways to better calibrate simulated to living microcircuits, and to effect real-time robotic behaviors.  
41 Under continuing ONR support, the investigators and two graduate students provide part-time assistance to  
42 external users at no cost through e-mail and online documentation. User manual and programmer specifications  
43 with examples are available<sup>18</sup>.

44  
45  
46  
47  
48  
49  
50  
51  
52  
53  
54  
55  
56  
57  
58 <sup>14</sup><http://brain.unr.edu/publications/neuroplot.m>; <http://brain.unr.edu/publications/EVALCELLTRACINGS.zip>

59 <sup>15</sup><http://brain.unr.edu/publications/MaciokasDissertationfinal.zip>

60 <sup>16</sup>[http://brain.unr.edu/publications/jcm.hierarch\\_robotics.unr.ms.thesis03.pdf](http://brain.unr.edu/publications/jcm.hierarch_robotics.unr.ms.thesis03.pdf);  
61 <http://brain.unr.edu/publications/JGKingThesis.pdf> (Macera-Rios et al., 2004)

62 <sup>17</sup><http://bluebrainproject.epfl.ch>

63 <sup>18</sup><http://brain.unr.edu/ncsDocs>

## 3.5 CSIM

### 3.5.1 Feature overview

The *Circuit SIMulator* CSIM is a tool for

simulating heterogeneous networks composed of (spike emitting) point neurons. CSIM is intended to simulate networks containing a few neurons, up to networks with a few thousand neurons and on the order of 100000 synapses. It was written to do modeling at the network level in order to analyze the computational effects which can not be observed at the single cell level. To study single cell computations in detail we give the advice to use simulators like GENESIS or NEURON.

*Easy to use Matlab interface:* The core of CSIM is written in C++ which is controlled by means of Matlab (there is no standalone version of CSIM). We have chosen Matlab since it provides very powerful graphics and analysis capabilities and is a widely used programming language in the scientific community. Hence it is not necessary to learn yet another script language to set up and run simulations with CSIM. Furthermore the results of a simulation are directly returned as Matlab arrays and hence any plotting and analysis tools available in Matlab can easily be applied.

Until now CSIM does not provide a GUI. However one can easily use Matlab powerful GUI builder to make a GUI for a specific application based on CSIM.

*Object oriented design:* We adopted an object oriented design for CSIM which is similar to the approaches taken in GENESIS and NEURON. That is there are objects (e.g. a `LifNeuron` object implements the standard leaky-integrate-and-fire model) which are interconnected by means of well defined signal channels. The creation of objects, the connection of objects and the setting of parameters of the objects is controlled at the level of Matlab whereas the actual simulation is done in the C++ core.

*Fast C++ core:* Since CSIM is implemented in C++ and is not as general as e.g. GENESIS simulations are performed quite fast. We also implemented some ideas from event driven simulators which result in a considerable speedup (up to a factor of three for low firing rates; see the subsection about implementation aspects below).

*Runs on Windows and Linux (Unix):* CSIM is developed on Linux (Matlab 6.5 and 7.2, gcc 4.0.2). From the site `www.lsm.tugraz.at/csm` precompiled versions for Linux and Windows are available. Since CSIM is pure C++ it should not be hard to port it to other platforms for which Matlab is available.

*Different levels of modeling:* By providing different neuron models CSIM allows to investigate networks at different levels of abstraction: sigmoidal neurons with analog output, linear and non-linear leaky-integrate-and-fire neurons and compartmental based (point) neurons with spiking output. A broad range of synaptic models is also available for both spiking and non-spiking neuron models: starting from simple static synapses ranging over synapses with short-term plasticity to synapse models which implement different models for long-term plasticity.

### 3.5.2 Built-in models

*Neuron models:* CSIM provides two different classes of neurons: neurons with analog output and neurons with spiking output. Neurons with analog output are useful for analyzing population responses in larger circuits. For example CSIM provides a sigmoidal neuron with leaky integration. However, there are much more different objects available to build models of spiking neurons:

- Standard (linear) leaky-integrate-and-fire neurons
- Non-linear leaky-integrate-and-fire neurons based on the models of Izhikevich
- Conductance based point neurons with and without a spike template. There are general conductance based neurons where the user can insert any number of available ion-channel models to build the neuron model. On the other hand there is a rich set of predefined point neurons available used in several studies.

1  
2  
3  
4 *Spiking Synapses:* As for the neurons CSIM also implements synapses which transmit analog values and  
5 spike transmitting synapses. Two types of synapses are implemented: static and dynamic synapses. While  
6 for static synapses the amplitude of each postsynaptic response (current or conductance change) is the same,  
7 the amplitude of an postsynaptic response in the case of a dynamic synapse depends on the spike train that it  
8 has seen so far, i.e. dynamic synapses implement a form of short term plasticity (depression, facilitation). For  
9 synapses transmitting spikes the time course of a postsynaptic response is modeled by  $A \times \exp(-t/\tau_{syn})$ , where  
10  $\tau_{syn}$  is the synaptic time constant and  $A$  is the synaptic strength which is constant for static synapses and given  
11 by the model described in (Markram et al., 1998b) for dynamic synapses.  
12

13 Note that static as well as dynamic synapses are available as current supplying or conductance based models.

14 *Analog Synapses:* For synapses transmitting analog values, such as the output of a sigmoidal neuron, static  
15 synapses are simply defined by their strength (weight), whereas for dynamic synapses we implemented a con-  
16 tinuous version of the dynamic synapse model for spiking neurons (Tsodyks et al. 1998).  
17

18 *Synaptic plasticity:* CSIM also supports spike time dependent plasticity, STDP, applying a similar model  
19 as in (Song et al., 2000). STDP can be modeled most easily by making the assumption that each pre- and  
20 postsynaptic spike pair contributes to synaptic modification independently and in a similar manner. Depending  
21 on the time difference  $\Delta t = t_{pre} - t_{post}$  between pre- and postsynaptic spike the absolute synaptic strength is  
22 changed by an amount  $L(\Delta t)$ . The typical shape for the function  $L(\Delta t)$  as found for synapses in neocortex layer  
23 5 (Markram et al., 1997) is implemented. Synaptic strengthening and weakening are subject to constraints so  
24 that the synaptic strength does not go below zero or above a certain maximum value. Furthermore additional  
25 variants as suggested in (Froemke and Dan, 2002) and (Gütig et al. 2003) are also implemented.  
26  
27  
28

### 29 3.5.3 Implementation aspects

30  
31 *Network input and output:* There are two forms of inputs which can be supplied to the simulated neural mi-  
32 crocircuit: spike trains and analog signals. To record the output of the simulated model special objects called  
33 Recorder are used. A recorder can be connected to any object to record any field of that object.  
34

35 *Simulation Strategy:* CSIM employees a clock based simulation strategy with a fixed simulation step width  
36  $dt$ . Typically the exponential Euler integration method is used. A spike which occurs during a simulation time  
37 step is assumed to occur at the end of that time step. That implies that spikes can only occur at multiples of  $dt$ .  
38

39 *Efficient processing of spikes:* In a typical simulation of a neural circuit based on simple neuron models  
40 the CPU time spent in advancing *all* the synapses may be larger then the time needed to integrate the neuron  
41 equations. However if one considers the fact that synapses are actually “idle” most of the time (at least in low  
42 firing rate scenarios) it makes sense to update during one time step only those synapses whose postsynaptic  
43 response is not zero, i.e. are active. CSIM implements this idea by dividing synapses into a list of idle and a  
44 list of active synapses where only the latter is updated during a simulation time step. A synapse becomes active  
45 (i.e. is moved from the idle list to the active list) if a spike arrives. After its postsynaptic response has vanished  
46 the synapse becomes idle again (i.e. is moved back from the active list to the idle list). This trick can result in  
47 considerable speed up for low firing rate scenarios.  
48  
49

### 50 3.5.4 Further information

51  
52 CSIM ins distributed under the GNU General Public License and is available for download<sup>19</sup>. Support for CSIM  
53 (and its related tools) can be obtained by writing email to [lsm@igi.tu-graz.ac.at](mailto:lsm@igi.tu-graz.ac.at)

54 At the site <http://www.lsm.tugraz.at> one can find besides the download area for CSIM (including the  
55 user manual and an object reference manual) a list of publications which used CSIM (and its related tools) and  
56 also the code of published models.  
57

58 *Related tools:* Furthermore the site <http://www.lsm.tugraz.at> provides two sets of Matlab scripts and  
59 objects which heavily build on CSIM. The *circuit tool* supports the construction of multi-column circuits by  
60 providing functionality to connect pools of neurons to pools of neurons. The *learning tool* was developed  
61

---

62 <sup>19</sup><http://www.lsm.tugraz.at/csim>  
63  
64  
65

1  
2  
3  
4 to analyze neural circuits in the spirit of the liquid state machine (LSM) approach (Maass et al., 2002) and  
5 therefore contains several machine learning methods (see (Natschläger et al., 2003) for more information about  
6 this tools).

7 As of this writing resources are devoted to develop a parallel version of CSIM called PCSIM which al-  
8 lows distributed simulation of large scale networks. PCSIM will have a python interface which allows an  
9 easy implementation of the upcoming PyNN application programming interface (see appendix 1). The current  
10 development version of PCSIM can be obtained from the SourceForge site<sup>20</sup>.

### 13 3.5.5 CSIM implementations of the benchmark simulations

15 We implemented the benchmark networks 1 to 3 as specified in Appendix 2.

16 The integrate-and-fire benchmark networks (Benchmark 1 and 2) are well suited to be simulated with CSIM  
17 and can be implemented by only using built-in objects: CbNeuron and StaticSpikingCbSynapse as the  
18 neuron and synapse model for the COBA network and LifNeuron and StaticSpikingSynapse as neuron  
19 and synapse model for the CUBA network.

20 To implement Benchmark 3 (HH network) it is necessary to add the desired channel dynamics to CSIM by  
21 implementing it at the C++ level. The user defined neuron model (TraubsHHNeuron) is easily implemented  
22 in C++ (see the files `traubs_hh_channels.[cpp|h]` and `TraubsHHNeuron.[cpp|h]`). After these files are  
23 compiled and linked to CSIM they are available for use in the simulation. We refer the user to the CSIM manual  
24 for details on how to add user defined models at C++ level to CSIM.

25 For each benchmark network we provide two implementations: the first implementation uses the plain  
26 CSIM interface only while the second implementation makes use of the *circuit tool* mentioned in the previous  
27 subsection (filename suffix `*_circuit.m`).

28 To provide the initial stimulation during the first 50 ms of the simulation we set up a pool of input neurons  
29 (SpikingInputNeuron objects) which provide random spikes to the network.

30 Results of CSIM simulations of all implemented benchmarks are depicted in Figure 12. This figures were  
31 produced by the simulation scripts provided for each benchmark using Matlab's powerful graphics capabilities  
32 (see the file `make_figures.m`) and illustrate the sustained irregular activity described by Vogels and Abbott  
33 (2005) for such networks.

34 The current development version of PCSIM has been used to perform scalability tests based on the CUBA  
35 benchmark (Benchmark 2). The results are summarized in Figure 13. For the small 4000 neuron network the  
36 speedup for more than four machines vanishes while for the larger networks a more than expected speedup  
37 occurs up to six machines. This shows that PCSIM is scalable with regard to the problem size and the number  
38 of available machines. The development version of PCSIM together with the python script for the CUBA  
39 benchmark can be obtained from the SourceForge site<sup>21</sup>.

---

40  
41  
42  
43  
44  
45  
46  
47  
48  
49  
50  
51  
52  
53  
54  
55  
56  
57  
58  
59  
60  
61  
62 <sup>20</sup><http://sourceforge.net/projects/pcsim>

63 <sup>21</sup><http://sourceforge.net/projects/pcsim>

### 3.6 XPPAUT

*XPPAUT* is a general numerical tool for simulating, animating, and analyzing dynamical systems. These can range from discrete finite state models (McCulloch-Pitts) to stochastic Markov models, to discretization of partial differential and integrodifferential equations. *XPPAUT* was not specifically developed for neural simulations but because of its ability to provide a complete numerical analysis of the dependence of solutions on parameters (“bifurcation diagrams”) it is widely used by the community of computational and theoretical neuroscientists. There are many online tutorials many of which are geared to neuroscience. While it can be used for modest sized networks, it is not specifically designed for this purpose and due to its history, there are limits on the size of problems which can be solved (about 2000 differential equations is the current limit). The benchmarks were not performed due to this limitation in size, however, a reduced version is included. Rather than a pure simulator, *XPPAUT* is a tool for understanding the equations and the results of simulating the equations. *XPPAUT* uses a highly optimized parser to produce a pseudocode which is interpreted and runs very fast – at about half the speed of directly compiled code. Since no compiler is required, *XPPAUT* is a stand alone program and runs on all platforms which have an X-windows interface available (UNIX, MAC OSX, Windows, etc.) The program is open source and available as source and various binary versions.

*XPPAUT* can be run interactively (the preferred method) but can also be run in batch mode with no GUI with the results dumped to one or more files. Graphical output in postscript, GIF, PBM, and animated GIF is possible. (There are codecs available for AVI format but these are not generally included in the compiled versions.) Numerous packages for controlling *XPPAUT* have been written, some stand-alone such as JigCell and others using Matlab or PERL. Data from simulations can be saved for other types of analysis and or plotting with other packages. The “state” of the program can be saved as well so that users can come back where they let off.

There are no limits as far as the form of the equations is concerned since the actual equations that you desire to solve are written down like you would write them in a paper. For example the voltage equation for a conductance-based model would be written as:

$$dv/dt = (-g_l*(v-e_l) - g_{na}*m^3*h*(v-e_{na})-g_k*n^4*(v-e_k))/cm$$

There is a method for writing indexed networks as well, so that one does not have to write every equation. Special operators exist for speeding up network functions like discrete convolutions and implementation of the stochastic Gillespie algorithm. Furthermore, the user can link the right-hand sides of differential equations to external C libraries to solve complex equations (for example, equation-free firing rate models, Laing JCNS 2006). Because it is a general purpose solver, the user can mix different types of equations for example stochastic discrete time events with continuous ODEs. Event driven simulations are also possible and can be performed in such a way that output occurs only when an event happens. There are many ways to display the results of simulations including color-coded plots showing space-time behavior, a built-in animation language, and one- two- and three-dimensional phase-space plots.

*XPPAUT* provides a variety of numerical methods for solving differential equations, stochastic systems, delay equations, Volterra integral equations, and boundary-value problems (BVP). The numerical integrators are very robust and vary from the simple Euler method to the standard method for solving stiff differential equations, CVODE. The latter allows the user to specify whether the system is banded and thus can improve calculation speed by up to two orders of magnitude. The use of BVP solvers is rare in neuroscience applications but they can be used to solve, for example, the steady-state behavior of Fokker-Planck equations for noisy neurons and to find the speed of traveling waves in spatially distributed models.

Tools for analysis dynamical properties such as equilibria, basins of attraction, Lyapunov exponents, Poincare maps, embedding, and temporal averaging are all available via menus. Some statistical analysis of simulations is possible such as power spectra, mean and variance, correlation analysis and histograms are also included in the package. There is a very robust parameter fitting algorithm (Marquardt-Levenburg) which allows the user to find parameters and initial conditions which best approximate specified data.

One part of *XPPAUT* which makes it very popular is the inclusion of the continuation package, AUTO. This package allows the user to track equilibria, limit cycles, and solutions to boundary-value problems as

1  
2  
3  
4  
5  
6  
7  
8  
9  
10  
11  
12  
13  
14  
15  
16  
17  
18  
19  
20  
21  
22  
23  
24  
25  
26  
27  
28  
29  
30  
31  
32  
33  
34  
35  
36  
37  
38  
39  
40  
41  
42  
43  
44  
45  
46  
47  
48  
49  
50  
51  
52  
53  
54  
55  
56  
57  
58  
59  
60  
61  
62  
63  
64  
65

parameters vary. The stability of the solutions is irrelevant so that users can track the entire qualitative behavior of a differential equation. *XPPAUT* provides a simple to use GUI for AUTO which allows the user to seamlessly switch back and forth between simulation and analysis.

*XPPAUT* is used in many different courses and workshops including the Methods in Computational Neuroscience course at the Marine Biological Laboratory (where it was developed 15 years ago), various European CNS courses as well as in classroom settings. Since equations are written for the software as you would write them on paper, it is easy to teach students how to use *XPPAUT* for their own problems. There are many features for the qualitative analysis of differential equations such as direction fields, nullclines and color coding of solutions by some property (such as energy or speed).

*XPPAUT* can be considered a stable mature package. It is developed and maintained by the author. While a list of users is not maintained, a recent Google search revealed 38500 hits and a search on Google Scholar showed over 250 papers citing the software. In the future, the parser will be rewritten so that there will be no limit to the number of equations and methods for implementing large spatially distributed systems will also be incorporated. Parts of the analysis code in *XPPAUT* may possible be included in NEURON in the near future. A book has been written on the use of the program (Ermentrout, 2004) and it comes with 120 pages of documentation and dozens of examples.

## 3.7 SPLIT

### 3.7.1 Parallel simulators

The development of parallel simulation in computational neuroscience has been relatively slow. Today there are a few publicly available parallel simulators, but they are far from as general, flexible, and documented as commonly used serial simulators such as Neuron (Hines and Carnevale, 1997) and Genesis (Bower and Beeman, 1998). For Genesis there is PGENESIS and the development of a parallel version of Neuron has started. In addition there exists simulators like NCS<sup>22</sup> (see Frye, 2005), NEST (Morrison et al., 2005), and our own parallelizing simulator SPLIT (Hammarlund and Ekeberg, 1998). However, they are in many ways still on the experimental and developmental stage.

### 3.7.2 The simulator

SPLIT is a tool specialized for efficiently simulating large-scale multicompartmental models based on Hodgkin-Huxley formalism. It should be regarded as experimental software for demonstrating the possibility and usefulness of very large scale biophysically detailed neuronal network simulations. Recently, this tool was used for one of the largest cortex simulations ever performed (Djurfeldt et al., 2005). It supports massive parallelism on cluster computers using MPI. The model is specified by a C++ program written by the SPLIT user. This program is then linked with the SPLIT library to obtain the simulator executable. Currently, there is no supported graphical interface, although an experimental Java/QT-based graphical interface has been developed. There is no built-in support for analysis of results. Rather, SPLIT should be regarded as a pure, generic, neural simulation kernel with the user program adapting it into a simulator specific to a certain model. Although this approach is in some sense “raw”, this means that the model specification benefits from the full power of a general purpose programming language.

SPLIT provides conductance-based synaptic interactions with short-term plasticity (facilitation and depression). Long-term plasticity (such as STDP) and integrate-and-fire formalism have not yet been implemented, although this is planned for the future.

The user program specifies the model through the SPLIT API which is provided by the class `split`. The user program is serial and parallelism is hidden from the user. The program can be linked with either a serial or parallel version of SPLIT. In the parallel case, some or all parts of the program run in a master node on the cluster while SPLIT internally sets up parallel execution on a set of slave nodes. As an option, parts of the user program can execute distributed onto each slave via a callback interface. However, SPLIT provides a set of tools which ensures that also such distributed code can be written without explicit reference to parallelism.

The SPLIT API provides methods to dynamically inject spikes to an arbitrary subset of cells during a simulation. Results of a simulation are logged to file. Most state variables can be logged. This data can be collected into one file at the master node or written down at each slave node. In the latter case, a separate program might be used to collect the files at each node after the simulation terminates.

### 3.7.3 Large scale simulations

Recently, Djurfeldt et al., 2005 have described an effort to optimize SPLIT for the Blue Gene/L supercomputer. BG/L (Gara et al., 2005) represents a new breed of cluster computers where the number of processors, instead of the computational performance of individual processors, is the key to higher total performance. By using a lower clock frequency, the amount of heat generated decreases dramatically. Therefore, CPU chips can be mounted more densely and need less cooling equipment. A node in the BG/L cluster is a true “system on a chip” with two processor cores, 512 MiB of on chip memory and integrated network logic. A BG/L system can contain up to 65536 processing nodes.

During this work, simulations of a neuronal network model of layers II/III of the neocortex were performed using conductance-based multicompartmental model neurons based on Hodgkin-Huxley formalism. These

---

<sup>22</sup><http://brain.cse.unr.edu/ncsdocs>

1  
2  
3  
4 simulations comprised up to 8 million neurons and 4 billion synapses. After a series of optimization steps, per-  
5 formance measurements showed linear scaling behavior both on the Blue Gene/L supercomputer (see Figure 1)  
6 and on a more conventional cluster computer. Optimizations included parallelization of model setup and do-  
7 main decomposition of connectivity meta data. Computation time was dominated by the synapses which allows  
8 for a “free” increase of cell model complexity. Furthermore, communication time was hidden by computation.  
9

### 10 11 **3.7.4 Implementation aspects**

12  
13 SPLIT has so far been used to model neocortical networks (Fransén and Lansner, 1998; Lundqvist et al., 2006),  
14 the Lamprey spinal cord (Kozlov et al., 2003; 2006) and the olfactory cortex (Sandström et al., 2006).

15 The library exploits data locality for better cache-based performance. In order to gain performance on vector  
16 architectures, state variables are stored as sequences. It uses techniques such as adjacency lists for compact  
17 representation of projections and AER (Address Event Representation; Bailey and Hammerstrom, 1988) for  
18 efficient communication of spike events.  
19

20 Perhaps the most interesting concept in SPLIT is its asynchronous design: On a parallel architecture, each  
21 slave process has its own simulation clock which runs asynchronously with other slaves. Any pair of slaves  
22 only need to communicate at intervals determined by the smallest axonal delay in connections crossing from  
23 one slave to the other.  
24

25 The neurons in the model can be distributed arbitrarily over the set of slaves. This gives great freedom in  
26 optimizing communication so that densely connected neurons reside on the same CPU and so that axonal delays  
27 between neurons simulated on different slaves are maximized. The asynchronous design, where a slave process  
28 does not need to communicate with all other slaves at each time step, gives two benefits: 1. By communicating  
29 more seldom, the communication overhead is reduced. 2. By allowing slave processes to run out of phase, to a  
30 degree determined by the mutually smallest axonal delay, the waiting time for communication is decreased.  
31  
32

### 33 **3.7.5 Benchmark**

34  
35 The SPLIT implementation of the HH benchmark (Benchmark 3 in Appendix 2) consists of a C++ program  
36 which specifies what entities are to be part of the simulation (cell populations, projections, noise-generators,  
37 plots), makes a call which distributes these objects onto the cluster slaves (in the parallel case), sets the param-  
38 eters of the simulation objects, initializes, and simulates. While writing the code, close attention needs to be  
39 paid to which parameters are scalar and which are vectorized over the sets of cells or axons. Channel equations  
40 are pre-compiled into the library, and a choice of which set of equations to use needs to be made. Parameters  
41 are specified using SI units.  
42  
43

44 The Benchmark 3 simulation (4000 cells, 5 s of simulated time) took 386 s on a 2 GHz Pentium M machine  
45 (Dell D810). Outputs are written in files on disk and can easily be displayed using `gnuplot`. Figure 17 shows  
46 a raster of spiking activity in 100 cells during the first second of activity. Figure 18 shows membrane potential  
47 traces of 3 of the cells during 5 s (left) and 100 ms (right).  
48  
49

### 50 **3.7.6 Future plans**

51 Ongoing and possible future developments of SPLIT include:

- 52
- 53
- 54 • a revision of the simulation kernel API
- 55
- 56 • the addition of a Python interpreter interface
- 57
- 58 • compatibility with channel models used in popular simulators such as Neuron and Genesis, enabling easy
- 59 transfer of neuron models
- 60
- 61 • gap junctions
- 62
- 63 • graded transmitter release
- 64
- 65



1  
2  
3  
4  
5  
6  
7  
8  
9  
10  
11  
12  
13  
14  
15  
16  
17  
18  
19  
20  
21  
22  
23  
24  
25  
26  
27  
28  
29  
30  
31  
32  
33  
34  
35  
36  
37  
38  
39  
40  
41  
42  
43  
44  
45  
46  
47  
48  
49  
50  
51  
52  
53  
54  
55  
56  
57  
58  
59  
60  
61  
62  
63  
64  
65

- better documentation and examples

Currently, SPLIT is developed, in part time, by two people. There exists some limited documentation and e-mail support.

## 3.8 Mvaspike

### 3.8.1 Modelling with events

It has been argued many times that action potentials as produced by many types of neurones can be considered as *events*: they consist of stereotypical impulses that appear superimposed on the internal voltage dynamics of the neurons. As a result, many models of neurons offer ways of defining event times associated with each emitted action potential, often through the definition of a firing threshold<sup>23</sup>. Neural simulation tools have taken advantage of this for a long time, through the use of *event driven algorithms* (see section 1). Indeed, when one speaks of *events* in the context of simulation of neural networks, *event-driven* algorithms come to mind and it is the author's impression that the use of events upstream, during the modeling stage, is often understated.

Mvaspike was designed as an event-based modeling and simulation framework. It is grounded on a well established set-theoretic modeling approach (DEVS: Discrete Event system Specification (Zeigler and Vahie, 1993; Zeigler et al., 2000)). Target models are discrete event systems: their dynamics can be described by changes of state variables at arbitrary moments in time<sup>24</sup>. One aspect of Mvaspike is to bridge the gap between the more familiar expression of continuous dynamics, generally in use in the neuroscience community, and the event-centric use of models in the simulator (see figure 19). This is conveniently easy for many simple models that represent the models of choice in Mvaspike (mostly integrate-and-fire or phase models, and SRMs). Watts (1994) already noted that many neuronal properties can be explicitly and easily represented in discrete event systems. Think of absolute refractory *periods*, rising *time* of PSPs, axonal propagation *delays*, these are notions directly related to time intervals (and therefore, events) that are useful to describe many aspects of the neuronal dynamics. This being obviously quite far from the well established, more electro-physiologically correct conductance based models, another aim of Mvaspike is therefore to take into account as much as possible of these more complex models, through the explicit support of discrete-time events, and, possibly, state space discretization for the integration of continuous or hybrid dynamics.

The DEVS formalism makes also possible the modeling of large, hierarchical or modular systems (e.g. networks of coupled populations of neurons, or micro-circuits, cortical columns etc.), through a well-defined coupling and composition system. This helps modeling large and complex networks, but also favors code reusability, prototyping, and the use of different levels of modeling. Additional tools have been implemented in Mvaspike to take into account e.g. synaptic or axonal propagation delays, the description of structured or randomly connected networks in an efficient way, through the use of generic iterators to describe the connectivity (Rochel and Martinez, 2003).

### 3.8.2 The simulator

The core simulation engine in Mvaspike is event-driven, meaning that it is aimed at simulating networks of neurons where event-times can be computed efficiently. Firing times will then be calculated exactly (in fact, to the precision of the machine). This does not mean however that it is restricted to models that offer analytical expressions of the firing times, as numerical approximations can be used in many situations.

Mvaspike consists of a core C++ library, implementing a few generic classes to describe networks, neurons and additional input/output systems. It has been designed to be easy to access from other programming languages (high level or scripting languages, e.g. Python) and extensible. Well established simulation algorithms are provided, based on state of the art priority queue data structures. They have been found to be sufficiently efficient on average; however, the object-oriented approach has been designed to permit the use of dedicated, optimized sub-simulators when possible.

On top of the core engine lies a library that includes a few common models of neurons, including linear or quadratic integrate-and-fire (or SRM) neurons, with Dirac synaptic interactions, or various forms of piecewise

---

<sup>23</sup>The firing threshold here has to be taken in a very broad sense, from a simple spike detection threshold in a continuous model (e.g. Hodgkin-Huxley) to an active threshold that is used in the mathematical expression of the dynamics (integrate-and-fire model)

<sup>24</sup>as opposed to discrete time systems, in which state changes occur periodically, and continuous systems where state changes occur continuously.

1  
2  
3  
4 linear and exponential PSPs. Other available ingredients include plasticity mechanisms (STDP), refractory  
5 periods, input spike trains generation (Poisson). Some connectivity patterns (e.g. all-to-all, ring, etc) are also  
6 included.

7 There is no graphical user interface, nor pre- and post-processing tools included, as these are elements of  
8 the modeling and simulation work-flow that we believe to be easy to handle using third-party environments or  
9 high level languages, tailored to the needs and habits of the user.

### 12 **3.8.3 Benchmarks**

14 The simplest model available in Mvaspike corresponds to the one defined for Benchmark 4 (see Appendix 2).  
15 A straightforward implementation of the corresponding network can be done using only available objects from  
16 the library.

17 The typical output of a Mvaspike simulation is a list of events, corresponding e.g. to spikes emitted (or  
18 received) by the neurons. In particular, the membrane potential is not available directly. In order to obtain  
19 the voltage trace presented in figure 20, a simple post-processing stage was necessary in order to obtain values  
20 for the membrane potential at different instants between the event times. To this aim, the differential equation  
21 governing the dynamics between events is used (in a integrated form), together with the values already available  
22 at each event times, to find new intermediary values. Here, this is as simple as computing the effect of the leak  
23 (exponential) and the refractory period. As this only has to be done between events, each neuron can be treated  
24 independently of the others. In a sense, this illustrates how the hybrid formalism (as presented in section 1.1)  
25 is handled in Mvaspike: the flow of discrete events is the main point of interest, continuous dynamics come  
26 second.  
27  
28  
29

### 31 **3.8.4 Current status and further perspectives**

33 Mvaspike is currently usable for the modeling of medium to large scale networks of spiking neurons. It is  
34 released under the GPL license, maintained and supported by its main author and various contributors.

35 It has been used to model networks of integrate-and-fire neurons, for e.g. modeling the early stages of the  
36 visual system (see eg. Hugues et al., 2002; Wohrer et al., 2006), and more theoretical research on computing  
37 paradigms offered by spiking neurons (for instance, Rochel and Cohen, 2005; Rochel and Vieville, 2006). A  
38 partial parallel implementation was developed and successfully tested on small clusters of PCs and parallel  
39 machines (16 processors max), and should be completed to take into account all aspects of the framework and  
40 more ambitious hardware platforms.  
41

42 Work is ongoing to improve the interface of the simulator regarding input and output data formatting,  
43 through the use of structured data language (XML). While a proof-of-concept XML extension has already been  
44 developed, this is not a trivial task, and further work is needed in the context of existing initiatives (such as  
45 NeuroML).  
46

47 Meanwhile, it is expected that the range of models available to the user will be extended, for instance  
48 through the inclusion of models of stochastic point processes, and generic implementation of state space dis-  
49 cretization methods.  
50  
51  
52  
53  
54  
55  
56  
57  
58  
59  
60  
61  
62  
63  
64  
65

1  
2  
3  
4  
5  
6  
7  
8  
9  
10  
11  
12  
13  
14  
15  
16  
17  
18  
19  
20  
21  
22  
23  
24  
25  
26  
27  
28  
29  
30  
31  
32  
33  
34  
35  
36  
37  
38  
39  
40  
41  
42  
43  
44  
45  
46  
47  
48  
49  
50  
51  
52  
53  
54  
55  
56  
57  
58  
59  
60  
61  
62  
63  
64  
65

## 4 Discussion

We have presented here an overview of different strategies and algorithms for simulating spiking neural networks, as well as an overview of most of the presently available simulation environment to implement such simulations. We also have conceived a set of benchmark simulations of spiking neural networks (Appendix 2) and provide as supplementary material (linked to ModelDB) the codes for implementing the benchmarks in the different simulators. We believe this should constitute a very useful resource, especially for new researchers in the field of computational neuroscience.

We voluntarily did not approach the difficult problem of simulation speed and comparison of different simulators in this respect. Evidently, each simulation environment is optimal for a given problem, as discussed in Section 3 for each specific case. It is interesting to note that the different simulation environments are obviously able to simulate the same models, but unfortunately the codes are not compatible with each-other. This underlines the need for a more transparent communication channel between simulators. Related to this, the present efforts with simulator-independent codes (such as NeuroML, see Appendix 1) constitutes the main advance for a future inter-operability. We illustrated here that, using a Python-based interface, one of the benchmarks can be run in either NEURON or NEST using the same code (see Fig. 24 and Appendix 1).

Thus, future work should focus on obtaining a full compatibility between simulation environments and XML-based specifications. Importing and exporting XML should enable to convert simulation codes between simulators, and thereby provide very efficient means of combining existing models. A second direction for future investigations is to adapt simulation environments to current hardware constraints, such as parallel computations on clusters. Finally, more work is also needed to clarify the differences between simulation strategies and integration algorithms, which may considerably differ for cases where the timing of spikes is important (Fig. 4).

## Acknowledgments

Research supported by the European Community (FACETS project, IST 15879), NIH (NS11613), CNRS and HFSP. We are also grateful for the feedback and suggestions from users that have led to improvements of the simulators reviewed here.

## Appendix 1: Simulator-independent model specification

As we have seen, there are many freely-available, open-source and well-documented tools for simulation of networks of spiking neurons. There is considerable overlap in the classes of network that each is able to simulate, but each strikes a different balance between efficiency, flexibility, scalability and user-friendliness, and the different simulators encompass a range of simulation strategies. This makes the choice of which tool to use for a particular project a difficult one. Moreover, we argue that using just one simulator is an undesirable state of affairs. This follows from the general principle that scientific results must be reproducible, and that any given instrument may have flaws or introduce a systematic bias. The simulators described here are complex software packages, and may have hidden bugs or unexamined assumptions that may only be apparent in particular circumstances. Therefore it is desirable that any given model should be simulated using at least two different simulators and the results cross-checked.

This is, however, more easily said than done. The configuration files, scripting languages or graphical interfaces used for specifying model structure are very different for the different simulators, and this, together with subtle differences in the implementation of conceptually-identical ideas, makes the conversion of a model from one simulation environment to another an extremely non-trivial task; as such it is rarely undertaken.

We believe that the field of computational neuroscience has much to gain from the ability to easily simulate a model with multiple simulators. First, it would greatly reduce implementation-dependent bugs, and possible subtle systematic biases due to use of an inappropriate simulation strategy. Second, it would facilitate communication between investigators and reduce the current segregation into simulator-specific communities; this, coupled with a willingness to publish actual simulation code in addition to a model description, would perhaps lead to reduced fragmentation of research effort and an increased tendency to build on existing models rather than redevelop them *de novo*. Third, it would lead to a general improvement in simulator technology since bugs could be more easily identified, benchmarking greatly simplified, and hence best-practice more rapidly propagated.

This goal of simulator independent model specification is some way off, but some small steps have been taken. There are two possible approaches (which will probably prove to be complementary) to developing simulator-independent model specification, which mirror the two approaches taken to model specification by individual simulators: declarative and programmatic. Declarative model specification is exemplified by the use of configuration files, as used for example by NCS. Here there is a fixed library of neuron models, synapse types, plasticity mechanisms, connectivity patterns, etc., and a particular model is specified by choosing from this library. This has the advantages of simplicity in setting up a model, and of well-defined behaviors for individual components, but has less flexibility than the alternative, programmatic model specification. Most simulators reviewed here use a more or less general purpose programming language, usually an interpreted one, which has neuroscience specific functions and classes together with more general control and data structures. As noted, this gives the flexibility to generate new structures beyond those found in the simulator's standard library, but at the expense of the very complexity that we identified above as the major roadblock in converting models between simulators.

### Declarative model specification using NeuroML

The NeuroML project<sup>25</sup> is an open-source collaboration<sup>26</sup> whose stated aims are:

1. To support the use of declarative specifications for models in neuroscience using XML.
2. To foster the development of XML standards for particular areas of computational neuroscience modeling.

The following standards have so far been developed:

---

<sup>25</sup><http://www.neuroml.org> (Crook et al., 2005)

<sup>26</sup><http://sourceforge.net/projects/neuroml>

- **MorphML**: specification of neuroanatomy (i.e. neuronal morphology)
- **ChannelML**: specification of models of ion channels and receptors (see Figure 21 for an example)
- **Biophysics**: specification of compartmental cell models, building on MorphML and ChannelML
- **NetworkML**: specification of cell positions and connections in a network.

The common syntax of these specifications is XML (Extensible Markup Language<sup>27</sup>). This has the advantages of being both human- and machine-readable, and standardized by an international organization, which in turn has led to wide uptake and developer participation.

Other XML-based specifications that have been developed in neuroscience and in biology more generally include BrainML<sup>28</sup> for exchanging neuroscience data, CellML<sup>29</sup> for models of cellular and subcellular processes and SBML<sup>30</sup> for representing models of biochemical reaction networks.

Although XML has become the most widely used technology for the electronic communication of hierarchically structured information, the real standardization effort is orthogonal to the underlying technology, and concerns the structuring of domain-specific knowledge, i.e. a listing of the objects and concepts of interest in the domain and of the relationships between them, using a standardized terminology. To achieve this, NeuroML uses the XML Schema Language<sup>31</sup> to define the allowed elements and structure of a NeuroML document. The validity of a NeuroML document may be checked with reference to the schema definitions. The NeuroML Validation service<sup>32</sup> provides a convenient way to do this.

### Using NeuroML for specifying network models

In order to use NeuroML to specify spiking neuronal network models we require detailed descriptions of

1. point spiking neurons (integrate and fire neurons and generalizations thereof),
2. compartmental models with Hodgkin-Huxley-like biophysics,
3. large networks with structured internal connectivity related to a network topology (e.g.: full-connectivity, 1D or 2D map with local connectivity, synfire chains patterns, with/without randomness) and structured map to map connectivity (e.g., point-to-point, point-to-many, etc.).

At the time of writing, NeuroML supports the second and third items, but not the first. However, an extension to support specification of integrate-and-fire-type neuron models is currently being developed, and will hopefully be incorporated into the NeuroML standard in the near future.

Specification of Hodgkin-Huxley-type models uses the MorphML, ChannelML and Biophysics standards of NeuroML (see Fig. 21 for an example. We focus here only on specification of networks, using the NetworkML standard.

A key point is that a set of neurons and network connectivity may be defined either by *extension* (providing the list of all neurons, parameters and connections), for example:

```

49 <population name="PopulationA">
50   <cell_type>CellA</cell_type>
51   <instances>
52     <instance id="0"><location x="0" y="0" z="0"/></instance>
53     <instance id="1"><location x="0" y="10" z="0"/></instance>
54     <instance id="2"><location x="0" y="20" z="0"/></instance>
55     . . .
56   </instances>
57 </population>

```

---

<sup>27</sup><http://www.w3.org/XML>

<sup>28</sup><http://brainml.org>

<sup>29</sup><http://www.cellml.org>

<sup>30</sup><http://sbml.org>

<sup>31</sup><http://www.w3.org/XML/Schema>

<sup>32</sup><http://morphml.org:8080/NeuroMLValidator>

(note that CellA is a cell model described earlier in the NeuroML document), or by *specification*, i.e. an implicit enumeration, for example:

```
<population name="PopulationA">
  <cell_type>CellA</cell_type>
  <pop_location>
    <random_arrangement>
      <population_size>200</population_size>
      <spherical_location>
        <meta:center x="0" y="0" z="0" diameter="100"/>
      </spherical_location>
    </random_arrangement>
  </pop_location>
</population>
```

Similarly, for connectivity, one may define an explicit list of connections,

```
<projection name="NetworkConnection1">
  <source>PopulationA</source>
  <target>PopulationB</target>
  <connections>
    <connection id="0">
      <pre cell_id="0" segment_id = "0"/>
      <post cell_id="1" segment_id = "1"/>
    </connection>
    <connection id="1">
      <pre cell_id="2" segment_id = "0"/>
      <post cell_id="1" segment_id = "0"/>
    </connection>
    . . .
  </connections>
</projection>
```

or specify an algorithm to determine the connections:

```
<projection name="NetworkConnection1">
  <source>PopulationA</source>
  <target>PopulationB</target>
  <connectivity_pattern>
    <num_per_source>3</num_per_source>
    <max_per_target>2</max_per_target>
  </connectivity_pattern>
</projection>
```

## Using NeuroML with a specific simulator

One very interesting feature of XML is that any language such as NeuroML is not fixed for ever:

- it may be adapted to your own<sup>33</sup> way of presenting data and models (e.g. words may be written in your own native language) as soon as the related logical-structure can be translated to/from standard NeuroML

<sup>33</sup>**Pragmatic generic coding-rules.** There are always several ways to represent information as a logical-structure. Here are a few key ideas to make such choices:

\* *Maximizing atomicity.* i.e. structure the data with a maximal decomposition (e.g. atomic values must only contain “words” else there is still a “structure” and is thus to be decomposed itself in terms of elements).

\* *Maximizing factorization.* i.e. prohibit data redundancy, but use references to index a data fragment from another part of the data. This saves place and time, but also avoid data inconsistency.

\* *Maximizing flat representation.* i.e. avoid complex tree structures, when the data can be represented as uniform lists of data, i.e. tables with simple records, such as a field-set.

\* *Maximizing generic description.* i.e. abstract representation, without any reference to file format or operating-system syntax: independent of how the data is going to be used.

\* *Maximizing parameterization of functionality.* i.e. specify, as much as possible, the properties (i.e. characteristics / parameters / options) of a software module or a function as a static set of data (instead of “putting-it-in-the-code”).

- add-ons are always easily defined, as soon as they are compatible with the original NeuroML specifications.

Then using NeuroML simply means editing such data-structures using a suitable XML editor, validating them (i.e. verify that the related logical-structures are well-formed and valid with respect to the specification, conditions, etc.) and normalizing them (i.e. translate it to an equivalent logical-structure but without redundancy, while some factorization simplifies subsequent manipulation).

Translation from this validated normalized form is efficient and safe. Translation can be achieved by one of two methods: Either a simulator may accept a NeuroML document as input, and translation from NeuroML elements to native simulator objects is performed by the simulator, or the XSL Transformation language<sup>34</sup> may be used to generate native simulator code (e.g. hoc or NMODL in the case of NEURON). For example, the NeuroML Validator service provides translation of ChannelML and MorphML files to NEURON and GENESIS formats.

The process of editing, validating, normalizing and translating NeuroML data-structures is summarized in Figure 22.

### Future extensions

The NetworkML standard is at an early stage of development. Desirable future extensions include:

- specification of point spiking models, such as the integrate-and-fire model.
- more flexible specification of numerical parameters. Numerical parameter values are not simple “numbers” but satisfy certain standard conditions (parameter values are physical quantities with a unit, may take a default value, have values bounded within a certain range with minimal/maximal values and are defined up to a certain precision) or specific conditions defined by a boolean expression, and may have their default value not simply defined by a constant but from an algebraic expression. In the current NeuroML standards all numerical parameters are simple numbers, and all units must be consistent with either a “physiological units” system or the SI system (they may not be mixed in a single NeuroML document).
- specifying parameter values as being drawn from a defined random distribution.

### Programmatic model specification using Python

For network simulations, we may well require more flexibility than can easily be obtained using a declarative model specification, but we still wish to obtain simple conversion between simulators, i.e. to be able to write the simulation code for a model only once, then run the same code on multiple simulators. This requires first the definition of an API (Application Programming Interface) or meta-language, a set of functions/classes which provides a superset of the capabilities of the simulators we wish to run on<sup>35</sup>. Having defined an API, there are two possible next stages: (i) each simulator implements a parser which can interpret the meta-language; (ii) a separate program either translates the meta-language into simulator-specific code or controls the simulator directly, giving simulator-specific function calls.

In our opinion, the second of these possibilities is the better one, since

1. it avoids replication of effort in writing parsers,
2. we can then use a general purpose, state-of-the-art interpreted programming language, such as Python or Ruby, rather than a simulator-specific language, and thus leverage the effort of outside developers in areas that are not neuroscience specific, such as data analysis and visualization<sup>36</sup>

---

<sup>34</sup><http://www.w3.org/TR/xslt>

<sup>35</sup>Note that since we choose a superset, the system must emit a warning/error if the underlying simulator engine does not support a particular feature.

<sup>36</sup>For Python, examples include efficient data storage and transfer (HDF5, ROOT), data analysis (SciPy), parallelization (MPI), GUI toolkits (GTK, QT).



1  
2  
3  
4 The PyNN project<sup>37</sup> has begun to develop both the API and the binding to individual simulation engines,  
5 for both purposes using the Python programming language. The API has two parts, a low-level, procedu-  
6 ral API (functions `create()`, `connect()`, `set()`, `record()`), and a high-level, object-oriented API (classes  
7 `Population` and `Projection`, which have methods like `set()`, `record()`, `setWeights()`, etc.). The low-  
8 level API is good for small networks, and perhaps gives more flexibility. The high-level API is good for  
9 hiding the details and the book-keeping, and is intended to have a one-to-one mapping with NeuroML, i.e. a  
10 population element in NeuroML will correspond to a `Population` object in PyNN.

11  
12 The other thing that is required to write a model once and run it on multiple simulators is standard cell mod-  
13 els. PyNN translates standard cell-model names and parameter names into simulator-specific names, e.g. stan-  
14 dard model `IF_curr_alpha` is `iaf_neuron` in NEST and `StandardIF` in NEURON, while `SpikeSourcePoisson`  
15 is a `poisson_generator` in NEST and a `NetStim` in NEURON.

16  
17 An example of the use of the API to specify a simple network is given in Figure 23.

18 Python bindings currently exist to control NEST (PyNEST<sup>38</sup>) and Mvaspike, and Python can be used as an  
19 alternative interpreter for NEURON (`nrnpython`), although the level of integration (how easy it is to access the  
20 native functionality) is variable. Currently PyNN supports PyNEST and NEURON (via `nrnpython`), and there  
21 are plans to add support for other simulators with Python bindings, initially Mvaspike and CSIM, and to add  
22 support for the distributed simulation capabilities of NEURON and NEST.

## 23 24 25 **Example simulations**

26  
27 Benchmarks 1 and 2 (see Appendix 2) have been coded in PyNN and run using both NEURON and NEST  
28 (Fig. 24). The results for the two simulators are not identical, since we used different random number sequences  
29 when determining connectivity, but the distributions of inter-spike intervals (ISIs) and of the coefficient of  
30 variation of ISI are almost indistinguishable. All the cell and synapse types used in the benchmarks are standard  
31 models in PyNN. Where these models do not come as standard in NEURON or NEST, the model code is  
32 distributed with PyNN (in the case of NEURON) or with PyNEST (in the case of NEST). We do not report  
33 simulation times, as PyNN has not been optimized for either simulator.

---

34  
35  
36  
37  
38  
39  
40  
41  
42  
43  
44  
45  
46  
47  
48  
49  
50  
51  
52  
53  
54  
55  
56  
57  
58  
59  
60  
61  
62 <sup>37</sup>pronounced 'pine'

63 <sup>38</sup>a Python interface to NEST  
64  
65

## Appendix 2: Benchmark simulations

In this appendix, we present a series of “benchmark” network simulations using both integrate-and-fire (IF) or Hodgkin-Huxley (HH) type neurons. They were chosen such that at least one of the benchmark can be implemented in the different simulators (the code corresponding to these implementations will be provided in the ModelDB database<sup>39</sup>).

The models chosen were networks of excitatory and inhibitory neurons inspired from a recent study (Vogels and Abbott, 2005). This paper considered two types of networks of leaky IF neurons, one with current-based synaptic interactions (CUBA model), and another one with conductance-based synaptic interactions (CUBA model; see below). We also introduce here a HH-based version of the COBA model, as well as a fourth model consisting of IF neurons interacting through voltage deflections (“voltage-jump” synapses).

### Network structure

Each model consisted of 4,000 IF neurons, which were separated into two populations of excitatory and inhibitory neurons, forming 80% and 20% of the neurons, respectively. All neurons were connected randomly using a connection probability of 2%.

### Passive properties

The membrane equation of all models was given by:

$$C_m \frac{dV}{dt} = -g_L(V - E_L) + S(t) + G(t) , \quad (5)$$

where  $C_m = 1 \mu\text{F}/\text{cm}^2$  is the specific capacitance,  $V$  is the membrane potential,  $g_L = 5 \times 10^{-5} \text{ S}/\text{cm}^2$  is the leak conductance density and  $E_L = -60 \text{ mV}$  is the leak reversal potential. Together with a cell area of  $20,000 \mu\text{m}^2$ , these parameters give a resting membrane time constant of 20 ms and an input resistance at rest of 100 M $\Omega$ . The function  $S(t)$  represents the spiking mechanism and  $G(t)$  stands for synaptic interactions (see below).

### Spiking mechanisms

#### IF neurons

In addition to passive membrane properties, IF neurons had a firing threshold of -50 mV. Once the  $V_m$  reaches threshold, a spike is emitted and the membrane potential is reset to -60 mV and remains at that value for a refractory period of 5 ms.

#### HH neurons

HH neurons were modified from Traub and Miles (1991) and were described by the following equations:

$$\begin{aligned} C_m \frac{dV}{dt} &= -g_L(V - E_L) - \bar{g}_{Na} m^3 h (V - E_{Na}) - \bar{g}_{Kd} n^4 (V - E_K) + G(t) \\ \frac{dm}{dt} &= \alpha_m(V) (1 - m) - \beta_m(V) m \\ \frac{dh}{dt} &= \alpha_h(V) (1 - h) - \beta_h(V) h \\ \frac{dn}{dt} &= \alpha_n(V) (1 - n) - \beta_n(V) n , \end{aligned} \quad (6)$$

---

<sup>39</sup><http://senselab.med.yale.edu/senselab/ModelDB>

where  $\bar{g}_{Na} = 100 \text{ mS/cm}^2$  and  $\bar{g}_{Kd} = 30 \text{ mS/cm}^2$  are the maximal conductances of the sodium current and delayed rectifier with reversal potentials of  $E_{Na} = 50 \text{ mV}$  and  $E_K = -90 \text{ mV}$ .  $m$ ,  $h$ , and  $n$  are the activation variables which time evolution depends on the voltage-dependent rate constants  $\alpha_m$ ,  $\beta_m$ ,  $\alpha_h$ ,  $\beta_h$ ,  $\alpha_n$  and  $\beta_n$ . The voltage-dependent expressions of the rate constants were modified from the model described by Traub and Miles (1991):

$$\begin{aligned}
\alpha_m &= 0.32 * (13 - V + V_T) / [\exp((13 - V + V_T)/4) - 1] \\
\beta_m &= 0.28 * (V - V_T - 40) / [\exp((V - V_T - 40)/5) - 1] \\
\alpha_h &= 0.128 * \exp((17 - V + V_T)/18) \\
\beta_h &= 4 / [1 + \exp((40 - V + V_T)/5)] \\
\alpha_n &= 0.032 * (15 - V + V_T) / [\exp((15 - V + V_T)/5) - 1] \\
\beta_n &= 0.5 * \exp((10 - V + V_T)/40) ,
\end{aligned}$$

where  $V_T = -63 \text{ mV}$  adjusts the threshold (which was around  $-50 \text{ mV}$  for the above parameters).

## Synaptic interactions

### Conductance-based synapses

For conductance-based synaptic interactions, the membrane equation of neuron  $i$  was given by:

$$C_m \frac{dV_i}{dt} = -g_L(V_i - E_L) + S(t) - \sum_j g_{ji}(t)(V_i - E_j) , \quad (7)$$

where  $V_i$  is the membrane potential of neuron  $i$ ,  $g_{ji}(t)$  is the synaptic conductance of the synapse from neuron  $j$  to neuron  $i$ , and  $E_j$  is the reversal potential of that synapse.  $E_j$  was of  $0 \text{ mV}$  for excitatory synapses, or  $-80 \text{ mV}$  for inhibitory synapses.

Synaptic interactions were implemented as follows: when a spike occurred in neuron  $j$ , the synaptic conductance  $g_{ji}$  was instantaneously incremented by a quantum value ( $6 \text{ nS}$  and  $67 \text{ nS}$  for excitatory and inhibitory synapses, respectively) and decayed exponentially with a time constant of  $5 \text{ ms}$  and  $10 \text{ ms}$  for excitation and inhibition, respectively.

### Current-based synapses

For implementing current-based synaptic interactions, the following equation was used:

$$C_m \frac{dV_i}{dt} = -g_L(V_i - E_L) + S(t) - \sum_j g_{ji}(t)(\bar{V} - E_j) , \quad (8)$$

where  $\bar{V} = -60 \text{ mV}$  is the mean membrane potential. The conductance quanta were of  $0.27 \text{ nS}$  and  $4.5 \text{ nS}$  for excitatory and inhibitory synapses, respectively. The other parameters are the same as for conductance-based interactions.

### Voltage-jump synapses

For implementing voltage-jump type of synaptic interactions, the membrane potential was abruptly increased by a value of  $0.25 \text{ mV}$  for each excitatory event, and it was decreased by  $2.25 \text{ mV}$  for each inhibitory event.

1  
2  
3  
4  
5  
6  
7  
8  
9  
10  
11  
12  
13  
14  
15  
16  
17  
18  
19  
20  
21  
22  
23  
24  
25  
26  
27  
28  
29  
30  
31  
32  
33  
34  
35  
36  
37  
38  
39  
40  
41  
42  
43  
44  
45  
46  
47  
48  
49  
50  
51  
52  
53  
54  
55  
56  
57  
58  
59  
60  
61  
62  
63  
64  
65

## Benchmarks

Based on the above models, the following four benchmarks were implemented.

*Benchmark 1: Conductance-based IF network.* This benchmark consists of a network of IF neurons connected with conductance-based synapses, according to the parameters above. It is equivalent to the COBA model described in Vogels and Abbott (2005).

*Benchmark 2: Current-based IF network.* This second benchmark simulates a network of IF neurons connected with current-based synapses, which is equivalent to the CUBA model described in Vogels and Abbott (2005). It has the same parameters as above, except that every cell needs to be depolarized by about 10 mV, which was implemented by setting  $E_L = -49$  mV (see Vogels and Abbott, 2005).

*Benchmark 3: Conductance-based HH network.* This benchmark is equivalent to Benchmark 1, except that the HH model was used.

*Benchmark 4: IF network with voltage-jump synapses.* This fourth benchmark used voltage-jump synapses, and has a membrane equation which is analytically solvable, and can be implemented using event-driven simulation strategies.

For all four benchmarks, the models simulate a self-sustained irregular state of activity, which is easy to identify: all cells fire irregularly and are characterized by important subthreshold voltage fluctuations. The neurons must be randomly stimulated during the first 50 ms in order to set the network in the active state.

## Supplementary material

The supplementary material to the paper contains the codes for implementing those benchmarks in the different simulators reviewed here (see Section 3 for details on specific implementations). We provide the codes for those benchmarks, implemented in each simulator, and this code is made available in the ModelDB database<sup>40</sup>.

In addition, we provide a clock-driven implementation of Benchmarks 1 and 2 with Scilab, a free vector-based scientific software. In this case, Benchmark 1 is integrated with Euler method, second order Runge-Kutta and Euler with spike timing interpolation (Hansel et al, 1998), while Benchmark 2 is integrated exactly (with spike timings aligned to the time grid). The event-driven implementation (Benchmark 4) is also possible with Scilab but very inefficient because the programming language is interpreted, and since the algorithms are asynchronous, the operations cannot be vectorized. Finally, we also provide a C++ implementation of Benchmark 2 and of a modified version of the COBA model (Benchmark 1, with identical synaptic time constants for excitation and inhibition).

---

<sup>40</sup><https://senselab.med.yale.edu/senselab/modeldb/ShowModel.asp?model=83319> (if necessary, use "reviewme" as password).

## References

- [1] Abbott LF, Nelson SB (2000). Synaptic plasticity: taming the beast. *Nat Neurosci*, 3 Suppl:1178-1283.
- [2] Arnold L (1974). *Stochastic Differential Equations: Theory and Applications*. J. Wiley and Sons.
- [3] Azouz R. (2005) Dynamic spatiotemporal synaptic integration in cortical neurons: neuronal gain, revisited. *J. Neurophysiol.* 94: 2785-2796.
- [4] Badoual M, Rudolph M, Piwkowska Z, Destexhe A and Bal T. (2005) High discharge variability in neurons driven by current noise. *Neurocomputing* 65: 493-498.
- [5] Bailey, J. and Hammerstrom, D. (1988) Why VLSI Implementations of Associative VLCNs Require Connection Multiplexing. *International Conference on Neural Networks (ICNN 88, IEEE)*: 173-180, San Diego, USA.
- [6] Banitt Y, Martin KAC and Segev I. (2005) Depressed responses of facilitatory synapses. *Journal of Neurophysiology* 94: 865-870.
- [7] Beeman D (2005) GENESIS Modeling Tutorial. *Brains, Minds, and Media*. 1: bmm220 (urn:nbn:de:0009-3-2206).
- [8] Bernard C, Ge YC, Stockley E, Willis JB, Wheal HV (1994) Synaptic integration of NMDA and non-NMDA receptors in large neuronal network models solved by means of differential equations. *Biol. Cybern.* 70(3): 267-73.
- [9] Bhalla U, Bilitch D, Bower JM (1992) Rallpacks: A set of benchmarks for neuronal simulators. *Trends in Neurosci.* 15: 453-458.
- [10] Bhalla US, Iyengar R (1999) Emergent properties of networks of biological signaling pathways. *Science* 283: 381-387.
- [11] Bhalla US (2004) Signaling in small subcellular volumes: II. Stochastic and diffusion effects on synaptic network properties. *Biophys. J.* 87: 745-753.
- [12] Blake JL, Goodman PH (2002) Speech perception simulated in a biologically-realistic model of auditory neocortex. (Abstract) *J. Investig. Med.* 50: 193S.
- [13] Bower JM (1995) Reverse engineering the nervous system: An in vivo, in vitro, and in computo approach to understanding the mammalian olfactory system. In: SF Zornetzer, JL Davis and C Lau, eds. *An Introduction to Neural and Electronic Networks*, second edn. Academic Press, New York. pp. 3-28.
- [14] Bower JM, Beeman D (1998) *The Book of GENESIS: Exploring Realistic Neural Models with the GENeral Neural Simulation System, second edition*. Springer, New York.
- [15] Brette R (2006a). Exact simulation of integrate-and-fire models with exponential currents. *Neural Computation* (in press).
- [16] Brette R (2006b) Exact simulation of integrate-and-fire models with synaptic conductances. *Neural Computation* 18: 2004-2027.
- [17] Brette R, Gerstner W (2005). Adaptive exponential integrate-and-fire model as an effective description of neuronal activity. *J Neurophysiol*, 94: 3637-3642.
- [18] Brown R (1988). Calendar queues: a fast  $O(1)$  priority queue implementation for the simulation event set problem. *J Commun. ACM*, 31(10):1220-1227.
- [19] Carnevale NT and Hines ML. (2006) *The NEURON Book*. Cambridge University Press, Cambridge, UK.
- [20] Carriero, N. and Gelernter, D. (1989) Linda in context. *Communications of the ACM* 32: 444-458.
- [21] Claverol E, Brown A, Chad J (2002). Discrete simulation of large aggregates of neurons. *Neurocomputing*, 47:277-297.
- [22] Connolly C, Marian I, Reilly R (2003). Approaches to efficient simulation with spiking neural networks. In WSPC .
- [23] Cormen T, Leiserson C, Rivest R, Stein C (2001). *Introduction to Algorithms, Second Edition*. MIT Press.
- [24] Crook S, Beeman D, Gleeson P, Howell F (2005) XML for model specification in neuroscience. *Brains, Minds and Media* 1: bmm228 (urn:nbn:de:0009-3-2282)
- [25] Daley D, Vere-Jones D (1988). *An Introduction to the Theory of Point processes*. Springer, New-York.
- [26] Day, M., Carr, D.B., Ulrich, S., Ilijic, E., Tkatch, T., and Surmeier, D.J. (2005) Dendritic excitability of mouse frontal cortex pyramidal neurons is shaped by the interaction among HCN, Kir2, and k(leak) channels. *J. Neurosci.* 25: 8776-8787.
- [27] Delorme A, Thorpe SJ (2003). Spikenet: an event-driven simulation package for modelling large networks of spiking neurons. *Network*, 14(4):613-627.
- [28] De Schutter E, Bower JM (1994) An active membrane model of the cerebellar Purkinje cell. I. Simulation of current clamps in slice. *J. Neurophysiol.* 71: 375-400.
- [29] Destexhe A, Mainen Z, Sejnowski T (1994a). An efficient method for computing synaptic conductances based on a kinetic model of receptor binding. *Neural Computation* 6: 14-18.
- [30] Destexhe A, Mainen Z, Sejnowski T (1994b). Synthesis of models for excitable membranes, synaptic transmission and neuromodulation using a common kinetic formalism. *J. Comput. Neurosci.* 1: 195-230.

- 1  
2  
3  
4 [31] Destexhe, A. and Sejnowski, T.J. (2001) *Thalamocortical Assemblies*. Oxford University Press, New York.  
5 [32] Diesmann, M. and Gewaltig, M.-O. (2002). NEST: An environment for neural systems simulations. In T. Plesser and  
6 V. Macho (Eds.), *Forschung und wissenschaftliches Rechnen, Beitrage zum Heinz-Billing-Preis 2001*, Volume 58  
7 of GWDG-Bericht, pp. 43-70. Gottingen: Ges. fur Wiss. Datenverarbeitung.  
8 [33] Djurfeldt, M., Johansson, C., Ekeberg, Ö., Rehn, M., Lundqvist, M., and Lansner, A. (2005). Massively parallel sim-  
9 ulation of brain-scale neuronal network models. Technical Report TRITA-NA-P0513, School of Computer Science  
10 and Communication, Stockholm.  
11 [34] Drewes R, Maciokas JB, Louis SJ, Goodman PH (2004) An evolutionary autonomous agent with visual cortex and  
12 recurrent spiking columnar neural network. *Lecture Notes in Computer Science* 3102: 257-258.  
13 [35] Drewes R (2005) Modeling the brain with NCS and Brainlab. *LINUX Journal* online.  
14 <http://www.linuxjournal.com/article/8038>  
15 [36] Ermentrout B. (2002) *Simulating, analyzing, and animating dynamical systems: A guide to XPPAUT for researchers*  
16 *and students*. SIAM  
17 [37] Ermentrout B, Kopell N (1986). Parabolic bursting in an excitable system coupled with a slow oscillation. *Siam J*  
18 *Appl Math* 46: 233-253.  
19 [38] Ferscha, A. (1996). Parallel and distributed simulation of discrete event systems. In A. Y. Zomaya (Ed.), *Parallel*  
20 *and Distributed Computing Handbook*, Chapter 35, pp. 1003–1041. McGraw-Hill.  
21 [39] Fransén, E. and Lansner, A. (1998). A model of cortical associative memory based on a horizontal network of  
22 connected columns. *Network: Computation in Neural Systems* 9: 235-264.  
23 [40] Froemke RC, Dan Y (2002). Spike-timing-dependent synaptic modification induced by natural spike trains. *Nature*  
24 416: 433-438.  
25 [41] Fujimoto, R. M. (2000). *Parallel and distributed simulation systems*. New York: Wiley.  
26 [42] Galassi, M., Davies, J., Theiler, J., Gough, B., Jungman, G., Booth, M. and Rossi, F. (2001) *Gnu Scientific Library:*  
27 *Reference Manual*. Bristol: Network Theory Limited.  
28 [43] Gara, A., Blumrich, M. A., Chen, D., Chiu, G. L.-T., Coteus, P., Giampapa, M. E., Haring, R. A., Heidelberger, P.,  
29 Hoenicke, D., Kopcsay, G. V., Liebsch, T. A., Ohmacht, M., Steinmacher-Burow, B. D., Takken, T., and Vranas, P.  
30 (2005). Overview of the Blue Gene/L system architecture. *IBM Journal of Research and Development* 49: 195-212.  
31 [44] Gerstner W, Kistler WM (2002). Mathematical formulations of hebbian learning. *Biol Cybern*, 87: 404-415.  
32 [45] Giugliano M (2000). Synthesis of generalized algorithms for the fast computation of synaptic conductances with  
33 markov kinetic models in large network simulations. *Neural Computation* 12: 903-931.  
34 [46] Giugliano M, Bove M, Grattarola M (1999). Fast calculation of short-term depressing synaptic conductances. *Neural*  
35 *Computation* 11: 1413-1426.  
36 [47] Goddard N, Hucka M, Howell F, Cornelis H, Shankar K, Beeman D (2001) Towards NeuroML: Model Description  
37 Methods for Collaborative Modelling in Neuroscience. *Phil. Trans. Royal Society B*. 356: 1209-1228.  
38 [48] Gupta A, Wang Y, Markram H (2000) Organizing principles for a diversity of GABAergic interneurons and synapses  
39 in the neocortex. *Science* 287: 273-278.  
40 [49] Gütig R, Aharonov R, Rotter S, Sompolinsky H (2003). Learning input correlations through non-linear asymmetric  
41 hebbian plasticity. *J. Neurosci*. 23: 3697-3714.  
42 [50] Gütig R, Sompolinsky H (2006). The tempotron: a neuron that learns spike timing-based decisions. *Nat Neurosci* 9:  
43 420-428.  
44 [51] Hammarlund, P. and Ekeberg, Ö. (1998). Large neural network simulations on multiple hardware platforms. *J.*  
45 *Comput. Neurosci*. 5: 443-459.  
46 [52] Hansel D, Mato G, Meunier C, Neltner L (1998). On numerical simulations of integrate-and-fire neural networks.  
47 *Neural Computation* 10: 467-483.  
48 [53] Hereld M, Stevens RL, Teller J, van Drongelen W (2005) Large Neural Simulations on Large Parallel Computers.  
49 *Int. J. Bioelectromagnetism* 7: 44-46.  
50 [54] Hindmarsh, A.C, Brown, P.N., Grant, K.E., Lee, S.L, Serban, R., Shumaker, D.E., Woodward, C.S. (2005) SUNDI-  
51 ALS: suite of nonlinear and differential/algebraic equation solvers. *ACM Transactions on Mathematical Software*  
52 31: 363-396.  
53 [55] Hines, M. (1984) Efficient computation of branched nerve equations. *Int. J. Bio-Med. Comput*. 15: 69-76.  
54 [56] Hines, M. (1989) A program for simulation of nerve equations with branching geometries. *Int. J. Bio-Med. Comput*.  
55 24: 55-68.  
56 [57] Hines, M. and Carnevale, N. T. (1997). The neuron simulation environment. *Neural Computation* 9: 1179-1209.  
57 [58] Hines, M.L. and Carnevale, N.T. (2000) Expanding NEURON's repertoire of mechanisms with NMODL. *Neural*  
58 *Computation* 12: 995-1007.  
59 [59] Hines, M.L. and Carnevale, N.T. (2001) NEURON: a tool for neuroscientists. *The Neuroscientist* 7: 123-135.  
60 [60] Hines, M.L. and Carnevale, N.T. (2004) Discrete event simulation in the NEURON environment. *Neurocomputing*  
61  
62  
63  
64  
65

- 58-60: 1117-1122.
- [61] Hirsch M, Smale S (1974). *Differential Equations, Dynamical Systems, and Linear Algebra. Pure and Applied Mathematics*. Academic Press.
- [62] Honeycutt RL (1992). Stochastic runge-kutta algorithms. I. White noise. *Physical Review A* 45: 600-603.
- [63] Houweling, A.R., Bazhenov, M., Timofeev, I., Steriade, M., and Sejnowski, T.J. (2005) Homeostatic synaptic plasticity can explain post-traumatic epileptogenesis in chronically isolated neocortex. *Cereb. Cortex* 15: 834-845.
- [64] Hugues E, Guilleux F, Rochel O (2002) Contour detection by synchronization of Integrate-and-Fire neurons. Proceedings of the 2nd Workshop on Biologically Motivated Computer Vision - BMCV 2002, Tbingen, Germany. *Lecture Notes in Computer Science* 2525: 60-69.
- [65] Izhikevich EM (2003). Simple model of spiking neurons. *IEEE Transactions on Neural Networks* 14: 1569-1572.
- [66] Jahnke A, Roth U, Schoenauer T (1998) Digital simulation of spiking neural networks. In: Maass W, Bishop CM, editors, *Pulsed Neural Networks*, MIT Press.
- [67] Johnston, D. and Wu, S.M.-S. (1995) *Foundations of Cellular Neurophysiology*. MIT Press, Cambridge, MA.
- [68] Kanold, P.O. and Manis, P.B. (2005) Encoding the timing of inhibitory inputs. *J. Neurophysiol.* 93: 2887-2897.
- [69] Kellogg MM, Wills HR, Goodman PH (1999) Cumulative synaptic loss in aging and Alzheimer's dementia: A biologically realistic computer model. (Abstract) *J Investig Med* 47: 17S.
- [70] Kernighan, B.W. and Pike, R. (1984) Appendix 2: Hoc manual. In: *The UNIX Programming Environment*. Englewood Cliffs, NJ: Prentice-Hall, pp. 329-333.
- [71] Kohn J, Wörgötter F (1998). Employing the Z-transform to optimize the calculation of the synaptic conductance of NMDA and other synaptic channels in network simulations. *Neural Computation* 10: 1639-1651.
- [72] Kozlov, A., Lansner, A., and Grillner, S. (2003). Burst dynamics under mixed nmda and ampa drive in the models of the lamprey spinal cpg. *Neurocomputing* 52-54: 65-71.
- [73] Kozlov, A., Lansner, A., Grillner, S., and Kotaleski, J. H. (2006). Locomotor rhythm generation in a population of excitatory interneurons of the lamprey hemicord network-a computer simulation study. *Submitted*.
- [74] Laing CR. (2006) On the application of "equation-free" modelling to neural systems. *J. Comput. Neurosci.*, in press.
- [75] Lee G, Farhat NH (2001). The double queue method: a numerical method for integrate-and-fire neuron networks. *Neural Networks* 14: 921-932.
- [76] Lundqvist, M., Rehn, M., Djurfeldt, M., and Lansner, A. (2006). Attractor dynamics in a modular network model of neocortex. *Network*, in press.
- [77] Lytton WW (1996). Optimizing synaptic conductance calculation for network simulations. *Neural Computation* 8: 501-509.
- [78] Lytton, W.W. (2002) *From Computer to Brain*. Springer-Verlag, New York.
- [79] Lytton WW, Hines ML (2005). Independent variable time-step integration of individual neurons for network simulations. *Neural Computation* 17: 903-921.
- [80] Macera-Rios JC, Goodman PH, Drewes R, Harris FC Jr (2004) Remote-Neocortex Control of Robotic Search and Threat Identification. *Robotics and Autonomous Systems* 46: 97-110.
- [81] Maciakas JB, Goodman PH, Kenyon JL, Toledo-Rodriquez M, Markram H (2005) Accurate dynamical model of interneuronal GABAergic channel physiologies. *Neurocomputing* 65: 5-14.
- [82] Makino T (2003). A discrete-event neural network simulator for general neuron models. *Neural Comput. and Applic.* 11: 210-223.
- [83] Marian I, Reilly R, Mackey D (2002). Efficient event-driven simulation of spiking neural networks. Proceedings of the 3rd WSEAS International Conference on Neural Networks and Applications.
- [84] Markram H, Lubke J, Frotscher M, Roth A, Sakmann B (1997a) Physiology and anatomy of synaptic connections between thick tufted pyramidal neurones in the developing rat neocortex. *J Physiol* 500: 409-440.
- [85] Markram H, Lubke J, Frotscher M, Sakmann B (1997b) Regulation of synaptic efficacy by coincidence of postsynaptic APs and EPSPs. *Science* 275: 213-215.
- [86] Markram H, Dimitri P, Gupta A, Tsodyks M. (1998a) Potential for multiple mechanisms, phenomena and algorithms for synaptic plasticity at single synapses. *Neuropharmacology* 37: 489-500.
- [87] Markram H, Wang Y, Tsodyks M (1998b). Differential signaling via the same axon of neocortical pyramidal neurons. *Proc. Natl. Acad. Sci.* 95: 5323-5328.
- [88] Mattia M, Del Giudice P (2000). Efficient event-driven simulation of large networks of spiking neurons and dynamical synapses. *Neural Computation* 12: 2305-2329.
- [89] Markaki, M., Orphanoudakis, S., and Poirazi, P. (2005) Modelling reduced excitability in aged CA1 neurons as a calcium-dependent process. *Neurocomputing* 65: 305-314.
- [90] Mayrhofer R, Affenzeller M, Prähofer H, Hfer G, Fried A (2002). Devs simulation of spiking neural networks. In Proceedings of Cybernetics and Systems (EMCSR), volume 2, pages 573-578. Austrian Society for Cybernetic Studies.

1  
2  
3  
4  
5  
6  
7  
8  
9  
10  
11  
12  
13  
14  
15  
16  
17  
18  
19  
20  
21  
22  
23  
24  
25  
26  
27  
28  
29  
30  
31  
32  
33  
34  
35  
36  
37  
38  
39  
40  
41  
42  
43  
44  
45  
46  
47  
48  
49  
50  
51  
52  
53  
54  
55  
56  
57  
58  
59  
60  
61  
62  
63  
64  
65

[91] Migliore, M., Hines, M.L., and Shepherd, G.M. (2005) The role of distal dendritic gap junctions in synchronization of mitral cell axonal output. *J. Computat. Neurosci.* 18: 151-161.

[92] Migliore, M., Cannia, C., Lytton, W.W., Markram, H. and Hines, M.L. (2006) Parallel network simulations with NEURON. *J. Comput. Neurosci.* 21: 119-129.

[93] Moffitt, M.A. and McIntyre, C.C. (2005) Model-based analysis of cortical recording with silicon microelectrodes. *Clin. Neurophysiol.* 116: 2240-2250.

[94] Moore, J.W. and Stuart, A.E. (2000) *Neurons in Action: Computer Simulations with NeuroLab*. Sinauer Associates, Sunderland, MA.

[95] Morrison, A., Aertsen, A. and Diesmann, M. (2006). Spike-timing dependent plasticity in balanced random networks. *Neural Computation*, in press.

[96] Morrison, A., Mehring, C., Geisel, T., Aertsen, A. and Diesmann, M. (2005). Advancing the boundaries of high connectivity network simulation with distributed computing. *Neural Computation* 17: 1776-1801.

[97] Morrison, A., Straube, S., Plesser, H. E. and Diesmann, M. (2006). Exact subthreshold integration with continuous spike times in discrete time neural network simulations. *Neural Computation*, in press.

[98] Natschläger T, Markram H, Maass W (2003). Computer models and analysis tools for neural microcircuits. In: Kötter, R, editor, *Neuroscience Databases. A Practical Guide*, chapter 9, pp. 123–138. Kluwer Academic Publishers, Boston, MA.

[99] Nenadic Z, Ghosh BK, Ulinski P (2003) Propagating waves in visual cortex: A large scale model of turtle visual cortex. *J. Comput. Neurosci.* 14: 161-184.

[100] Olshausen BA, Field DJ (2005). How close are we to understanding V1? *Neural Computation* 17: 1665-1699.

[101] Opitz BA, Goodman PH (2005) In silico knockin/knockout in model neocortex suggests role of Ca-dependent K+ channels in spike-timing information. (Abstract) *J. Investig. Med.* 53: 193S.

[102] Prescott, S.A. and De Koninck, Y. (2005) Integration time in a subset of spinal lamina I neurons is lengthened by sodium and calcium currents acting synergistically to prolong subthreshold depolarization. *J. Neurosci.* 25: 4743-4754.

[103] Press WH, Flannery BP, Teukolsky SA, Vetterling WT (1993). *Numerical Recipes in C: The Art of Scientific Computing*. Cambridge University Press.

[104] Reutimann J, Giugliano M, Fusi S (2003). Event-driven simulation of spiking neurons with stochastic dynamics. *Neural Computation* 15: 811-830.

[105] Ripplinger MC, Wilson CJ, King JG, Frye J, Drewes R, Harris FC, Goodman PH. (2004) Computational model of interacting brain networks. (Abstract) *J. Investig. Med.* 52: 155S.

[106] Rochel O, Martinez D (2003) An event-driven framework for the simulation of networks of spiking neurons. in proc. 11th European Symposium On Artificial Neural Networks - ESANN'2003, Bruges, Belgium. pp. 295-300

[107] Rochel O, Vieville T (2006) One step towards an abstract view of computation in spiking neural networks (abstract). 10th international conference on cognitive and neural systems, Boston , Massachusetts 02215 USA.

[108] Rochel O, Cohen N (2006) Real time computation: zooming in on population codes. *BioSystems*, in press (doi:10.1016/j.biosystems.2006.09.021).

[109] Rotter S, Diesmann M (1999). Exact digital simulation of time-invariant linear systems with applications to neuronal modeling. *Biol. Cybern.* 81: 381-402.

[110] Rubin, J., Lee, D. and Sompolinsky, H. (2001) Equilibrium properties of temporally asymmetric Hebbian plasticity. *Phys. Rev. Lett.* 86: 364367.

[111] Rudolph M, Destexhe A (2006). Analytical integrate-and-fire neuron models with conductance-based dynamics for event-driven simulation strategies. *Neural Computation* 18: 2146-2210.

[112] Rudolph M, Destexhe A (2007). How much can we trust neural simulation strategies ? *Neurocomputing*, in press.

[113] Saghatelian, A., Roux, P., Migliore, M., Rochefort, C., Desmaisons, D., Charneau, P., Shepherd, G.M., and Lledo, P.M. (2005) Activity-dependent adjustments of the inhibitory network in the olfactory bulb following early postnatal deprivation. *Neuron* 46: 103-116.

[114] Sanchez-Montanez M (2001). Strategies for the optimization of large scale networks of integrate and fire neurons. In Mira J, Prieto A, editors, *IWANN*, volume 2084/2001 of *Lecture Notes in Computer Science*. Springer-Verlag.

[115] Sandström, M., Kotaleski, J. H., and Lansner, A. (2006). Scaling effects in a model of the olfactory bulb. *Neuro-computing*, in press.

[116] Shelley, MJ, Tao, L (2001). Efficient and accurate time-stepping schemes for integrate-and-fire neuronal networks. *J Comput. Neurosci.* 11: 111-119.

[117] Sleator, D. and Tarjan, R. (1983) Self-adjusting binary trees. *Proceedings of the 15th ACM SIGACT Symposium on Theory of Computing*, pp. 235-245.

[118] Sloot, A., Kaandorp, J. A., Hoekstra, G., & Overeinder, B. J. (1999). Distributed simulation with cellular automata: Architecture and applications. In J. Pavelka, G. Tel, & M. Bartosek (Eds.), *SOFSEM'99*, LNCS, Berlin, Heidelberg,



- 1  
2  
3  
4 pp. 203–248. Springer-Verlag.
- 5 [119] Song S, Abbott LF (2001) Cortical development and remapping through spike timing-dependent plasticity. *Neuron* 32: 339-350.
- 6  
7 [120] Song S, Miller KD, Abbott LF (2000). Competitive hebbian learning through spike-timing-dependent synaptic  
8 plasticity. *Nature Neurosci.* 3: 919-926.
- 9 [121] Stricanne B, Bower JM (1998) A network model of the somatosensory system cerebellum, exploring recovery from  
10 peripheral lesions at various developmental stages in rats. (Abstract) *Soc. Neurosci. Abstr.* 24: 669.
- 11 [122] Tonnelier A, Belmabrouk H, Martinez D (2006). Event-driven simulations of nonlinear integrate-and-fire neurons.  
12 Submitted.
- 13 [123] Traub, R.D. and Miles, R. (1991) *Neuronal Networks of the Hippocampus*. Cambridge University Press, Cambridge  
14 UK.
- 15 [124] Traub, R.D., Contreras, D., Cunningham, M.O., Murray, H., LeBeau, F.E.N., Roopun, A., Bibbig, A., Wilent,  
16 W.B., Higley, M.J., and Whittington, M.A. (2005) Single-column thalamocortical network model exhibiting gamma  
17 oscillations, sleep spindles, and epileptogenic bursts. *J. Neurophysiol.* 93: 2194-2232.
- 18 [125] Tsodyks M, Pawelzik K, Markram H (1998). Neural networks with dynamic synapses. *Neural Computation* 10:  
19 821-835.
- 20 [126] Tuckwell H (1988) *Introduction to Theoretical Neurobiology, Vol 1: Linear Cable Theory and Dendritic Structure*.  
21 Cambridge University Press, Cambridge UK.
- 22 [127] van Emde Boas P, Kaas R, Zijlstra E (1976). Design and implementation of an efficient priority queue. *Theory of*  
23 *Computing Systems* 10: 99-127.
- 24 [128] Vitko, I., Chen, Y.C., Arias, J.M., Shen, Y., Wu, X.R., and Perez-Reyes, E. (2005) Functional characterization and  
25 neuronal modeling of the effects of childhood absence epilepsy variants of CACNA1H, a T-type calcium channel. *J.*  
26 *Neurosci.* 25: 4844-4855.
- 27 [129] Vogels TP, Abbott LF. (2005) Signal propagation and logic gating in networks of integrate-and-fire neurons. *J.*  
28 *Neurosci.* 25: 10786-10795.
- 29 [130] Waikul KK, Jiang, LJ, Wilson, EC, Harris, FC Jr, Goodman, PH. (2002) Design and implementation of a web portal  
30 for a NeoCortical Simulator. *Proceedings of the 17th International Conference on Computers and Their Applications*  
31 (CATA 2002), pp. 349-353.
- 32 [131] Wang Y, Markram H, Goodman PH, Berger TK, Ma J, Goldman-Rakic PS (2006) Heterogeneity in the pyramidal  
33 network of the medial prefrontal cortex. *Nat. Neurosci.* 9: 534-542.
- 34 [132] Watts L (1994). Event-driven simulation of networks of spiking neurons. *Advances in Neural Information Process-*  
35 *ing Systems*, pages 927-934.
- 36 [133] Wiebers JL, Goodman PH, Markram H. (2000) Blockade of A-type potassium channels recovers memory impair-  
37 ment caused by synaptic loss: Implications for Alzheimer’s dementia. (Abstract) *J. Investig. Med.* 48: 283S.
- 38 [134] Wills HR, Kellogg MM, Goodman PH. (1999) A biologically realistic computer model of neocortical associative  
39 learning for the study of aging and dementia. (Abstract) *J. Investig. Med.* 47: 11S.
- 40 [135] Wilson, MA, Bower, JM (1989) The simulation of large-scale neural networks. In *Methods in neuronal modeling:*  
41 *From synapses to networks, eds C Koch and I Segev, MIT Press*, 291-333.
- 42 [136] Wohrer A, Kornprobst P, Vieville T (2006) From Light to Spikes: a Large-Scale Retina Simulator. *Proceedings of*  
43 *the IJCNN 2006, Vancouver, Canada.* pp. 8995–9003, ISBN: 0-7803-9490-9.
- 44 [137] Wolf, J.A., Moyer, J.T., Lazarewicz, M.T., Contreras, D., Benoit-Marand, M., O’Donnell, P., and Finkel, L.H.  
45 (2005) NMDA/AMPA ratio impacts state transitions and entrainment to oscillations. *J. Neurosci.* 25: 9080-9095.
- 46 [138] Zeigler B, Praehofer H, Kim T (2000). *Theory of Modeling and Simulation. Second Edition. Integrating Discrete*  
47 *Event and Continuous Complex Dynamic Systems*. Academic Press.
- 48 [139] Zeigler BP, Vahie S (1993) DEVS formalism and methodology: unity of conception/diversity of application. In.  
49 *Proceedings of the 1993 Winter Simulation Conference, Los Angeles, CA, December 12-15.* pp. 573-579.
- 50  
51  
52  
53  
54  
55  
56  
57  
58  
59  
60  
61  
62  
63  
64  
65

1  
2  
3  
4  
5  
6  
7  
8  
9  
10  
11  
12  
13  
14  
15  
16  
17  
18  
19  
20  
21  
22  
23  
24  
25  
26  
27  
28  
29  
30  
31  
32  
33  
34  
35  
36  
37  
38  
39  
40  
41  
42  
43  
44  
45  
46  
47  
48  
49  
50  
51  
52  
53  
54  
55  
56  
57  
58  
59  
60  
61  
62  
63  
64  
65

Question	NEURON	GENESIS	NEST	NCS	CSIM	XPP	SPLIT	Mvaspike
HH	B.I.	B.I.	YES	B.I.	B.I.	YES	B.I.	POSS
leaky IF	B.I.	POSS	YES	B.I.	B.I.	YES	POSS**	B.I.
Izhikevich IF	YES	B.I.	YES	NO	B.I.	YES	POSS**	POSS**
Cable eqs	B.I.	B.I.	NO	NO	NO	YES	B.I.	NO
ST plasticity	YES	B.I.	YES	B.I.	B.I.	YES	B.I.	YES
LT Plasticity	YES	YES	YES	B.I.	B.I.	YES	NO**	YES
Event-based	B.I.	NO	YES	NO	NO	YES	NO	YES
exact	B.I.	-	YES	-	-	NO	-	YES
Clock-based	B.I.	B.I.	YES	B.I.	YES	YES	YES	POSS**
extrapolated	B.I.	NO	YES	NO	?	YES	B.I.	POSS
G synapses	B.I.	B.I.	YES	B.I.	B.I.	YES	B.I.	POSS**
parallel	B.I.	YES	B.I.	B.I.	NO**	NO	B.I.	NO**
graphics	B.I.	B.I.	NO(*)	NO(*)	NO(*)	YES	NO	NO
simple analysis	B.I.	B.I.	YES	NO(*)	NO(*)	YES	NO	NO
complx analysis	B.I.	YES	NO(*)	NO(*)	NO(*)	YES	NO	NO
development	YES	YES	YES	YES	YES	YES	YES	YES
how many p.	3	2-3	4	2-3	2	1	2	1
support	YES	YES	YES	YES	YES	YES	YES	YES
type	e,p,c	e	e	e	e	e	e	e
user forum	YES	YES	YES	NO	NO	YES	YES	NO
publ list	YES	YES	YES	YES	YES	NO	NO	NO
codes	YES	YES	YES	YES	YES	YES	NO	NO
online manual	YES	YES	YES	YES	YES	YES	YES	YES
book	YES	YES	NO	NO	NO	YES	NO	NO
XML import	NO**	POSS	NO**	NO**	NO	YES	NO	NO**
XML export	B.I.	NO**	NO**	NO**	NO	NO	NO	NO**
web site	YES	YES	YES	YES	YES	YES	YES	YES
LINUX	YES	YES	YES	YES	YES	YES	YES	YES
Windows	YES	YES	YES	YES	YES	YES	NO	NO
Mac-Os	YES	YES	YES	NO	NO	YES	NO	NO
Interface	B.I.	B.I.	POSS	B.I.	YES	POSS	POSS	POSS
Save option	B.I.	YES	NO**	B.I.	NO	NO	NO	NO

Table 1: Comparison of features of the different simulators.

1  
2  
3  
4 **Table caption**

5  
6 Table 1: Comparison of features of the different simulators

7  
8 Different questions were asked (see below), and for each question, the answer is either:  
9 B.I. = Built-in feature, incorporated in the simulator without need to load additional mechanisms;  
10 YES = feature very easy to simulate or implement (ie., a few minutes of programming);  
11 POSS = feature possible to implement, but requires a bit of user programming;  
12 NO = feature not implemented, would require modifying the code;  
13 \*\* = feature planned to be implemented in a future version of the simulator;  
14 (\*) graphical interface and analysis possible via front-ends like Python or MATLAB.  
15  
16

17 The list of questions were:

18 HH: can it simulate HH models?;  
19 leaky IF: can it simulate leaky IF models?;  
20 Izhikevich IF: can it simulate multivariable IF models, for example Izhikevich type?;  
21 Cable eqs: can it simulate compartmental models with dendrites?;  
22 ST plasticity: can it simulate short-term synaptic plasticity? (facilitation, depression);  
23 LT Plasticity: can it simulate long-term synaptic plasticity? (LTP, LTD, STDP);  
24 Event-based: can it simulate event-based strategies?;  
25 exact: in this case, is the integration scheme exact?;  
26 Clock-based: can it simulate clock-based strategies? (e.g., Runge-Kutta);  
27 interpolated: in this case, does it use extrapolation for spike times?;  
28 G synapses: can it simulate conductance-based synaptic interactions?;  
29 parallel: does it support parallel processing?;  
30 graphics: does it have a graphical interface?;  
31 simple analysis: is it possible to use the interface for simple analysis? (spike count, correlations, etc);  
32 complx analysis: can more complex analysis be done? (parameter fitting, fft, matrix operations, ...);  
33 development: is it currently developed?;  
34 how many p.: if yes, how many developers are working on it?;  
35 support: is it supported? (help for users);  
36 type: what type of support (email, phone, consultation?);  
37 user forum: is there a forum of users or mailing list?;  
38 publ list: is there a list of publications of articles that used it?;  
39 codes: are there codes available on the web of published models?;  
40 online manual: are there tutorials and reference material available on the web?;  
41 book: are there published books on the simulator?  
42 XML import: can it import model specifications in XML?  
43 XML export: can it export model specifications in XML?  
44 web site: is there a web site of the simulator where all can be found? (including help and source codes)  
45 LINUX: does it run on LINUX?  
46 Windows: does it run on Windows? (98, 2K, XP)  
47 Mac-Os: does it run on Mac-OS X?  
48 Interface: Is there a possibility to interface the simulator to outside signals ? (such as a camera, or a real neuron)  
49 Save option: Does it have a "save option", (different than ctrl-z), allowing the user to interrupt a simulation,  
50 and continue it later on ? (this feature is important on a cluster when simulations must be interrupted)  
51  
52  
53  
54  
55  
56  
57  
58  
59  
60  
61  
62  
63  
64  
65

1  
2  
3  
4  
5  
6  
7  
8  
9  
10  
11  
12  
13  
14  
15  
16  
17  
18  
19  
20  
21  
22  
23  
24  
25  
26  
27  
28  
29  
30  
31  
32  
33  
34  
35  
36  
37  
38  
39  
40  
41  
42  
43  
44  
45  
46  
47  
48  
49  
50  
51  
52  
53  
54  
55  
56  
57  
58  
59  
60  
61  
62  
63  
64  
65

```
t=0
while t<duration
  for every neuron
    process incoming spikes
    advance neuron dynamics by dt
  end
  for every neuron
    if vm>threshold
      reset neuron
      for every connection
        send spike
      end
    end
  end
  t=t+dt
end
```

*State updates*

*Propagation of spikes*

Figure 1: A basic clock-driven algorithm

```
while queue not empty and t<duration
  extract event with lowest timing
  (= timing t, target i, weight w)
  compute state of neuron i at time t
  update state of neuron i (+w)
  if vm>threshold
    for each connection i->j
      insert event in the queue
    end
    reset neuron i
  end
end
```

*Process event*

*Propagate spike*

Figure 2: A basic event-driven algorithm with instantaneous synaptic interactions

```

20 for every neuron i
21     compute timing of next spike           Initialization
22     insert event in priority queue
23 end
24
25
26 while queue not empty and t<duration
27     extract event with lowest timing       Process spike
28     (event = timing t, neuron i)
29     compute state of neuron i at time t
30     reset membrane potential
31     compute timing of next spike
32     insert event in queue
33
34
35
36     for every connection i->j           Communicate spike
37         compute state of neuron j at time t
38         change state with weight w(i,j)
39         compute timing of next spike
40         insert/change/suppress event in queue
41     end
42 end
43 end
44

```

Figure 3: A basic event-driven algorithm with non-instantaneous synaptic interactions

1  
2  
3  
4  
5  
6  
7  
8  
9  
10  
11  
12  
13  
14  
15  
16  
17  
18  
19  
20  
21  
22  
23  
24  
25  
26  
27  
28  
29  
30  
31  
32  
33  
34  
35  
36  
37  
38  
39  
40  
41  
42  
43  
44  
45  
46  
47  
48  
49  
50  
51  
52  
53  
54  
55  
56  
57  
58  
59  
60  
61  
62  
63  
64  
65

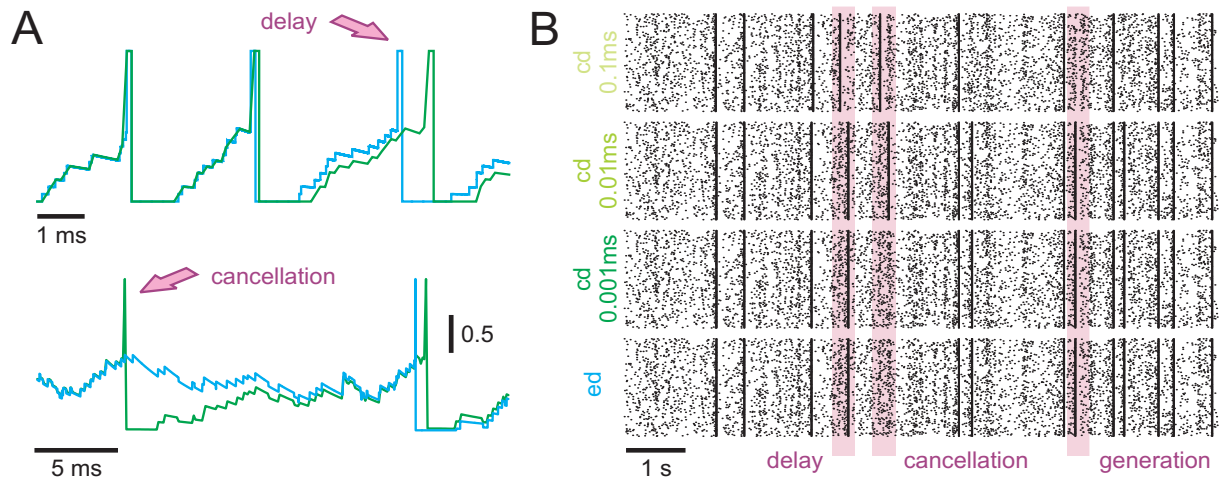


Figure 4: Modelling strategies and dynamics in neuronal systems without STDP.

A: Small differences in spike times can accumulate and lead to severe delays or even cancellation (see arrows) of spikes, depending on the simulation strategy utilized or the temporal resolution within clock-driven strategies used. B: Rasterplots of spike events in a small neuronal network of LIF neurons simulated with event-driven and clock-driven approaches with different temporal resolutions. Observed differences in neural network dynamics include delays, cancellation or generation of synchronous network events (Figure modified from Rudolph & Destexhe, 2007).

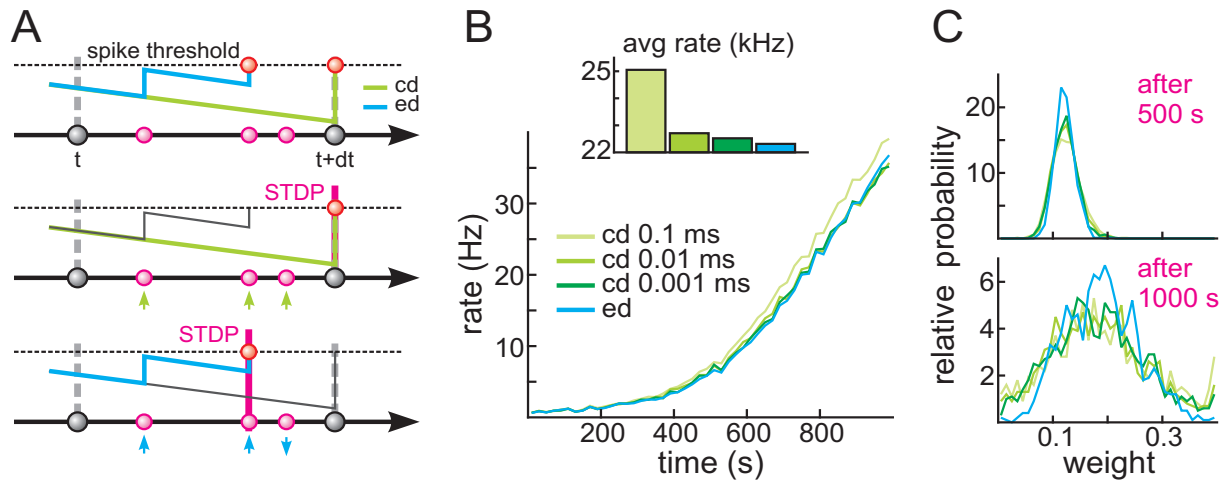


Figure 5: Dynamics in neuronal systems with STDP.

A: Impact of the simulation strategy (clock-driven: *cd*; event-driven: *ed*) on the facilitation and depression of synapses. B: Time course and average rate (inset) in a LIF model with multiple synaptic input channels for different simulation strategies and temporal resolution. C: Synaptic weight distribution after 500 s and 1,000 s (Figure modified from Rudolph & Destexhe, 2007).

1  
2  
3  
4  
5  
6  
7  
8  
9  
10  
11  
12  
13  
14  
15  
16  
17  
18  
19  
20  
21  
22  
23  
24  
25  
26  
27  
28  
29  
30  
31  
32  
33  
34  
35  
36  
37  
38  
39  
40  
41  
42  
43  
44  
45  
46  
47  
48  
49  
50  
51  
52  
53  
54  
55  
56  
57  
58  
59  
60  
61  
62  
63  
64  
65

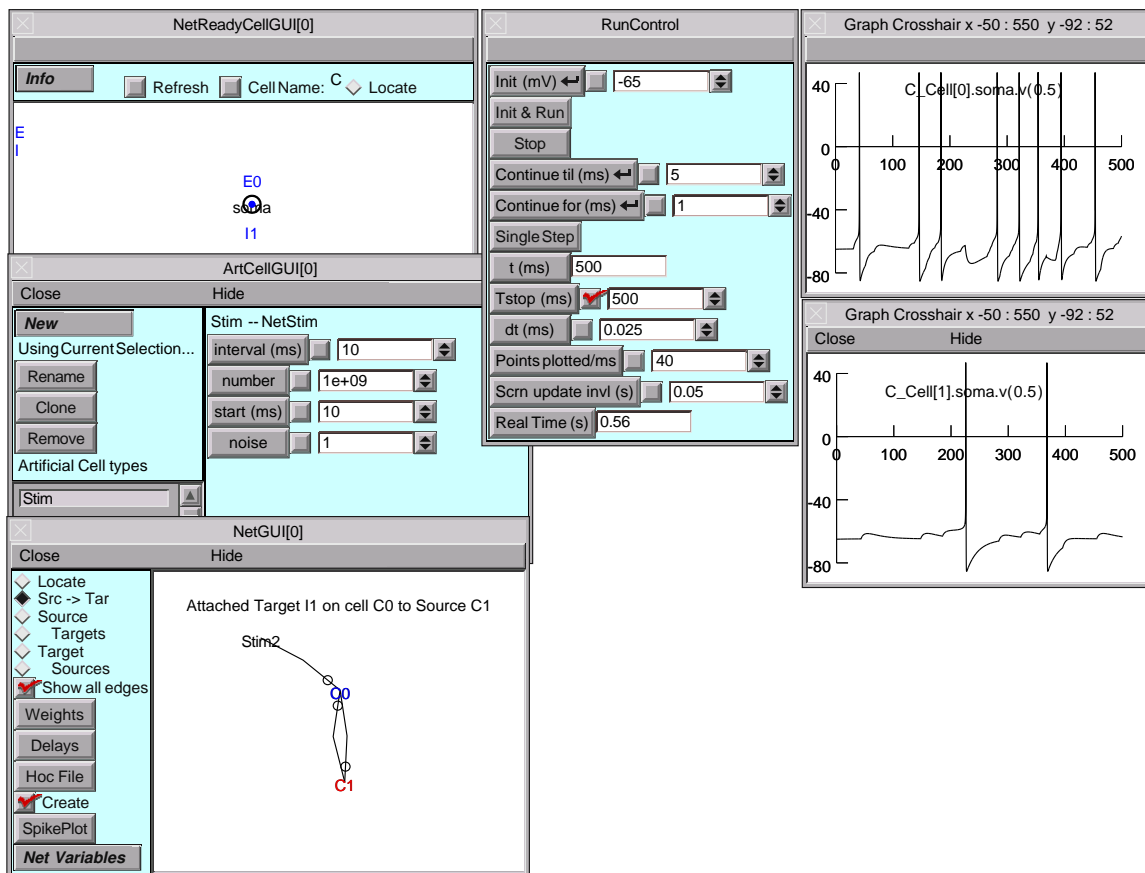


Figure 6: NEURON graphical user interface.

In developing large scale networks, it is helpful to start by debugging small prototype nets. NEURON's GUI, especially its Network Builder (shown here), can simplify this task. Also, at the click of a button the Network Builder generates hoc code that can be reused as the building blocks for large scale nets (see chapter 11, *Modeling networks* in Carnevale and Hines 2006).

1  
2  
3  
4  
5  
6  
7  
8  
9  
10  
11  
12  
13  
14  
15  
16  
17  
18  
19  
20  
21  
22  
23  
24  
25  
26  
27  
28  
29  
30  
31  
32  
33  
34  
35  
36  
37  
38  
39  
40  
41  
42  
43  
44  
45  
46  
47  
48  
49  
50  
51  
52  
53  
54  
55  
56  
57  
58  
59  
60  
61  
62  
63  
64  
65

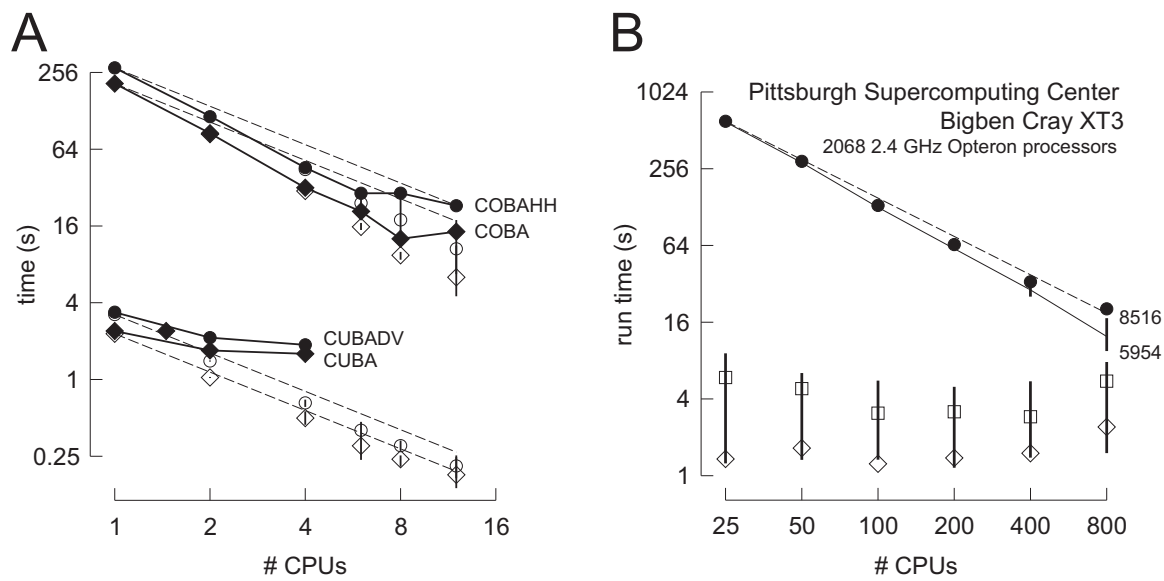


Figure 7: Parallel simulations using NEURON.

A. Four benchmark network models were simulated on 1, 2, 4, 6, 8, and 12 CPUs of a Beowulf cluster (6 nodes, dual CPU, 64-bit 3.2 GHz Intel Xeon with 1024 KB cache). Dashed lines indicate "ideal speedup" (run time inversely proportional to number of CPUs). Solid symbols are run time, open symbols are average computation time per CPU, and vertical bars indicate variation of computation time. The CUBA and CUBADV models execute so quickly that little is gained by parallelizing them. The CUBA model is faster than the more efficient CUBADV because the latter generates twice as many spikes (spike counts are COBAHH 92,219, COBA 62,349, CUBADV 39,280, CUBA 15,371). B. The Pittsburgh Supercomputing Center's Cray XT3 (2.4 GHz Opteron processors) was used to simulate a NEURON implementation of the thalamocortical network model of Traub et al. (2005). This model has 3,560 cells in 14 types, 3,500 gap junctions, 5,596,810 equations, and 1,122,520 connections and synapses, and 100 ms of model time it generates 73,465 spikes and 19,844,187 delivered spikes. The dashed line indicates "ideal speedup" and solid circles are the actual run times. The solid black line is the average computation time, and the intersecting vertical lines mark the range of computation times for each CPU. Neither the number of cell classes nor the number of cells in each class were multiples of the number of processors, so load balance was not perfect. When 800 CPUs were used, the number of equations per CPU ranged from 5954 to 8516. Open diamonds are average spike exchange times. Open squares mark average voltage exchange times for the gap junctions, which must be done at every time step; these lie on vertical bars that indicate the range of voltage exchange times. This range is large primarily because of synchronization time due to computation time variation across CPUs. The minimum value is the actual exchange time.



1  
2  
3  
4  
5  
6  
7  
8  
9  
10  
11  
12  
13  
14  
15  
16  
17  
18  
19  
20  
21  
22  
23  
24  
25  
26  
27  
28  
29  
30  
31  
32  
33  
34  
35  
36  
37  
38  
39  
40  
41  
42  
43  
44  
45  
46  
47  
48  
49  
50  
51  
52  
53  
54  
55  
56  
57  
58  
59  
60  
61  
62  
63  
64  
65

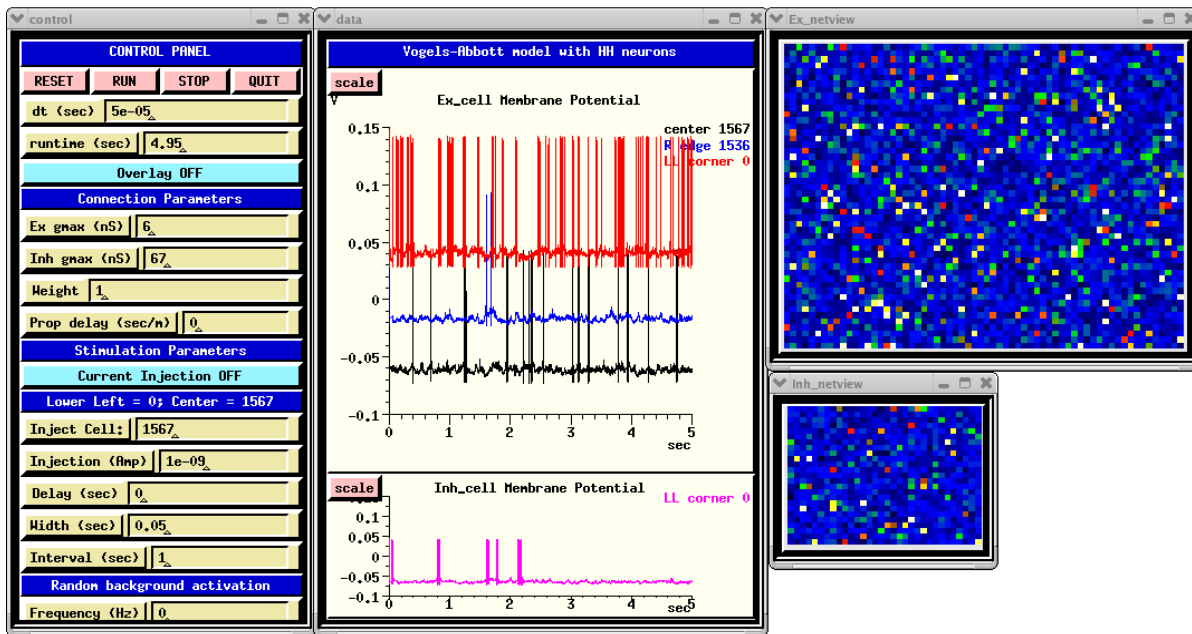


Figure 8: The GUI for the GENESIS implementation of the HH benchmark, using the dual-exponential form of synaptic conductance.

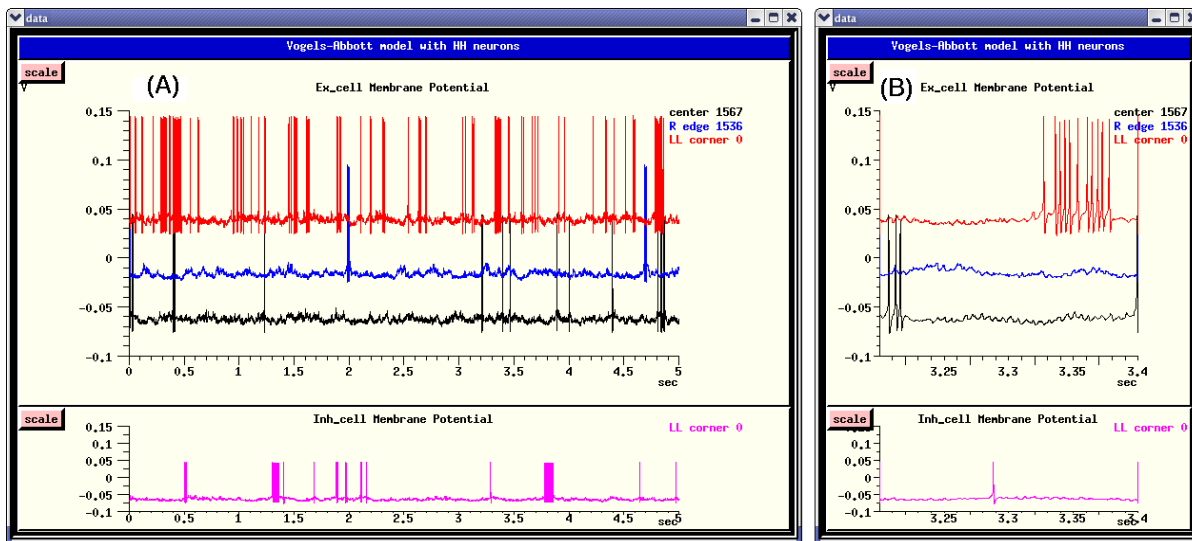


Figure 9: Membrane potentials for four selected neurons of the Instantaneous Conductance VA HH Model in GENESIS.

A. The entire 5 seconds of the simulation. B. Detail of the interval 3.2–3.4 sec.

1  
2  
3  
4  
5  
6  
7  
8  
9  
10  
11  
12  
13  
14  
15  
16  
17  
18  
19  
20  
21  
22  
23  
24  
25  
26  
27  
28  
29  
30  
31  
32  
33  
34  
35  
36  
37  
38  
39  
40  
41  
42  
43  
44  
45  
46  
47  
48  
49  
50  
51  
52  
53  
54  
55  
56  
57  
58  
59  
60  
61  
62  
63  
64  
65

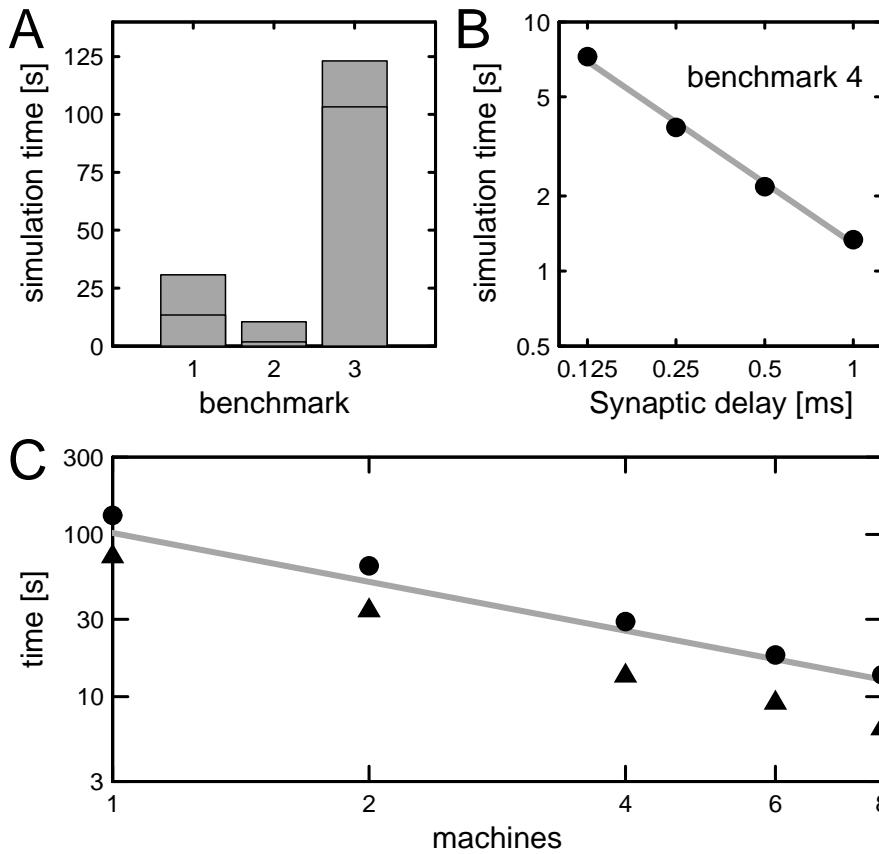


Figure 10: Performance of NEST on Benchmarks 1-4 and an additional benchmark (5) with spike timing dependent plasticity (STDP).

A. Simulation time for one biological second of Benchmarks 1-3 distributed over two processors, spiking suppressed, with a synaptic delay of 0.1 ms. The horizontal lines indicate the simulation times for the benchmarks with the synaptic delay increased to 1.5 ms. B. Simulation time for one biological second of Benchmark 4 as a function of the minimum synaptic delay in double logarithmic representation. The gray line indicates a linear fit to the data (slope $-0.8$ ). C. Simulation time for one biological second of Benchmark 5, a network of 11250 neurons and connection probability of 0.1 (total number of synapses:  $12.7 \times 10^6$ ) as a function of the number of processors in double logarithmic representation. All synapses static, triangles; excitatory-excitatory synapses implementing multiplicative STDP with an all-to-all spike pairing scheme, circles. The gray line indicates a linear speed-up.

1  
2  
3  
4  
5  
6  
7  
8  
9  
10  
11  
12  
13  
14  
15  
16  
17  
18  
19  
20  
21  
22  
23  
24  
25  
26  
27  
28  
29  
30  
31  
32  
33  
34  
35  
36  
37  
38  
39  
40  
41  
42  
43  
44  
45  
46  
47  
48  
49  
50  
51  
52  
53  
54  
55  
56  
57  
58  
59  
60  
61  
62  
63  
64  
65

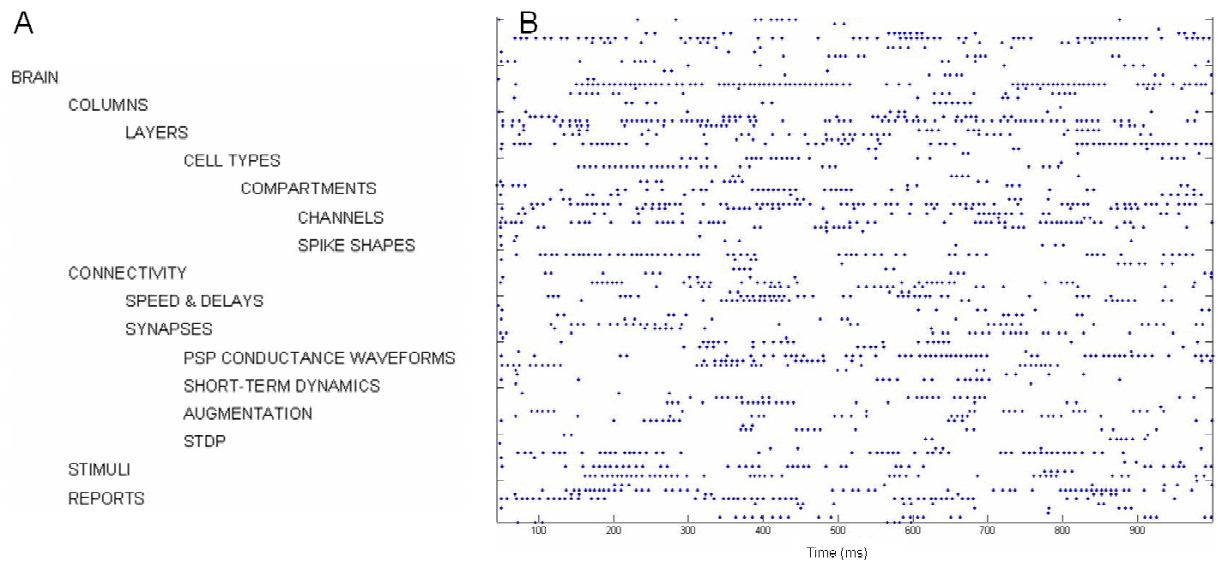


Figure 11: NCS file specifications and example of simulation.

A. Hierarchy of the NCS Command File Objects. The file is ASCII-based with simple object delimiters. Brainlab scripting tools are available for repetitive structures (Drewes, 2005). B. 1-second spike rastergram of 100 arbitrarily selected neurons in the benchmark simulation.

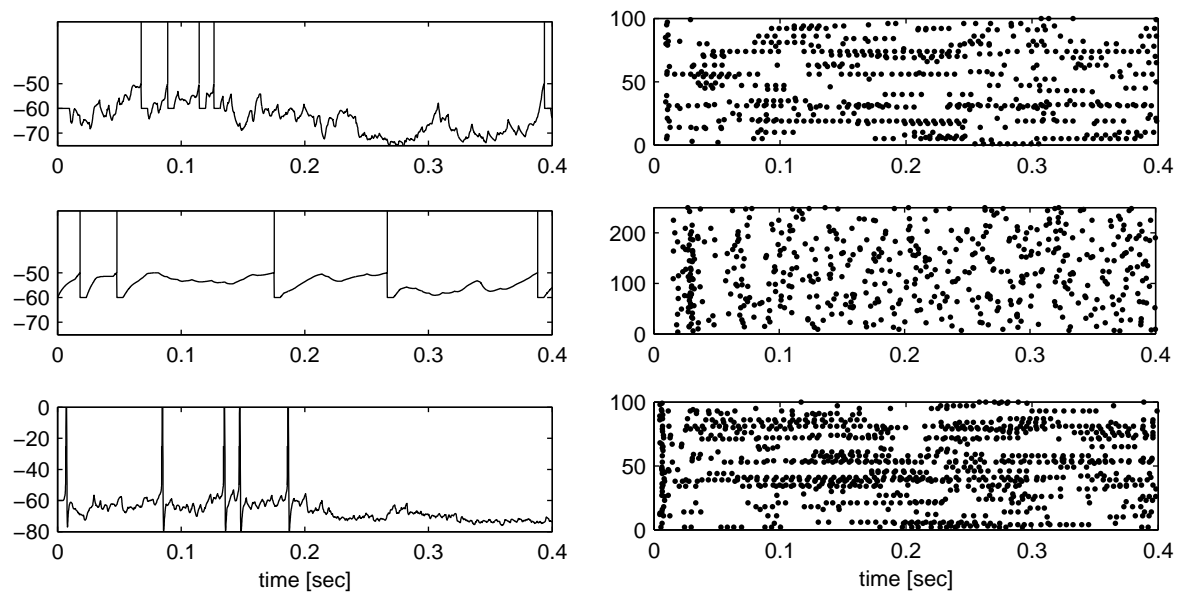


Figure 12: Results of CSIM simulations of the benchmarks 1 to 3 (top to bottom).

The left panels show the voltage traces (in mV) of a selected neuron. For Benchmark 1 (COBA) and Benchmark 2 (CUBA) models (top two rows), the spikes superimposed as vertical lines. The right panels show the spike raster for randomly selected neurons for each of the three benchmarks.

1  
2  
3  
4  
5  
6  
7  
8  
9  
10  
11  
12  
13  
14  
15  
16  
17  
18  
19  
20  
21  
22  
23  
24  
25  
26  
27  
28  
29  
30  
31  
32  
33  
34  
35  
36  
37  
38  
39  
40  
41  
42  
43  
44  
45  
46  
47  
48  
49  
50  
51  
52  
53  
54  
55  
56  
57  
58  
59  
60  
61  
62  
63  
64  
65

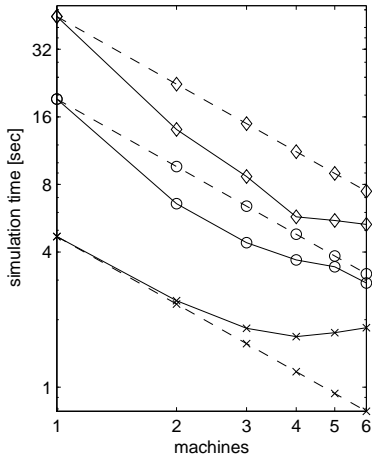


Figure 13: Performance of PCSIM.

The time needed to simulate the Benchmark 2 (CUBA) network (1ms synaptic delay, 0.1ms time step) for one second of biological time (solid line) as well as the expected times (dashed line) are plotted against the number of machines (Intel Xeon, 3.4 Ghz, 2 Mb cache). The CUBA model was simulated for three different sizes: 4000 neurons and  $3.2 \times 10^5$  synapses (stars), 10000 neurons and  $2 \times 10^6$  synapses (circles), and 20000 neurons and  $20 \times 10^6$  synapses (diamonds).

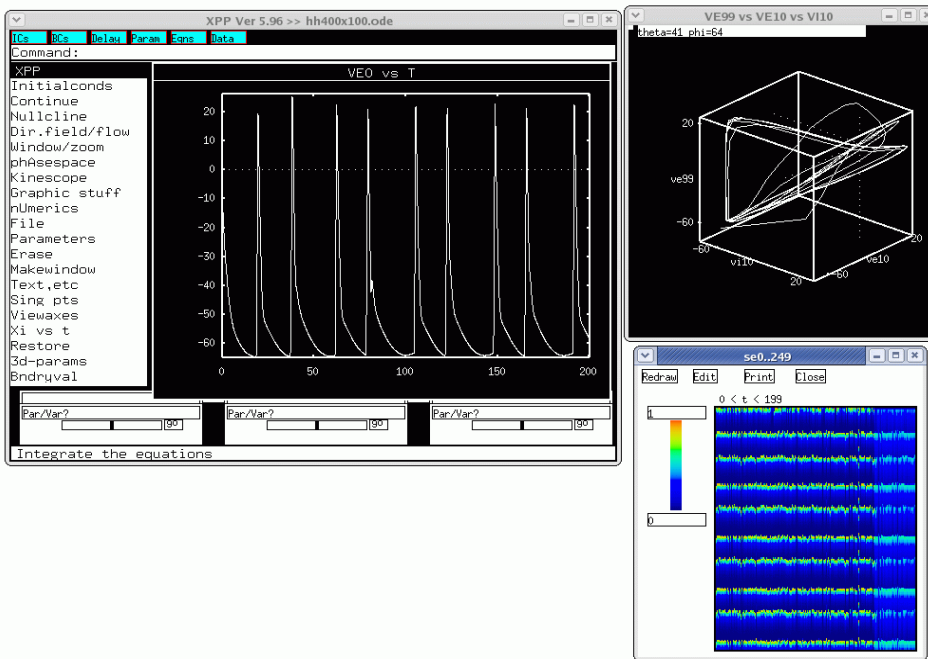


Figure 14: *XPPAUT* interface for a network of 200 excitatory and 50 inhibitory Hodgkin-Huxley neurons with random connectivity, conductance-based dynamical synapses. Each neuron is also given a random drive. Main window, a three-dimensional phase plot, and an array plot are shown.

1  
2  
3  
4  
5  
6  
7  
8  
9  
10  
11  
12  
13  
14  
15  
16  
17  
18  
19  
20  
21  
22  
23  
24  
25  
26  
27  
28  
29  
30  
31  
32  
33  
34  
35  
36  
37  
38  
39  
40  
41  
42  
43  
44  
45  
46  
47  
48  
49  
50  
51  
52  
53  
54  
55  
56  
57  
58  
59  
60  
61  
62  
63  
64  
65

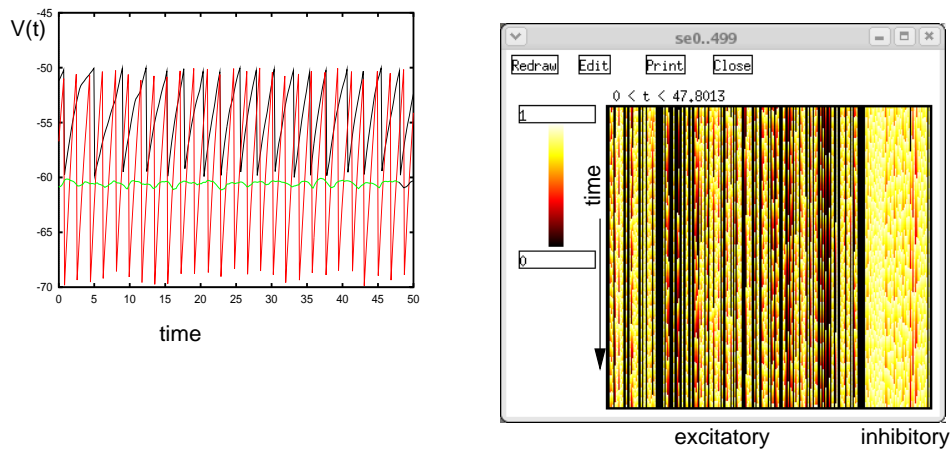


Figure 15: Persistent state in an integrate-and-fire network with 400 excitatory and 100 inhibitory cell. *XPPAUT* simulation with exponential conductance-based synapses, sparse coupling and random drive. Excitatory and inhibitory synapses are shown as well as voltages traces from 3 neurons.

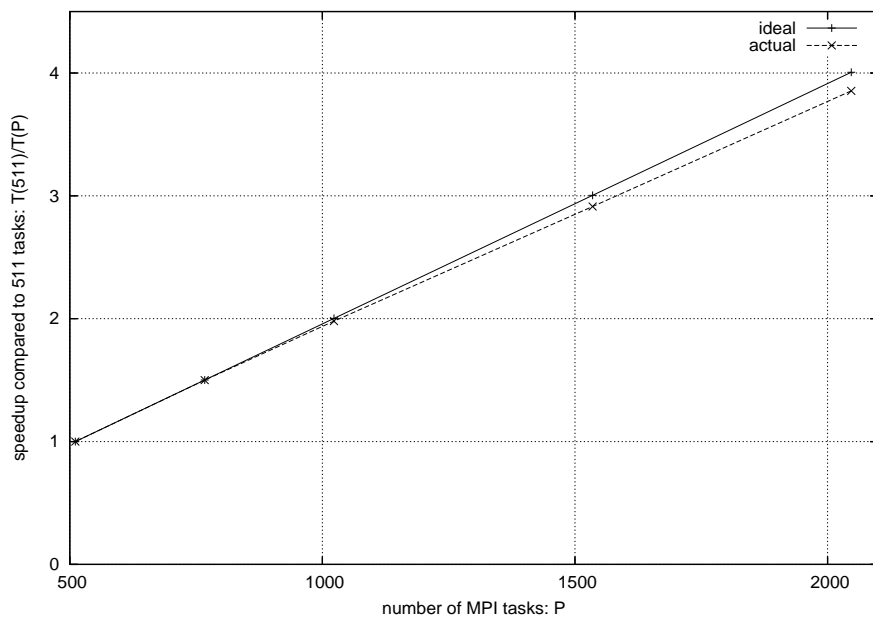


Figure 16: Speedup for model with 4 million cells and 2 billion synapses simulated with SPLIT on BG/L (from Djurfeldt et al., 2005).

1  
2  
3  
4  
5  
6  
7  
8  
9  
10  
11  
12  
13  
14  
15  
16  
17  
18  
19  
20  
21  
22  
23  
24  
25  
26  
27  
28  
29  
30  
31  
32  
33  
34  
35  
36  
37  
38  
39  
40  
41  
42  
43  
44  
45  
46  
47  
48  
49  
50  
51  
52  
53  
54  
55  
56  
57  
58  
59  
60  
61  
62  
63  
64  
65

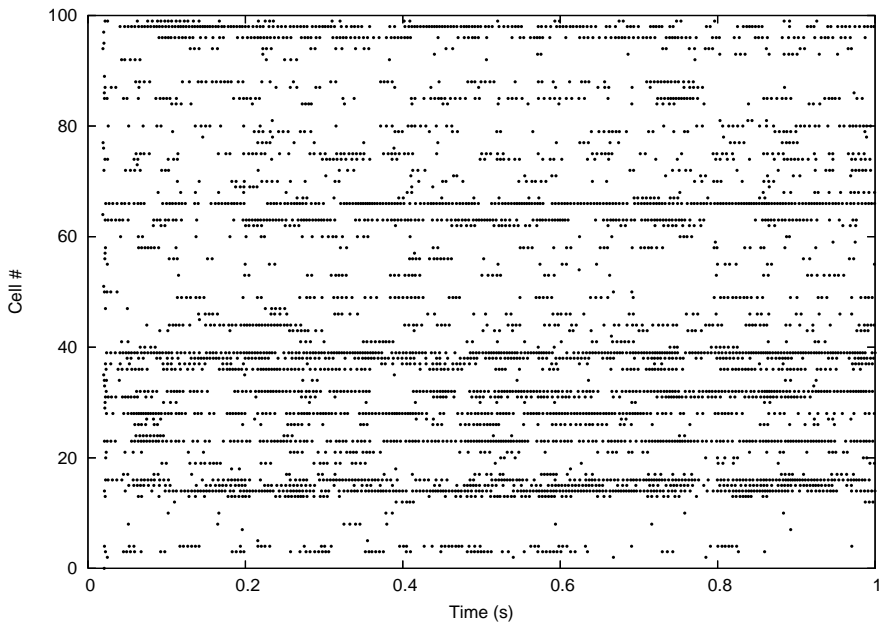


Figure 17: Raster plot showing spikes of 100 cells during the first second of activity (SPLIT simulation of Benchmark 3).

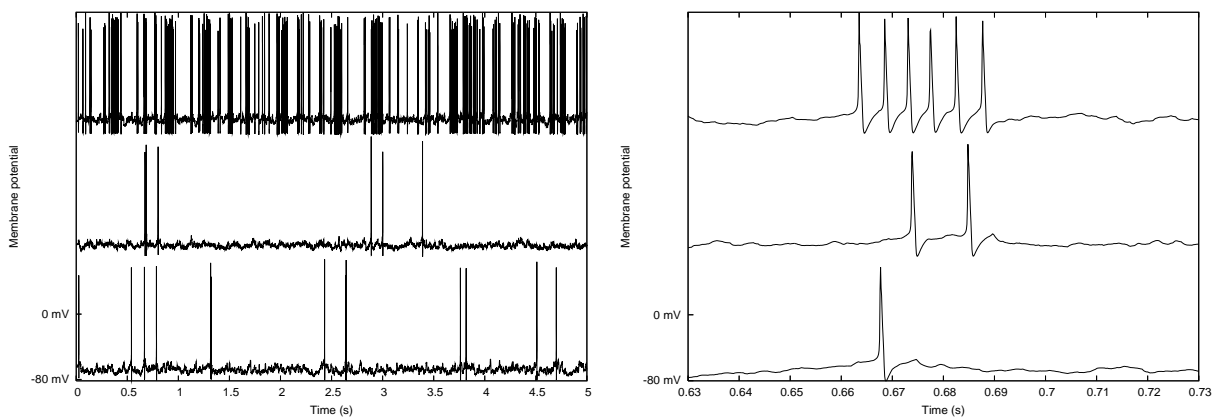


Figure 18: Plots of the membrane potential for 3 of the 4000 cells. The right plot shows a subset of the data in the left plot, with higher time resolution (SPLIT simulation of Benchmark 3).

1  
2  
3  
4  
5  
6  
7  
8  
9  
10  
11  
12  
13  
14  
15  
16  
17  
18  
19  
20  
21  
22  
23  
24  
25  
26  
27  
28  
29  
30  
31  
32  
33  
34  
35  
36  
37  
38  
39  
40  
41  
42  
43  
44  
45  
46  
47  
48  
49  
50  
51  
52  
53  
54  
55  
56  
57  
58  
59  
60  
61  
62  
63  
64  
65

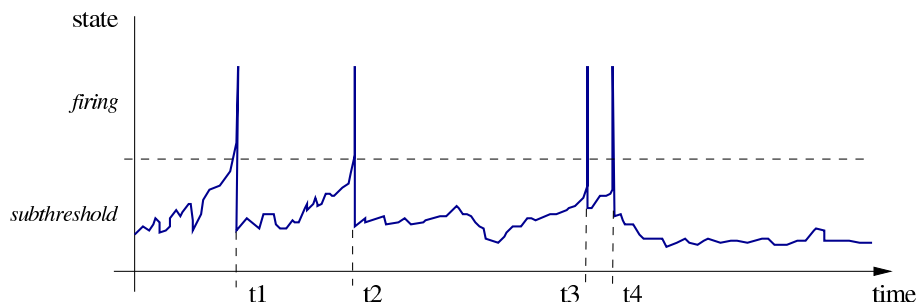


Figure 19: Neuronal dynamics from a discrete-event dynamical systems perspective. Events (t1-t4), corresponding to the state variable switching from the sub-threshold to the firing dynamics, can occur at any arbitrary point in time. They correspond here to change of the neuron output that can be passed to the rest of the systems (e.g. other neurons). Internal changes (e.g. end of the refractory period) can also be described in a similar way.

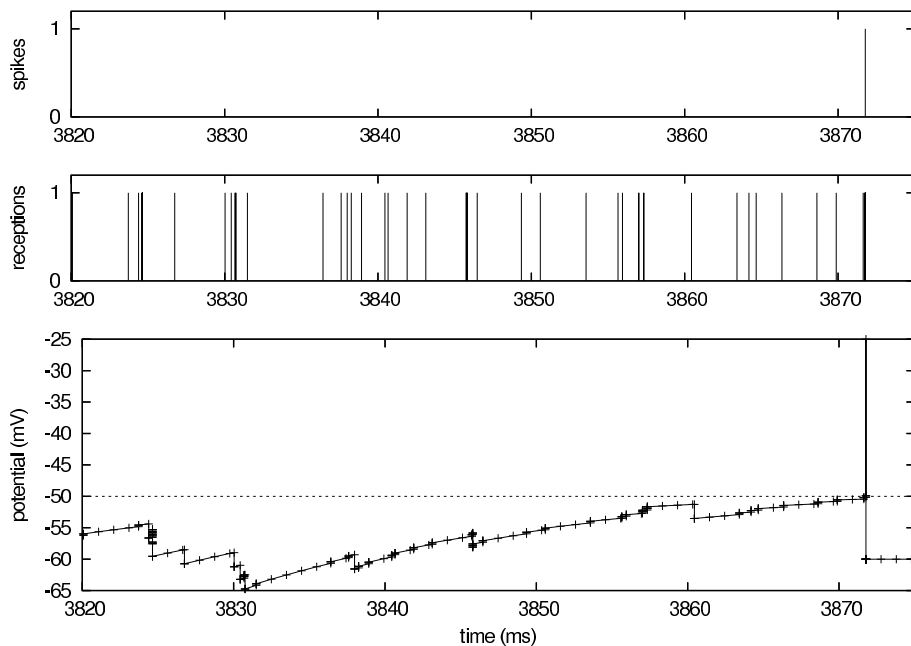


Figure 20: Membrane potential of a single neuron, from a Mvaspike implementation of Benchmark 4. Top: membrane potential dynamics (impulses have been superimposed at firing time to make them more apparent). Bottom: Mvaspike simulation result typically consists of lists of events (here, spiking and reception time, top and middle panels) and the corresponding state variables at these instants (not shown). In order to obtain the full voltage dynamics, a post-processing stage is used to add new intermediary values between events (bottom trace).

1  
2  
3  
4  
5  
6  
7  
8  
9  
10  
11  
12  
13  
14  
15  
16  
17  
18  
19  
20  
21  
22  
23  
24  
25  
26  
27  
28  
29  
30  
31  
32  
33  
34  
35  
36  
37  
38  
39  
40  
41  
42  
43  
44  
45  
46  
47  
48  
49  
50  
51  
52  
53  
54  
55  
56  
57  
58  
59  
60  
61  
62  
63  
64  
65

```
<?xml version="1.0" encoding="UTF-8"?>
<channelml xmlns="http://morphml.org/channelml/schema"
  xmlns:xsi="http://www.w3.org/2001/XMLSchema-instance"
  xmlns:meta="http://morphml.org/metadata/schema"
  xsi:schemaLocation="http://morphml.org/channelml/schema
  ../../Schemata/v1.1/Level2/ChannelML_v1.1.xsd"
  units="Physiological Units">
  <ion name="k" default_erev="-77.0" charge="1"/> <!-- phys units: mV -->
  <channel_type name="KChannel" density="yes">
    <meta:notes>Simple example of K conductance in squid giant axon.
      Based on channel from Hodgkin and Huxley 1952</meta:notes>
    <current_voltage_relation>
      <ohmic ion="k">
        <conductance default_gmax="36"> <!-- phys units: mS/cm2-->
          <gate power="4">
            <state name="n" fraction="1">
              <transition>
                <voltage_gate>
                  <alpha>
                    <parameterised_hh type="linoid" expr="A*(k*(v-d))/(1 - exp(-(k*(v-d))))">
                      <parameter name="A" value="0.1"/>
                      <parameter name="k" value="0.1"/>
                      <parameter name="d" value="-55"/>
                    </parameterised_hh>
                  </alpha>
                  <beta>
                    <parameterised_hh type="exponential" expr="A*exp(k*(v-d))">
                      <parameter name="A" value="0.125"/>
                      <parameter name="k" value="-0.0125"/>
                      <parameter name="d" value="-65"/>
                    </parameterised_hh>
                  </beta>
                </voltage_gate>
              </transition>
            </state>
          </gate>
        </conductance>
      </ohmic>
    </current_voltage_relation>
  </channel_type>
</channelml>
```

Figure 21: Example of Hodgkin-Huxley K<sup>+</sup> conductance specified in ChannelML, a component of NeuroML.



1  
2  
3  
4  
5  
6  
7  
8  
9  
10  
11  
12  
13  
14  
15  
16  
17  
18  
19  
20  
21  
22  
23  
24  
25  
26  
27  
28  
29  
30  
31  
32  
33  
34  
35  
36  
37  
38  
39  
40  
41  
42  
43  
44  
45  
46  
47  
48  
49  
50  
51  
52  
53  
54  
55  
56  
57  
58  
59  
60  
61  
62  
63  
64  
65

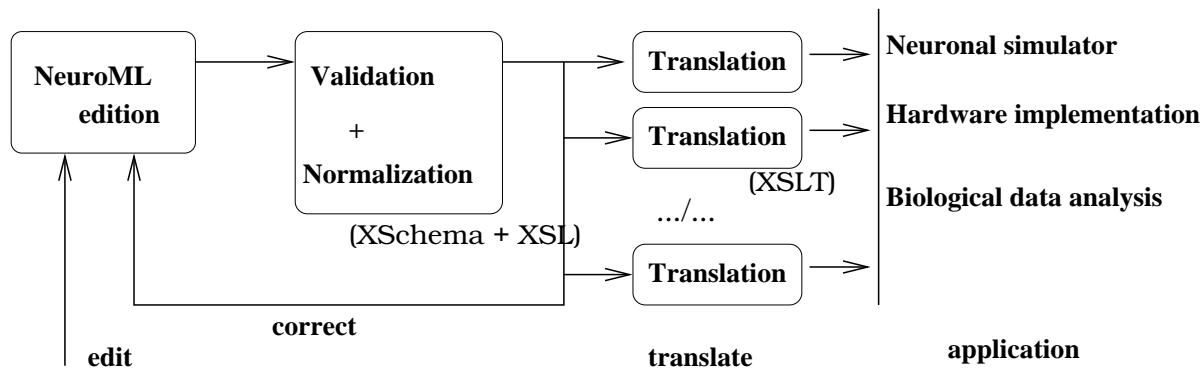


Figure 22: From NeuroML to simulator

```
cell_params = { 'tau_m' : 20.0, 'tau_syn' : 2.0, 'tau_refrac': 1.0,
                'v_rest': -65.0, 'v_thresh': -50.0, 'cm': 1.0}

populationA = Population((10,), "IF_curr_alpha", cell_params)
populationB = Population((5,5), "IF_curr_alpha", cell_params)
populationA.randomInit('uniform', v_reset, v_thresh)

connAtoB = Projection(populationA, populationB, 'fixedProbability', 0.2)
connAtoA = Projection(populationA, populationA, 'distanceDependentProbability', "exp(-abs(d))")
connBtoA = Projection(populationB, populationA, 'allToAll')

connAtoB.setWeights(w_AB)
connAtoA.setWeights(w_AA)
connBtoA.setWeights(w_BA)

populationA.record()
populationB.record()

run(1000.0)

populationA.printSpikes("populationA.spiketimes")
populationB.printSpikes("populationA.spiketimes")
```

Figure 23: Example of the use of the PyNN API to specify a network that can then be run on multiple simulators.

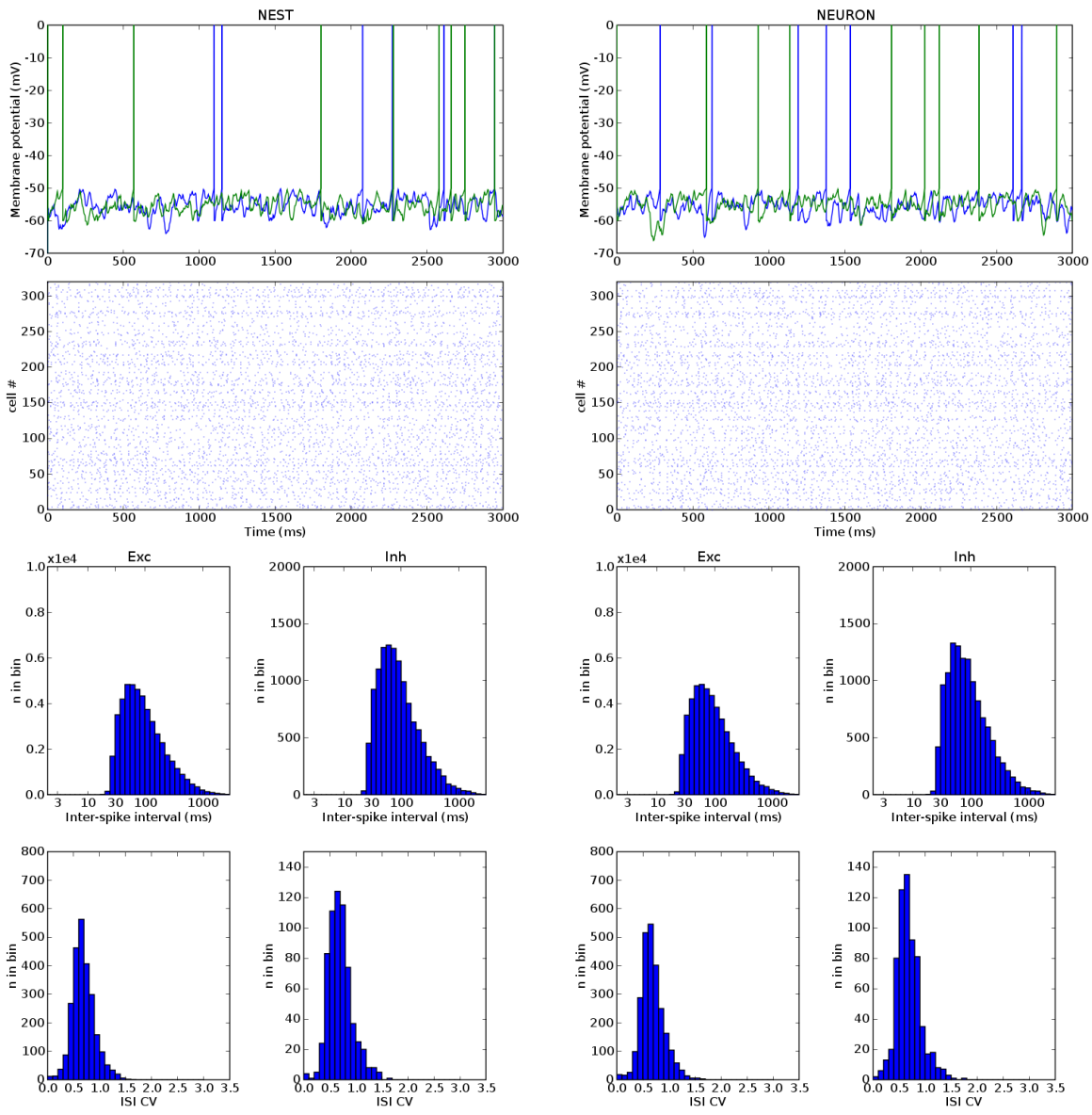


Figure 24: Same network model run on two different simulators using the same source code.

The model considered was the Vogels-Abbott integrate-and-fire network with current-based synapses and displaying self-sustained irregular activity states (benchmark 2 in Appendix 2). This network implemented with the PyNN simulator-independent network modelling API, and simulated using NEST (left column) and NEURON (right column) as the simulation engines. The same sequence of random numbers was used for each simulator, so the connectivity patterns were rigorously identical. The membrane potential trajectories of individual neurons simulated in different simulators rapidly diverge, as small numerical differences are rapidly amplified by the large degree of recurrency of the circuit, but the interspike interval (ISI) statistics of the populations are almost identical for the two simulators. (Top row) Voltage traces for two cells chosen at random from the population. (Second row) Spike raster plots for the first 320 neurons in the population. (Third row) Histograms of ISIs for the excitatory and inhibitory cell populations. (Bottom row) Histograms of the coefficient of variation (CV) of the ISIs.